Towards applications of the gauge-gravity duality to condensed matter physics

Fábio Diales da Rocha

A Dissertation

Presented to the Faculty

of Princeton University

in Candidacy for the Degree

of Doctor of Philosophy

Recommended for Acceptance

by the Department of

Physics

Adviser: Steven S. Gubser

September, 2010

Abstract

String theory offers, through the gauge-gravity dualities, powerful methods to study strongly coupled field theories. In this dissertation, we will be concerned with applying these methods to topics related to condensed matter physics.

The Abelian Higgs model coupled to gravity with a negative cosmological constant provides a gravitational dual to a strongly coupled field theory that has superconducting or superfluid phases. We construct zero-temperature solutions of this model that interpolate between two copies of anti-de Sitter space and which we identify with gravitational duals of quantum critical points. We will do this both for an *ad hoc* Abelian Higgs model and for closely related gravitational Lagrangians arising as consistent truncations of string theory and M-theory. We also compute their frequency-dependent conductivities and find power law behavior at low frequencies.

We will introduce spin-$\frac{1}{2}$ fermions in these domain wall geometries and find continuous bands of fermionic normal modes. These bands can be either partially filled or totally empty and gapped. We will consider fermionic normal modes and correlators in other gravitational backgrounds and find other interesting features. For certain dilatonic black holes in AdS_5 and AdS_4 in the extremal limit, we find isolated fermionic normal modes at zero frequency and finite momentum. We will also find that these dilatonic black holes have linear specific heat at low temperatures, which combined with the previous property makes them an interesting candidate for a gravitational dual of a Fermi liquid.

Finally, we will consider fermion correlators in non-abelian holographic superconductors and find that their spectral function exhibits several interesting features such as support in displaced Dirac cones and an asymmetric distribution of normal modes. We compare these features to similar ones observed in angle resolved photoemission experiments on high T_c superconductors.

Acknowledgements

I owe a huge debt of gratitude to my advisor, Steven S. Gubser, from whom I have learned a tremendous amount during my time at Princeton. The work in this dissertation was only made possible by his guidance and encouragement. He always had time for his students and never failed to have new and interesting projects to work on.

I am also extremely grateful to other faculty at Princeton for their time and patience. Christopher Herzog, Igor Klebanov and Herman Verlinde provided invaluable advice in matters related to physics and more. I also thank Christopher Tully for all his help with my experimental project.

Without the help of my collaborators I would have certainly accomplished much less. Dan Gulotta, Abhi Nellore, Silviu Pufu, Pedro Talavera, and Amos Yarom were also good friends and I owe them a great deal.

There are many other great friends I met while at Princeton to whom I must express my heartfelt gratitude. Aakash Pushp, Andrea Civelli, Charles Mathy, Chris Laumann, Diego Hofman, and Sid Parameswaran made the time I spent at Princeton better in many ways and I thank them for it.

I am also greatly indebted to several people outside Princeton. Without Miguel Costa I would have probably not have come to Princeton in the first place, and I owe him much more besides that.

To my family I owe everything and I cannot thank them enough for all their love and support throughout the years. My father Jaime, my mother Cristina, and my sister Mariana always gave me good advice and were always there when I needed them.

Finally, for all her love and patience and never having given up on me, I thank Tânia. Even across an ocean, you gave me strength and made it all worthwhile.

Contents

List of Figures

List of Tables

Chapter 1

Introduction

The discovery of the gauge-gravity duality [1, 2, 3] was one of the most influential developments to come out of the study of string theory. It continues to have a profound impact on the understanding of both gauge theories and quantum gravity. One of the ramifications of this discovery was that it provides powerful new tools to study quantum field theories in regimes where traditional perturbative methods fail (i.e., in the strong coupling regime). This opens up the exciting possibility of applying these string theoretic methods to the study of real physical systems where strong coupling plays a role. In this dissertation, we will focus on applications of the gauge-gravity duality to condensed matter topics. This is a subject that has already attracted substantial attention (for reviews see [4, 5, 6, 7]). In the remainder of this introductory chapter we will review some relevant aspects of the duality.

1.1 Overview of the gauge-gravity duality

The gauge-gravity duality, also referred to as the gauge-string duality or the AdS/CFT correspondence, in its most general form is the statement that

> *Some quantum field theories (QFTs) are dual to quantum theories of gravity defined in a higher number of dimensions.*

Here by *dual* we mean that the theories are in some sense exactly equivalent and that each of them can, in principle, be used as an alternative formulation of the other, enabling us to compute any physical quantity of interest from the second theory. Since it constitutes a correspondence between theories in defined in different numbers of dimensions, this is often called an *holographic* duality. To those unfamiliar with it, this claim, will seem very surprising. However, although it has not yet been rigorously proven, the duality has passed a wide array of qualitative and quantitive tests and is widely believed to be true. A vast swathe of literature has been devoted to studying implications of the duality from many different points of view.

The claim above is, as it stands, rather vague. To make things more concrete, consider the more specific version of this claim

> $\mathcal{N} = 4$ *supersymmetric* $SU(N_c)$ *Yang-Mills (SYM) is dual to Type IIB string theory on an* $AdS_5 \times S_5$ *background.*

This is the most studied gauge/gravity duality and hence also the best established. Before describing how the duality works out in practice, let us say something about the two theories that participate in it.

The QFT in this case is $\mathcal{N} = 4$ Super-Yang Mills. This is the unique 4-dimensional maximally supersymmetric[1] field theory. The field content of this theory is one gauge field A_μ, 4 spin-$\frac{1}{2}$ fermions λ^a and 6 real scalars X^i, each in the adjoint representation of the $SU(N_c)$ group. The Lagrangian is given by

$$\mathcal{L}_{\text{SYM}} = \frac{1}{g_{\text{YM}}^2} \operatorname{tr} \left(-\frac{1}{4}F^2 - \frac{1}{2}D_\mu X^i D^\mu X^i - \frac{i}{2}\bar{\lambda}^a \not{D} \lambda^a + \frac{1}{2}\sum_{i<j} \left[X^i, X^j\right]^2 + \frac{1}{2}\Gamma^i_{ab}\bar{\lambda}^a \left[X^i, \lambda^b\right] \right) \tag{1.1}$$

In addition to the $SU(N_c)$ gauge symmetry the theory has a $SU(4)$ global symmetry under which the λ^a and X^i transform (with the Γ^i_{ab} an intertwiner of the respective representations). Furthermore, SYM is a conformal field theory (CFT) and therefore has an $SO(4, 2)$ group of symmetries that contains the (3+1)-dimensional the Poincaré group and also includes dilations and special conformal transformations. Note that there are two dimensionless parameters in the theory, the number of colors N_c and the Yang-Mills coupling g_{YM}.

[1] Note that $\mathcal{N}$ refers to the number of supersymmetries the theory has. For four-dimensional theories that do not contain gravity 4 is the maximum amount of supersymmetries.

We are going to be interested in taking the large-N_c limit, and for that purpose it is useful to introduce the 't Hooft coupling $\lambda \equiv g_{\rm YM}^2 N_c$ which should be kept fixed as N_c is taken to infinity to obtain a sensible limit.

Type IIB string theory is a supersymmetric chiral string theory defined in 10 spacetime dimensions. The fundamental objects of the theory are strings, one-dimensional objects that propagate in spacetime and whose action principle dictates the minimization of the area they sweep out in spacetime. In addition to the fundamental strings, the theory also contains Dp-branes, objects which extend in p space dimensions, and exist for p equal to $1, 3, 5, 7$, or 9. The strings can be closed or open, in which case their endpoints are constrained to move on the Dp-branes that are present. The spectrum of excitations of the strings can be organized into an infinite set of fields transforming in representations of the 10-dimensional Lorentz group with masses and spins that grow arbitrarily large. Particularly important is the massless part of this spectrum, which, in the absence of Dp-branes, consists of a graviton $g_{\mu\nu}$, a gravitino ψ^μ, two scalar fields ϕ and C, a dilatino χ, two 2-form fields B_2 and C_2 and a 4-form C_4 with a self dual field strength F_5. In the low energy limit, the massive fields decouple and Type IIB string theory reduces to a theory that only involves these massless fields: Type IIB 10d supergravity. The $AdS_5 \times S_5$ geometry is a classical solution of this low energy theory. The nonzero fields in this background are the metric and the self-dual 5-form, and are given by

$$\begin{aligned} ds^2 &= \left[\frac{r^2}{L^2}\left(-dt^2 + dx_1^2 + dx_2^2 + dx_3^2\right) + \frac{L^2}{r^2} dr^2\right] + L^2 d\Omega_5 \\ F_5 &= \mathcal{F}_5 + *\mathcal{F}_5 \qquad \mathcal{F}_5 = \frac{4r^3}{L^4} dt \wedge dx_1 \wedge dx_2 \wedge dx_3 \wedge dr \,, \end{aligned} \tag{1.2}$$

where $d\Omega_5^2$ is the metric on a unit radius 5-sphere and L is a constant with dimensions of length, the radius of curvature of both factors of the geometry. The term in the square brackets in the first line of (1.2) is the metric of AdS_5 or 5-dimensional Anti de Sitter space. This is a maximally symmetric geometry, with constant negative curvature which is a solution of Einstein's equations with a negative cosmological constant. Its group of isometries is $SO(4,2)$. Since the group of isometries of the S_5 factor is $SO(6)$ (which is isomorphic to $SU(4)$) we see that the 10-dimensional geometry has a $SO(4,2) \otimes SU(4)$ isometry group, precisely matching the continuous global symmetries of $\mathcal{N} = 4$ SYM.

In addition to the length scale L that appears in (1.2), there are is one more dimensionful parameter in the theory: the Regge slope α' which determines the string tension and hence the mass of the massive part of the string spectrum. These parameters are related to the gauge-theory parameter λ by

$$\frac{L^4}{\alpha'^2} = \lambda \,. \tag{1.3}$$

The duality between SYM and Type IIB string theory is a statement of the equality of the partition function of the two theories,

$$Z_{\text{SYM}} = Z_{\text{string}} \,. \tag{1.4}$$

This equality holds not only for the vacuum partition functions but also in the presence of sources for all the operators in the theory and therefore encapsulates the fact that all the physics of one theory can be expressed in terms of that of the other. Of course, the two theories have distinct field contents and some care must be taken in interpreting this statement, and to this purpose a dictionary relating fields of SYM to those of string theory has been developed.

If one takes the large-N_c limit something remarkable happens on the the string side of the duality: the theory becomes classical, i.e., the string partition function can be approximated by its saddle point:

$$Z_{\text{SYM}} = Z_{\text{string}} \approx e^{iS_{\text{on-shell}}} \qquad (N_c \to \infty) \,. \tag{1.5}$$

This a tremendous simplification, and a further one happens if one also takes $\lambda \to \infty$ simultaneously. From (1.3), this means that α' will be very small relatively to L, which allows us to ignore the effects of massive string states (their mass is $\propto 1/\sqrt{\alpha'}$). Therefore, in the $N_c \to \infty$, $\lambda \to +\infty$ string theory reduces to classical supergravity. Computational methods for classical supergravity are much more developed than those for strongly coupled gauge-theory, and therefore the gauge-gravity duality provides us with powerful new tools to study the latter.

$\mathcal{N} = 4$ is SYM is not the only theory with a known gravity dual - the correspondence has been generalized in many different ways. A simple generalization is that duality accommodates a simple way of deforming $\mathcal{N} = 4$ by appropriate gauge-invariant operators contained in the theory itself (a procedure we will outline in section 1.2). In a different direction, there are many known dualities between field theories and string theory on geometries of the type $AdS_p \times M_{10-p}$, where M_{10-p} is an appropriate compact manifold (with isometry group equal to the group of global symmetries of the dual field theory) and AdS_p is p-dimensional Anti de Sitter space. Its metric is a simple generalization of the first factor of (1.2):

$$ds^2 = \frac{r^2}{L^2}\left(-dt^2 + \sum_{i=1}^{p-2} dx_i^2\right) + \frac{L^2}{r^2} dr^2 \,. \tag{1.6}$$

This metric has $SO(p-1,2)$ isometry group, which is the same as the conformal group in $p-1$ dimensions. The field theory dual to the $AdS_p \times M_{10-p}$ will therefore be a conformal field theory in $p-1$ dimensions, that for heuristic purposes can be thought of living in the boundary of the AdS_p space at $r = +\infty$.

A further possibility is gravity duals where the geometry of the product type $AdS_p \times M_{11-p}$. In this case the full geometry is 11-dimensional and the quantum gravity theory that one should have in mind in this background is M-theory rather than string theory. The low energy theory on the gravity side will be given by 11-dimensional supergravity. The canonical example corresponds to $p = 4$, $M_7 = S_7$ and in this case the dual gauge theory is a supersymmetric Chern-Simons $(2+1)$-dimensional conformal field theory, often referred to as ABJM theory [8].

In practice, we do not even need to consider a the full 10-dimensional (or 11-dimensional) gravity theory. We can exploit the product form of the full metric to Kaluza-Klein reduce onto the AdS_p factor, i.e., write an arbitrary 10-dimensional (11-dimensional) field as an infinite sum over p-dimensional fields on AdS_p times harmonics of the M_{10-p} (M_{11-p}). Having done this, we will obtain a p-dimensional theory that is *completely equivalent* to its higher dimensional uplift. Of course, the lower dimensional theory will have an infinite number of fields (corresponding to the infinite number of harmonics of the M_{10-p} manifold). However, we will be often interested in describing situations where only a finite number of these lower dimensional fields are nonzero and can for this purpose use effective p-dimensional actions with a finite number of fields. Through the course of this dissertation we will be concerned with studying gravity side actions of the type

$$S = \frac{1}{2\kappa^2}\int d^p x\sqrt{-g}\,(R - 2\Lambda + \mathcal{L}_{\text{matter}})\ , \tag{1.7}$$

where R is the Ricci scalar and Λ is the cosmological constant[2] and $\mathcal{L}_{\text{matter}}$ is a lagrangian that can involve different types of matter fields but always a finite number of them. In the course of this dissertation we will have occasion to consider $\mathcal{L}_{\text{matter}}$ involving abelian gauge fields and scalar fields (Chapters 2,3,4, and 5), non-Abelian gauge fields (Chapter 6) and spin-$\frac{1}{2}$ fermions (Chapters 4,5, and 6). We will be mostly focusing on $p = 4$, and therefore on gravity duals to $(2+1)$-dimensional field theories (in Chapter 4 we will also consider a $p = 5$ geometry).

Note that actions of the type (1.7) can, as we have just argued, be derived rigorously from dimensionally reducing an higher-dimensional gravity action that has a known gauge-theory dual. If this is is done, the p-dimensional classical solutions of the lower dimensional action can always be uplifted to solutions of the higher dimensional theory. However, an alternative useful approach is to simply postulate an *ad hoc* action of the type in (1.7) and study its properties (this is the approach we will take in Chapters 2, 5, and 6 and in part in Chapter 4). This allows us to study simpler gravity Langrangians and impose whatever features are necessary to obtain interesting physics. The price of this simplicity and flexibility is however that in these *ad hoc* phenomenological models, much less information about the gauge-theory dual is available.

1.2 Field theory correlators from gravity duals

Let us now be more concrete and sketch a simple calculation using a gravity dual. Let us take $p = 4$ and assume the background geometry is given by AdS_4. Consider the action

[2]We should take $\Lambda = -(p-1)(p-2)/(2L^2)$ to obtain an asymptotically AdS_p geometry with radius L.

(1.7) with $\mathcal{L}_{\text{matter}}$ given by

$$\mathcal{L}_{\text{matter}} = -\frac{1}{2}\partial_\mu\phi\partial^\mu\phi - \frac{1}{2}m^2\phi^2\,, \tag{1.8}$$

i.e., that for a simple real scalar ϕ with mass m. In the context of the gauge-gravity duality, ϕ is a gravity side field that will be dual to some gauge-theory side operator $\mathcal{O}$. Without some embedding of the action corresponding to (1.8) in higher dimensional action with a known gravity dual, there is no way of knowing precisely what this is operator is. Nevertheless, (1.8) provides us with enough information to compute correlation functions of $\mathcal{O}$. To this end, let us be a little more explicit on the meaning of (1.5). If we are only turning on a source for operator $\mathcal{O}$ then (1.5) can be written as

$$Z^{\text{QFT}}_{\phi_0} \equiv \left\langle e^{i\int d^3x\,\phi_0(x^m)\mathcal{O}(x^m)}\right\rangle_{\text{QFT}} = e^{iS_{\text{gravity}}}\Big|_{\lim_{r\to+\infty}\phi(x^m,r)=\phi_0(x^m)}\,. \tag{1.9}$$

Here S_{gravity} should be understood as (1.7) with $\mathcal{L}_{\text{matter}}$ given by (1.8) and evaluated on shell with the boundary condition on ϕ given above. Note that ϕ_0 is 3-dimensional classical field (it does not have an r dependence) that acts as a source for the operator $\mathcal{O}(x^m)$. According to the AdS/CFT dictionary, we should identify it with the limit of the 4-dimensional ϕ field as r becomes large. From (1.9) it is clear how to compute correlators: we should simply evaluate the on-shell action and take functional derivatives with respect to ϕ_0:

$$G_{\mathcal{O}}(x_1^m, x_2^m) \equiv \langle\mathcal{O}(x_1^m)\mathcal{O}(x_2^m)\rangle = \frac{\delta S_{\text{gravity}}}{\delta\phi_0(x_1^m)\delta\phi_0(x_2^m)}\Big|_{\phi_0=0}\,. \tag{1.10}$$

Let us now see how this works in more detail. In practice, it is useful to exploit the translation symmetry in the x^m and working in Fourier space. This can be done by setting

$$\phi(x^m, r) = e^{-iwt+ik_1x^1+ik_2x^2}\tilde{\phi}(r)\,. \tag{1.11}$$

and taking functional derivatives with respect to $\tilde{\phi}$ to obtain the correlator in Fourier space $G(k^m)$.

In order to extremize (1.8), $\phi(r)$ must be a solution of the Klein-Gordon equation $(\Box - m^2)\phi = 0$. This leads to the following equation for $\tilde{\phi}(r)$

$$r^2\tilde{\phi}'' + 4r\tilde{\phi}' - \left(m^2L^2 + \frac{L^4k^2}{r^2}\right)\tilde{\phi} = 0 \qquad k^2 \equiv -\omega^2 + k_1^2 + k^2\,, \tag{1.12}$$

where the prime denotes the derivative with respect to r. The generic solution to (1.12) is given by

$$\tilde{\phi}(r) = U r^{-\frac{3}{2}} K_{\Delta-\frac{3}{2}}\left(\frac{L^2 k}{r}\right) + V r^{-\frac{3}{2}} I_{\Delta-\frac{3}{2}}\left(\frac{L^2 k}{r}\right) \tag{1.13}$$

where U and V are arbitrary constants, K and I are modified Bessel functions of the second and first kinds respectively, and we have defined

$$\Delta \equiv \frac{3}{2} + \sqrt{\frac{9}{4} + m^2 L^2}\,. \tag{1.14}$$

If we expand (1.13) for large r, we obtain

$$\tilde{\phi} \approx A r^{\Delta-3} + B r^{-\Delta}\,, \tag{1.15}$$

where A and B are constants that can easily be written in terms of U and V. From (1.14), we see that if $m^2 \geq 0$ then $\Delta \geq 3$. Lower values of Δ are possible even though this implies that the scalar must be tachyonic, as in AdS spaces the negative curvature can stabilize tachyons, provided the squared mass is not too negative. The condition for no instability is the *Breitenlohner-Freedman bound* [9, 10] and corresponds to demanding that Δ in (1.14) be real, i.e, to imposing $m^2 L^2 > -9/4$. Provided this Breitenlohner-Freedman bound is satisfied, we see that $\Delta \geq \frac{3}{2}$ and that the A term in (1.15) dominates for sufficiently large r_0. This term, and therefore $\tilde{\phi}(r)$, does not in general approach a constant as $r \to +\infty$ so it is not clear how to identify $\tilde{\phi}_0(k^m)$ (by which we mean the Fourier transform of $\phi_0(x^m)$). The correct procedure is to identify $\tilde{\phi}_0$ with $r_0^{3-\Delta}\tilde{\phi}(r_0)$ for some large but finite r_0, take functional derivatives and at the end of the calculation send $r_0 \to \infty$ (or, in other words, to identify $\tilde{\phi}_0$ with A). When doing this we should also restrict the range of integration when computing the on-shell action, i.e.,

$$S_{\text{gravity}} = -\frac{1}{2\kappa^2}\int_0^{r_0} dr \int d^3x \sqrt{-g}\left(\partial_\mu \phi \partial^\mu \phi + m^2 \phi^2\right)\,, \tag{1.16}$$

where we have only included the contribution from $\mathcal{L}_{\text{matter}}$ because to the order we will be working with the scalar field ϕ does not back react on the geometry and therefore the Einstein-Hilbert term does not depend on ϕ_0.

Let us compute the first functional derivative. After integrating by parts, the variation of the action (1.16) can be written

$$\delta S_{\text{gravity}} = \frac{1}{2\kappa^2}\left[\int_0^{r_0} dr \int d^3x\sqrt{-g}\,\delta\phi\,\left(\Box - m^2\right)\phi + \int d^3x\,\delta\phi\,\Pi_\phi(x^m, r^0)\right], \tag{1.17}$$

with Π_ϕ the momentum conjugate to ϕ with respect to the r coordinate, i.e.,

$$\Pi_\phi = \frac{\delta\mathcal{L}_{\text{matter}}}{\delta\partial_r\phi} = \sqrt{-g}g^{rr}\partial_r\phi = \frac{r^4}{L^4}\partial_r\phi\,. \tag{1.18}$$

Now, since we are only interested in evaluating (1.17) on-shell, the first term will vanish identically since it is proportional to the equations of motion. We conclude that

$$\frac{\delta S_{\text{gravity}}}{\delta\phi_0} = r_0^{\Delta-3}\frac{\delta S_{\text{gravity}}}{\delta\phi} = \frac{1}{2\kappa^2}r_0^{\Delta-3}\Pi_\phi(r^0)\,. \tag{1.19}$$

To obtain the correlator, we just need to take a further functional derivative, obtaining the final expression

$$G(k^m) = \lim_{r_0\to+\infty}\frac{1}{2\kappa^2}r_0^{\Delta-3}\frac{\delta\Pi_\phi}{\delta\phi_0}\,. \tag{1.20}$$

If we now extract the finite part of the right hand side we obtain

$$G(k^m) = \frac{1}{2\kappa^2}(2\Delta-3)\frac{\delta B(k^m)}{\delta A(k^m)}\,. \tag{1.21}$$

Note that in writing (1.21) we droped terms in (1.20) that diverge in the limit $r_0 \to +\infty$ and kept only the finite part. This can be justified more rigorously by a procedure termed *holographic renormalization* in which counterterms localized at $r = r_0$ are added to the gravity action in order to cancel these divergences.

Until now we have not imposed any relationship between A and B - they are simply the two independent integration constants of a second order differential equation - and the meaning of (1.21) is not clear. To see where the relationship between A and B originates, consider first the case $k^2 > 0$ (i.e., we are outside the light-cone). It is easily seen that the $I_{\Delta-3/2}$ term in (1.13) diverges exponentially as $r \to 0$ and we must therefore set $V = 0$ to obtain well behaved $\tilde{\phi}$. It is then a simple exercise to use the large r expansion of $K_{\Delta-3/2}(L^2k/r)$ to write B in terms of A and obtain

$$G(k^m) \propto \frac{B}{A} \propto k^{2\Delta-3}\,. \tag{1.22}$$

By Fourier transforming (1.22), we obtain the real space correlator. A simple variable change will show that this will scale as

$$G(x^m) = \langle \mathcal{O}(x^m)\mathcal{O}(0)\rangle \propto \frac{1}{x^{2\Delta}}\,, \tag{1.23}$$

i.e., $\mathcal{O}$ is an operator with conformal dimension Δ, justifying our notation.

Consider now the case $k^2 < 0$. In this case, the generic solution (1.13) is oscillatory as $r \to 0$, and $\tilde{\phi}$ will always be well behaved, seeming to imply an ambiguity for the correlator. This is related to the fact the we are computing correlators for a theory with Lorentzian signature and there are therefore different useful definitions of the correlator: Feynman, retarded and advanced. Formula (1.21) can reproduce each of these different correlators, depending on the boundary conditions imposed as $r \to 0$. For instance, to obtain the retarded correlator we should impose that $\tilde{\phi}$ is a purely infalling wave as $r \to 0$ [11, 12]. Equivalently, we could use the usual $i\epsilon$ prescription for the retarded correlator, i.e., do the calculation with the replacement $\omega \to \omega + i\epsilon$ with ϵ a small positive number. By demanding regularity for nonzero ϵ and taking ϵ to zero at the end of the calculation, we will obtain the same results as from the purely infalling prescription. The other correlators can be obtained by the appropriate usual $i\epsilon$ prescriptions.

We have described a method to compute correlators of scalar operators using gravity duals for a simple AdS_4 background. This method generalizes straightforwardly for fields of higher spin and also to different background geometries provided that they are asymptotically AdS. The general strategy is the same in all cases:

1. Solve the classical equations of motion for the field, imposing appropriate boundary conditions in the interior of the manifold (i.e., regularity or purely infalling b.c.). Numerical methods might be necessary for this step in general.

2. Regulate the on-shell action by introducing a large r cut off r_0 and evaluate it with the result from the previous step.

3. Take functional derivatives and extract the finite part as r_0 is taken to infinity.

1.3 Gravity duals at finite temperature and chemical potential

To have any hope of applying the gauge-gravity duality to condensed matter topics it is essential to be able to study gravity duals in canonical and macro-canonical ensemble. Happily, this is something the duality accommodates in a straightforward way. To turn on a finite temperature, we should consider geometries that are asymptotically AdS_4 but that have an event horizon in the interior. More explicitly, let us consider geometries of the form

$$ds^2 = e^{2A(r)}\left(-h(r)dt^2 + dx_1^2 + dx_2^2\right) + e^{-2A(r)}\frac{dr^2}{h(r)}\,. \tag{1.24}$$

The condition that this geometry is asymptotically AdS_4 means that for large r it should approach the AdS_4 metric, i.e, $A \approx \log(r/L)$, $h \approx 1$. We also demand that the metric is an extremum of an action of the type (1.7), i.e., it must be a solution of Einstein's equations

$$G_{\mu\nu} + \Lambda g_{\mu\nu} = \frac{1}{2}T_{\mu\nu} \qquad G_{\mu\nu} = R_{\mu\nu} - \frac{1}{2}Rg_{\mu\nu}\,, \tag{1.25}$$

where $T_{\mu\nu} = -2\delta\mathcal{L}_{\text{matter}}/\delta g^{\mu\nu} + g_{\mu\nu}\mathcal{L}_{\text{matter}}$ is the bulk stress-energy tensor. Additionally, we must impose the equations of motion resulting from varying the action with respect to each matter field.

If we take $\mathcal{L}_{\text{matter}} = 0$ then there is a unique asymptotically AdS family of solutions, AdS-Schwarzschild, which corresponds to choice of metric coefficients

$$A = \log\frac{r}{L}, \qquad h = 1 - \frac{r_H^3}{r^3}\,. \tag{1.26}$$

Note that this geometry has an event horizon at the zero of h, $r = r_H$. This horizon has an associated Bekenstein-Hawking entropy and temperature, which will equal the temperature and entropy of the quantum field theory dual. The entropy is simply proportional to the area of the event horizon. Since this is infinite, it is more useful to consider the entropy density s per unit field theory area, and the result is

$$s = \frac{2\pi}{\kappa^2}\frac{A_h}{V_2} = \frac{2\pi}{\kappa^2}e^{2A(r_H)} = \frac{2\pi}{L^2\kappa^2}r_H^2\,, \tag{1.27}$$

where the last expression only applies to AdS-Schwarzschild. To compute the temperature of the background, we can Wick rotate to Euclidean time (i.e., send $t \to i\tau$) and impose periodicity in the Euclidean time, with period equal to the inverse temperature. When this procedure is applied to the metric (1.24), one finds that the resulting geometry will have a conical singularity at $r = r_H$, except for a special value of this period. This sets the temperature to be

$$T = \frac{1}{4\pi} e^{2A(r_H)} |h'(r_H)| = \frac{3}{4\pi} \frac{r_H}{L} \,. \tag{1.28}$$

Comparing (1.28) and (1.27), one sees that $s \propto T^2$, which is precisely what is expected for a conformal field theory in $(2+1)$ dimensions.

To introduce a chemical potential in relativistic field theory, the theory must posses a global symmetry and an associated conserved current J^m. Turning on a chemical potential μ is then equivalent to deforming the Lagrangian of the QFT by the time component of the conserved current J^t, i.e., sending

$$\mathcal{L}_{QFT} \to \mathcal{L}_{QFT} - \mu J^t \,. \tag{1.29}$$

The gravity dual of a conserved current J^m is a gauge field A^μ. The gauge symmetry of A^μ is the expression on the gravity side of the global symmetry associated to J^m on the field theory side. The minimal gravity side action that incorporates a gauge field is given by (1.7) with

$$\mathcal{L}_{\text{matter}} = -\frac{1}{4} F_{\mu\nu} F^{\mu\nu} , \qquad F_{\mu\nu} = \partial_\mu A_\nu - \partial_\nu A_\mu \,. \tag{1.30}$$

As before, one can consider more general $\mathcal{L}_{\text{matter}}$ that contain other fields but his minimal case has the virtual of leading to analytical solutions and illustrating all the relevant features. The background must obey Einstein's equations (1.25) with

$$T_{\mu\nu} = F_{\mu\alpha} F^{\alpha}{}_{\nu} - \frac{1}{4} F^2 g_{\mu\nu} \,, \tag{1.31}$$

and must also solve Maxwell's equation $\nabla_\mu F^{\mu\nu} = 0$. If we take the ansatz (1.24) for the metric and take the gauge field to be a of the form $A_\mu dx^\mu = \Phi(r) dt$, the asymptotically AdS solutions are of the form:

$$A = \log\left(\frac{r}{L}\right) \qquad h = 1 - m/r^3 + \frac{1}{4}\frac{q^2 L^2}{r^4} \qquad \Phi = \frac{q}{r} - \frac{q}{r_H} \tag{1.32}$$

where m and q are parameters that set the mass and charge of the black hole and r_H is the largest zero of $h(r)$ (we can easily solve for r_H explicitly but the expression is not particularly illuminating). This blackhole is the asymptotically AdS generalization of the Reissner-Nördstrom blackhole and is often referred to as the Reissner-Nördstrom-AdS (RNAdS) metric. It would seem that we can add an arbitrary constant to Φ since this a gauge transformation that does not affect the equations of motion. However, since $h(r)$ has a zero at $r = r_H$, $\Phi(r)dt$ is not a well defined 1-form at $r = r_H$ unless $\Phi(r_H) = 0$, fixing the constant in (1.32). Applying the formulae (1.28) and (1.27) we obtain

$$T_{\rm RN} = \frac{12r_H^4 - q^2L^2}{16\pi r_H^3} \qquad s_{\rm RN} = \frac{2\pi r_H^2}{L^2\kappa^2}\,, \tag{1.33}$$

where we have eliminated m in favor of r_H by using the condition $h(r_H) = 0$.

To identify the chemical potential μ and its thermodynamical conjugate the charge density ρ, we need to examine the behavior of $A_t = \Phi(r)$ for large r. The situation is entirely analogous to the case of the scalar operators discussed in section 1.2: by turning on $\Phi(r)$ we are deforming the dual field theory with respect to the operator dual to it (i.e, J_t) with the coefficient of the deformation (i.e., μ) being equal to the limiting value of $\Phi(r)$ near the boundary,[3] i.e., $\mu = \lim_{r\to+\infty}\Phi(r)/L$. To obtain the charge density $\rho = \langle J_t\rangle$ we should evaluate the on-shell action and take a μ derivative. If we do this for the RNAdS background (1.32), we obtain

$$\mu_{\rm RN} = -\frac{q}{Lr_H} \qquad \rho_{\rm RN} = -\frac{Q}{2L\kappa^2}\,. \tag{1.34}$$

We can combine (1.33) and (1.34) to write an equation of state for RNAdS that does not involve q or r_H:

$$4L\pi T s^{\frac{3}{2}} = 3s^2 - 4\pi^2\rho^2\,. \tag{1.35}$$

From this equation of state we immediately see that if we set the temperature to zero, then $s = 2\pi\rho/\sqrt{3}$, i.e., RNAdS has finite entropy density at zero temperature. We shall have more to say about this in Chapter 4, but for now note that this zero temperature geometry

[3]Note that we have introduced a factor of $1/L$ in the formula for μ. This is purely conventional as long as it is done consistently and was done so μ has the dimensions of energy.

corresponds to setting $m = 4r_H^3$, $q = \sqrt{6}r_H^2/L$ and that for these value of the parameters the near horizon geometry is $AdS_2 \times \mathbf{R}^2$, i.e.,

$$ds^2_{\text{nearhorizon}} \approx -\frac{\tilde{r}^2}{\tilde{L}^2}dt^2 + \frac{\tilde{L}^2}{\tilde{r}^2}d\tilde{r}^2 + \frac{r_H^2}{L^2}\left(dx_1^2 + dx_2^2\right) \qquad \tilde{L} \equiv \frac{L}{\sqrt{6}}\,, \tag{1.36}$$

where $\tilde{r} \equiv r - r_H$. For large r, it of course asymptotically AdS_4 and this zero temperature geometry can therefore be thought of as an AdS_4 to $AdS_2 \times \mathbf{R}^2$ domain wall. Through the course of this dissertation we will find other types of domain wall arising as interesting zero-temperature limits of gravitational backgrounds.

1.4 Holographic superconductors

We are now ready to introduce what has so far been one of the main topics of interest in condensed matter applications of the gauge-gravity dualities: holographic models of superconductivity. Superconductivity can be thought of as arising from a spontaneously broken gauge symmetry [13]. The gauge symmetry in question is, of course, the $U(1)$ electromagnetic gauge symmetry and it is broken by charged operator gaining an expectation value (in conventional superconductors this operator is a Cooper pair, a bilinear in the electron creation operator). This results in an effective mass for the photon, explaining much of the phenomenology of superconductors.

The simplest gravity dual that captures similar physics is the holographic Abelian Higgs model [14, 15]. This corresponds to taking the action (1.7) with

$$\mathcal{L}_{\text{matter}} = -\frac{1}{4}F_{\mu\nu}^2 - |D_\mu\psi|^2 - V(|\psi|) \qquad D_\mu\psi = \partial_\mu\psi - iqA_\mu\psi \tag{1.37}$$

where ψ is a complex scalar with so far arbitrary potential $V(|\psi|)$. Note that (1.37) is essentially a relativistic version of the Landau-Ginzburg free energy, and it is therefore not surprising that will encode some version of superconductivity. There are however, important differences. Firstly, in this context we are allowing a (asymptotically AdS) curved geometry that is back-reacted upon by the gauge field and complex scalar. Secondly, we are interpreting extrema of (1.37) in the context of the dual field theory. This in particular means that the $U(1)$ gauge symmetry manifest in (1.37) leads only to a global $U(1)$ symmetry in the field theory dual. Therefore, (1.37) can be more properly thought of as holographic model of *superfluidity* rather than superconductivity. However nothing prevents us from *a posteriori* gauging the $U(1)$ global symmetry of the field theory. In fact, even in conventional theories of superconductivity, such as BCS theory, there are no dynamical photons (i.e., a global rather than gauge $U(1)$ symmetry is studied).

As we have reviewed, Lagrangians like (1.37) allow asymptotically AdS charged black-hole solutions that are dual to field theory configurations at finite temperature and chemical potential. In particular, and provided $V'(0)$, (1.37) always has RNAdS extrema that correspond simply to setting $\psi = 0$. Additionally, (1.37) can have blackhole solutions that can be described as superconducting. These are solutions for which the gauge symmetry is broken, which will happen if $\psi(r)$ is nonzero, i.e., if the blackhole has charged scalar hair. The dual field theory interpretation of this is that the charged operator dual to ψ has gained an expectation value and broken the global symmetry of the theory.

Let us review how these superconducting blackhole solutions can be found in a little more detail. The equations of motion following from (1.7) and (1.37), are, once more, Einstein's equations (1.25) with

$$T_{\mu\nu} = F_{\mu\alpha}F^{\alpha}{}_{\nu} + 2D_{\mu}\psi^{*}D_{\nu}\psi + g_{\mu\nu}\mathcal{L}_{\text{matter}} \tag{1.38}$$

and the Maxwell and scalar equations

$$\begin{aligned} \nabla_{\mu}F^{\mu\nu} &= iq\left(\psi\partial_{\nu}\psi^{*} - \psi^{*}\partial_{\nu}\psi\right) \\ D^{\mu}D_{\mu}\psi &= V'(|\psi|)\,. \end{aligned} \tag{1.39}$$

We again take the metric ansatz (1.24) and the gauge field to be of the form $A_{\mu}dx^{\mu} = \Phi(r)dt$ a take $\psi = \psi(r)$. The equations of motion (1.39) then imply that the phase of the complex scalar ψ is constant, and by a gauge transformation we can take therefore take ψ to be real. Given this ansatz, the equations of motion become a set of coupled nonlinear ordinary differential equations which can be reduced to

$$\begin{aligned} A'' - A'^2 + \frac{1}{2}\psi'^2 + \frac{q^2\Phi^2\psi^2}{2h^2} &= 0 \\ A'h' + \frac{1}{2}e^{2A}V(\psi) - \frac{q^2\Phi^2\psi^2}{2h} + \frac{1}{4}e^{-2A}\phi'^2 + \frac{1}{2}h\left(6A'^2 - \psi'^2\right) &= 0 \\ \psi'' + \left(2A' + \frac{h'}{h}\right)\psi' + \frac{q^2\phi^2\psi}{h^2} - \frac{e^{2A}V'(\psi)}{2h} &= 0 \\ \phi'' - \frac{2q^2e^{2A}\Phi\psi^2}{h} &= 0\,. \end{aligned} \tag{1.40}$$

These equations do not generically have analytical solutions and recourse recourse to numerical methods is necessary in order to solve them.

Let us now discuss the boundary conditions. For large r, we wish the geometry to be asymptotically AdS, i.e., that $A \to \log \frac{r}{L}$ and $h \to 1$. This fixes the large r behavior of $\Phi(r)$ to be $\Phi \approx C_1 + C_2/r$ and we place no restrictions on C_1 (which we recall is related to the chemical potential) or C_2 (which will proportional to the charge density). The generic large r behavior of ψ will be, as discussed in section 1.2,

$$\psi \approx Ar^{\Delta-3} + Br^{-\Delta} \qquad \Delta = \frac{3}{2} + \sqrt{\frac{9}{4} + L^2V''(0)}\,. \tag{1.41}$$

We remind the reader that allowing A to be nonzero would correspond to turning on a deformation with respect the charged operator dual to ψ. This would mean that we would be breaking the $U(1)$ symmetry *explicitly* by this deformation. Since we are interested in studying spontaneously broken symmetry we will demand that $A = 0$ and allow only nonzero B.

We also wish the geometry to exhibit an event horizon, i.e., a value r_H of r such that $h(r_H) = 0$. To have a well defined gauge field we will also demand that $\Phi(r_H) = 0$. As for A and ψ we merely demand that they not diverge as $r \to r_H$.

We thus have boundary conditions both at $r = r_H$ and $r = +\infty$ and are therefore led to a boundary value problem. This can be solved numerically using a shooting method, and superconducting blackhole solutions can in this way be found, at least for appropriate choices of $V(\psi)$ and q.

Let us now focus on a particularly simple potential, the quadratic $V(|\psi|) = m^2|\psi|^2$. Even with this simple potential which lacks secondary extrema, the Abelian Higgs model

(1.37) will have a preferred superconducting phase at low temperatures for appropriate value of m and q. Furthermore, the RNAdS solution of (1.37) will be unstable and want to become superconducting. To see this consider the zero temperature limit of the RNAdS blackhole, which has we have reviewed at the end of section 1.3, is domain wall interpolating between AdS_4 and an $AdS_2 \times \mathbf{R}^2$ near horizon region. The scalar ψ leads to no instability in the AdS_4 large r region provided m^2 obeys the AdS_4 Breitenlohner-Freedman bound, i.e, $m^2 L^2 > -9/4$, which we will assume to be the case. However, in the AdS_2 region, the scalar has an effective mass to which the gauge field contributes given by

$$m_{\text{near}}^2 = \lim_{r \to r_H} m^2 + q^2 g^{tt}(r) \Phi(r)^2 = m^2 - 2q^2 \,. \tag{1.42}$$

This leads to violation of the AdS_2 Breitenlohner-Freedman bound, and hence an instability, whenever

$$m_{\text{near}}^2 \tilde{L}^2 < -\frac{1}{4} \,, \tag{1.43}$$

where $\tilde{L}$ is given by (1.36). This can be rewritten purely in terms of quantities in the Lagrangian as

$$m^2 L^2 - 2q^2 L^2 < -\frac{3}{2} \,, \tag{1.44}$$

which gives a sufficient condition for RNAdS to be unstable. Note that large enough charges q lead to a superconducting instability.

1.5 Outline of dissertation

The rest of this dissertation is organized as follows. In Chapter 2, which is based on [16], we will describe a zero temperature gravitational background that is an extremum of the holographic Abelian Higgs model. This background has properties that will lead us to identify it with the gravitational dual of a quantum critical point. It is also a zero temperature limit of the finite temperature holographic superconductor solutions of the same model. In Chapter 3, which is based on [17], we will discuss zero temperature gravitational backgrounds similar to the ones discussed in Chapter 2 but this time arising as extrema of gravitational actions derived from string theory and M-theory constructions, rather than from and *ad hoc* phenomenological action. Afterwards, in Chapter 4, which was based on [18], we will discuss some interesting black holes with uncharged scalar hair, arising from string theory and M-theory constructions. We will be particularly interested in their thermodynamical properties and in the spectrum of fermionic fields in these backgrounds. In Chapter 5, which was based on [19], we will again consider the spectrum of fermionic fields but this time in the zero temperature limit of holographic superconductors discussed in Chapters 2 and 3. In Chapter 6, which is based on [20], we will be concerned with some properties of p-wave holographic superconductors including, once more, the spectrum of fermionic fields in these backgrounds. We will find some interesting points of contact with non-conventional superconductors. Finally, in Chapter 7 we present some concluding remarks.

Chapter 2

The gravity dual to a quantum critical point with spontaneous symmetry breaking

In [21, 22, 23], it was proposed that AdS_4 black holes could be compared to the pseudogap state of high T_c materials, along the lines of the gauge-string duality [1, 2, 3]. This proposal hinges on the hypothesis that the properties of the pseudogap are largely controlled by a quantum critical point. A quantum critical point is a phase transition that occurs at zero temperature and is driven by quantum rather than thermal fluctuations. An example is the Bose-Hubbard model in $2+1$ dimensions, where there are quantum critical points with relativistic conformal symmetry in the plane parametrized by the hopping matrix element and the chemical potential (with the on-site repulsion held fixed) [24].

It is clearly desirable to understand better the general proposal that an AdS_4 vacuum could describe a quantum critical point. For a system to exhibit quantum critical behavior, it must have massless excitations. That usually means a linear dispersion relation, with some characteristic speed v less than the speed of light, and an associated Lorentz group. Quantum criticality is often (though not necessarily) characterized by relativistic conformal symmetry, which is an enlargement of the Lorentz group: for example, from $SO(2,1)$ to

$SO(3,2)$ for theories in two plus one dimensions. And $SO(3,2)$ is the isometry group of AdS_4. Symmetries of a quantum critical point are emergent in the sense that they characterize the infrared (IR) physics of a medium.

Consider the line element

$$ds^2 = e^{2A}(-hdt^2 + dx^2 + dy^2) + \frac{dr^2}{h}\,, \tag{2.1}$$

where A and h are functions of r, which encodes energy scale in the dual field theory.[1] The effective speed of transmission of signals in the field theory depends on scale: it is the coordinate speed dx/dt corresponding to a null vector $v^\mu = (1, \sqrt{h(r)}, 0, 0)$. That is,

$$v_{\rm eff}(r) = \sqrt{h(r)}\,. \tag{2.2}$$

Although the value of $v_{\rm eff}(r)$ can be changed by scaling t and/or x, ratios of $v_{\rm eff}(r)$ at different values of r are diffeomorphism-invariant.

In order to have $SO(2,1)$ Lorentz symmetry emerge in the infrared, one needs h to approach a constant in the region where $A \to -\infty$. (This region is generally understood to correspond to infrared physics in a gravity dual.) In order for $SO(3,2)$ conformal symmetry to emerge, one must also have A approach a linear function of r in the infrared region, so that the geometry is asymptotically AdS_4. Likewise, in the ultraviolet (UV) region, where $A \to +\infty$, Lorentz symmetry arises if $h \to$ constant, and conformal symmetry arises if $h \to$ constant and A is asymptotically linear. Thus we may envision domain wall geometries, where an ultraviolet and infrared geometry, each possessing Lorentzian or conformal symmetry, are separated by a finite region possessing neither. The UV and IR Lorentz groups (or conformal groups) differ because they are characterized by different values of $v_{\rm eff}$. Using the null energy condition, we will show that $v_{\rm eff}$ is never greater in the infrared than it is in the ultraviolet.

For definiteness, we will focus on an example where there is conformal invariance both in the ultraviolet and in the infrared. The action we are going to study is the one proposed

[1] Note that this metric is equivalent to the metric (1.24) by a redefinition of the r coordinate. In the present Chapter we prefer to use (2.1) as it will prove more convenient for numerical purposes.

in [14] for describing black holes that superconduct at finite temperature:

$$S = \int d^4x \sqrt{g} \left[R - \frac{1}{4} F_{\mu\nu}^2 - |\partial_\mu \psi - iqA_\mu \psi|^2 - V(\psi) \right] \tag{2.3}$$

where $V(\psi)$ depends only on $|\psi|$. Crucially, we assume that $V(\psi)$ has a negative local maximum at $\psi = 0$ and a gauge-equivalent family of minima at some value $|\psi| = \psi_{\text{IR}}$. The simplest example of a suitable potential is

$$V(\psi) = -\frac{6}{L^2} + m^2 |\psi|^2 + \frac{u}{2} |\psi|^4 \,, \tag{2.4}$$

where $m^2 < 0$ and $u > 0$. Then

$$\psi_{\text{IR}} = \sqrt{\frac{-m^2}{u}} \,. \tag{2.5}$$

We can choose coordinates such that the infrared limit of the metric is, call it AdS_{IR}, is

$$ds_{\text{IR}}^2 = e^{2r/L_{\text{IR}}}(-dt^2 + dx^2 + dy^2) + dr^2 \,, \tag{2.6}$$

where L_{IR} is defined through the equation

$$-\frac{6}{L_{\text{IR}}^2} = V(\psi_{\text{IR}}) \,. \tag{2.7}$$

We need to deform AdS_{IR} at large r in order to get it to match onto the ultraviolet geometry, call it AdS_{UV}. This could be done just with an r dependent profile $\psi(r)$, but then the $SO(2,1)$ symmetry acting on (t, x, y) would remain unbroken. To break it without breaking the $SO(2)$ subgroup acting on (x, y), we have to turn on the t component of the gauge field. The dual statement is that a quantum critical point whose characteristic velocity is less than the speed of light requires the presence of matter. We set $A_\mu dx^\mu = \Phi dt$ for some $\Phi(r)$, which must vanish as $r \to -\infty$ because there is a degenerate Killing horizon there where the norm of dt diverges.

The infrared asymptotics of the scalar and the gauge field are easily found to be

$$\begin{aligned} \psi(r) &= \psi_{\text{IR}} + a_\psi e^{(\Delta_{\text{IR}}-3)r/L_{\text{IR}}} + \ldots \\ \Phi(r) &= \phi_0 e^{(\Delta_\Phi - 1)r/L_{\text{IR}}} + \ldots \,, \end{aligned} \tag{2.8}$$

where a_ψ and ϕ_0 are undetermined coefficients, and $\Delta_{\rm IR}$ and Δ_Φ are the larger roots of

$$\begin{aligned} \Delta_{\rm IR}(\Delta_{\rm IR}-3) &= \frac{1}{2}V''(\psi_{\rm IR})L_{\rm IR}^2 \\ \Delta_\Phi(\Delta_\Phi-1) &= 2q^2\psi_{\rm IR}^2 L_{\rm IR}^2\,. \end{aligned} \tag{2.9}$$

Terms omitted in (2.8) vanish faster than the ones shown as $r\to-\infty$. We assume $\phi_0>0$, but there is a $\mathbf{Z}_2$ symmetry between configurations with positive and negative ϕ_0.

The equations of motion following from the action (2.3) are

$$A'' = -\frac{1}{2}\psi'^2 - \frac{q^2}{2h^2e^{2A}}\Phi^2\psi^2 \tag{2.10}$$

$$h''+3A'h' = e^{-2A}\Phi'^2 + \frac{2q^2}{he^{2A}}\Phi^2\psi^2 \tag{2.11}$$

$$\Phi''+A'\Phi' = \frac{2q^2}{h}\Phi\psi^2 \tag{2.12}$$

$$\psi''+\left(3A'+\frac{h'}{h}\right)\psi' = \frac{1}{2h}V'(\psi) - \frac{q^2}{h^2e^{2A}}\Phi^2\psi\,, \tag{2.13}$$

and there is a first order constraint, which if satisfied at one value of r must hold everywhere, provided the equations of motion (2.10-2.13) are also satisfied:

$$\begin{aligned} &h^2\psi'^2 + e^{-2A}q^2\Phi^2\psi^2 - \frac{1}{2}he^{-2A}\Phi'^2 - 2hh'A' \\ &\quad - 6h^2A'^2 - hV(\psi) = 0\,. \end{aligned} \tag{2.14}$$

The left hand side of (2.10) is proportional to $G_t^t - G_r^r$, where $G_{\mu\nu}$ is the Einstein tensor. So the right hand side of (2.10) is proportional to $T_t^t - T_r^r$. This quantity is evidently negative for the theory (2.3). If one considers a more general matter theory coupled to gravity, $T_t^t - T_r^r$ must still be non-positive provided the null energy condition is obeyed: $T_{\mu\nu}\xi^\mu\xi^\nu \geq 0$ for null ξ^ν. This shows that the argument of [25] demonstrating the holographic c-theorem extends to this case. Similarly, the left hand side of (2.11) is proportional to $G_x^x - G_t^t$, so the right hand side—call it $s(r)$—must be non-negative of the null energy condition is obeyed. We can formally solve (2.11) in terms of $s(r)$:

$$h(r) = 1 + \int_{-\infty}^{r} dr_1\, e^{-3A(r_1)} \int_{-\infty}^{r_1} dr_2\, e^{3A(r_2)} s(r_2)\,. \tag{2.15}$$

There are no free integration constants in (2.15) because we assume $h\to 1$ in the infrared, which implies $e^{3A(r)}h'(r)\to 0$ there as well. We learn from (2.15) that $h(r)$, and hence

$v_{\rm eff}(r)$, are monotonically increasing functions of r. We do not need to assume that there is conformal invariance in the UV or the IR to obtain (2.15).

Before exhibiting an explicit, numerical solution to (2.10)-(2.14), let's count the scaling symmetries and parameters that characterize a solution. The upshot of the discussion will be that, given a definite potential, an extremal solution of the form (2.1), with suitable asymptotic behaviors prescribed for the various fields involved, is essentially unique.

Equations (2.10-2.14) have two scaling symmetries that are summarized in Table 2.1, in which assigning a charge α to a quantity X means that $X \to \lambda^\alpha X$. Of the eight

	dr	e^A	h	Φ	ψ	ω	$a_x^{(0)}$	$a_x^{(1)}$
I	1	0	2	1	0	1	0	0
II	0	1	0	1	0	1	0	1

Table 2.1: Charges under scaling symmetries of quantities in (2.10-2.14) and (2.22).

integration constants in the equations (2.10-2.13), one is used up by (2.14). Two are used up by insisting $\psi \to \psi_{\rm IR}$ and $\Phi \to 0$ as $r \to -\infty$. One is used up by insisting that h is finite as $r \to -\infty$ (meaning that the horizon is degenerate, or zero-temperature). Using scaling symmetries I and II, we can ensure that $h \to 1$ and that $A(r) - r/L_{\rm IR} \to 0$ as $r \to -\infty$, which uses up two more integration constants and guarantees that the metric in the far infrared takes the form (2.6). The last two integration constants are the parameters a_ψ and ϕ_0 in (2.8). But by rescaling $x^m \to \lambda x^m$ and shifting $r/L_{\rm IR} \to r/L_{\rm IR} - \log\lambda$ (which preserves that metric ansatz (2.1) and the property $A - r/L_{\rm IR} \to 0$ as $r \to -\infty$), we can choose any prescribed value for ϕ_0. It appears then that there is a one-parameter family of solutions to (2.10-2.14), parametrized by a_ψ. However, the asymptotic behavior of ψ near the conformal boundary is constrained once one chooses a lagrangian for the UV field theory. For the sake of definiteness, we will assume that the appropriate boundary condition on ψ near the conformal boundary is

$$\psi \propto e^{-\Delta_\psi A}\,, \tag{2.16}$$

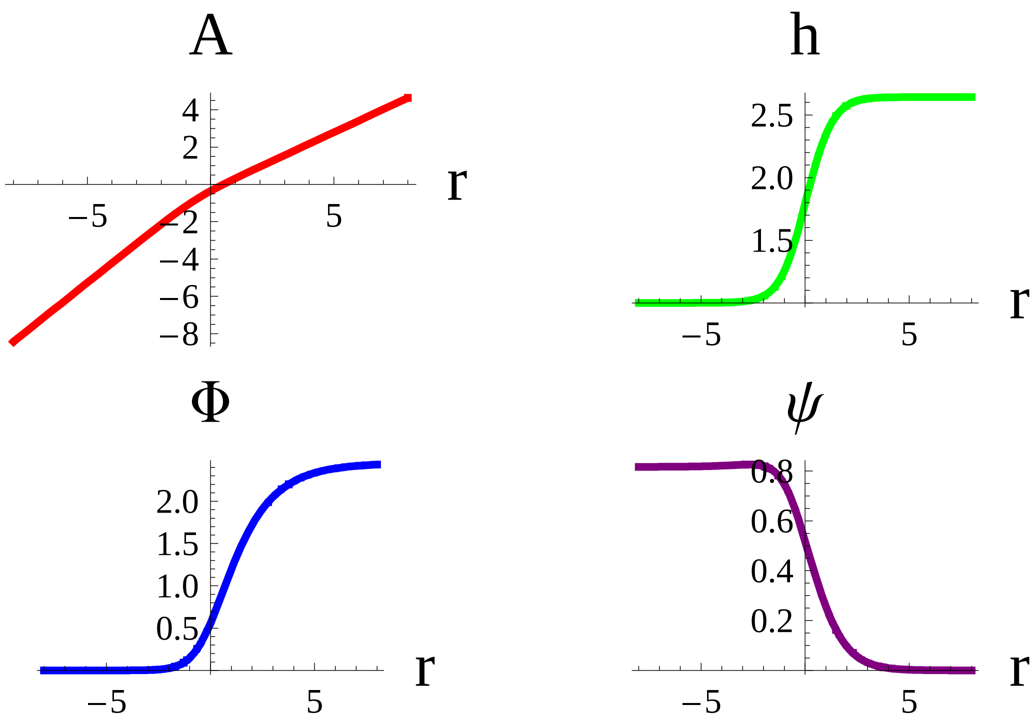

Figure 2.1: An example of a solution connecting two AdS vacua with different effective velocities of signal transmission.

where Δ_ψ is the larger root of

$$\Delta_\psi(\Delta_\psi - 3) = m^2 L^2 \,. \tag{2.17}$$

After this constraint is imposed, there can only be discretely many solutions. There may be none. If there is a stable solution, it represents a quantum critical point.

To give an explicit example, we used the potential (2.4) and made the following choice of parameters:

$$L = 1 \qquad q = 2 \qquad m^2 = -2 \qquad u = 3 \qquad \phi_0 = 1 \,. \tag{2.18}$$

A simple shooting algorithm suffices to find a solution satisfying both the infrared and ultraviolet asymptotic properties discussed in the previous paragraphs. We show the result in figure 2.1. The solution has $a_\psi = 0.312$, and the ratio of its characteristic velocity in the infrared to the speed of light in the ultraviolet is $v/c = \sqrt{h_{\rm IR}/h_{\rm UV}} = 0.615$.

It is reasonable to expect the transport coefficients of a quantum critical point to have power-law dependence on frequency. The example that is readiest to hand in our setup is the conductivity. Consider a complexified perturbation of the gauge field:

$$A_x = e^{-i\omega t} a_x(r)\,. \tag{2.19}$$

Following [26], if the leading behavior near the conformal boundary is

$$a_x(r) = a_x^{(0)} + a_x^{(1)} e^{-A(r)} + \ldots\,, \tag{2.20}$$

and if A_x is constrained to have purely infalling behavior as one approaches the degenerate Killing horizon of AdS_{IR}, then

$$\sigma \propto \tilde{\sigma} \equiv \frac{-i}{\omega} \frac{a_x^{(1)}}{a_x^{(0)}} \sqrt{h_{\mathrm{UV}}}\,. \tag{2.21}$$

The constant of proportionality in (2.21) is ω-independent. To relate σ to the resistance entering Ohm's Law, one must include factors of the electric charge relating to a weak gauging of the $U(1)$ symmetry of the boundary theory by a boundary gauge field. We will only be interested in the frequency dependence, so we will not try to track down the constant of proportionality and instead simply compute $\tilde{\sigma}$. The factor of $\sqrt{h_{\mathrm{UV}}}$ ensures that this expression is invariant under the scaling symmetries of Table 2.1. In other words, if we chose to perturb A_y instead of A_x, we would get the same answer for the conductivity.

The equation of motion obeyed by a_x is

$$\begin{aligned} a_x'' &+ \left(A' + \frac{h'}{h}\right) a_x' \\ &+ \frac{1}{h}\left(\frac{\omega^2}{he^{2A}} - 2q^2\psi^2 - e^{2A}\Phi'^2\right) a_x = 0\,. \end{aligned} \tag{2.22}$$

To derive (2.22), one must also consider a complexified metric perturbation δg_{tx}. This metric perturbation mixes with a_x in the linearized equations, but thanks to a constraint from the xr Einstein equation, δg_{tx} can be eliminated altogether from the Maxwell equations, and (2.22) follows more or less immediately.

Modulo three technical assumptions, it is easy to extract the scaling of $\tilde{\sigma}$ in the limit of small but non-zero ω. First, $\mathrm{Im}\,\tilde{\sigma} \sim 1/\omega$, because this is what Kramers-Kronig requires based on the existence of a delta function in $\mathrm{Re}\,\tilde{\sigma}$ at $\omega = 0$ [2] . In other words, the $1/\omega$ scaling

[2] Our first technical assumption is that the continuous part of $\mathrm{Re}\,\tilde{\sigma}$ is integrable at $\omega = 0$. This can be checked *a posteriori*.

of $\operatorname{Im}\tilde{\sigma}$ is a consequence of the infinite DC conductivity associated with the spontaneous breaking of the $U(1)$ symmetry. Next, $\operatorname{Re}\tilde{\sigma}$ is related to a conserved flux: if we define

$$\mathcal{F} = -\frac{he^A}{2i} a_x^* \overleftrightarrow{\partial}_r a_x \tag{2.23}$$

then $\partial_r \mathcal{F} = 0$ follows from (2.22), and

$$\operatorname{Re}\tilde{\sigma} = \frac{L}{\omega\sqrt{h_{\mathrm{UV}}}} \frac{\mathcal{F}}{|a_x^{(0)}|^2} \tag{2.24}$$

by direct computation. Deep in the AdS_{IR} region, where we can ignore deviations from $\psi = \psi_{\mathrm{IR}}$ and $\Phi = 0$ [3] , (2.22) can be solved explicitly:

$$a_x = e^{-r/2L_{\mathrm{IR}}} H^{(1)}_{\Delta_\Phi - 1/2}\left(\omega L_{\mathrm{IR}} e^{-r/L_{\mathrm{IR}}}\right) , \tag{2.25}$$

where $H^{(1)}_{\Delta_\Phi-1/2}$ is a Hankel function. Passing (2.25) through (2.23) gives an ω-independent flux, so to determine the scaling of $\operatorname{Re}\tilde{\sigma}$ we need only find $a_x^{(0)}$. The trick that makes this possible is that a solution, call it $a_x(r) = Z_x(r)$, to the $\omega \to 0$ limit of (2.22), can be combined with (2.25) using the method of matched asymptotic expansions, provided ω is small. Z_x should be chosen so that $e^{-(\Delta_\phi - 1)r/L_{\mathrm{IR}}} Z_x \to 1$ as $r \to -\infty$. Assume that ω is small enough so that the radius $r_* \equiv L \log \omega L$ is much less than the radius r_{IR} at which AdS_{IR} is significantly deformed. In the matching window $r_* \ll r \ll r_{\mathrm{IR}}$, one finds by expanding the Hankel function that[4]

$$a_x(r) \approx i \sec \pi \Delta_\phi \left(\frac{\omega L}{2}\right)^{-\Delta_\Phi + 1/2} Z_x(r)\,. \tag{2.26}$$

In fact, the approximate equality (2.26) must hold for all $r \gg r_*$, because the ω^2 term in (2.22) is negligible in this region. So we conclude

$$a_x^{(0)} = \lim_{r\to\infty} a_x(r) \propto \omega^{-\Delta_\Phi + 1/2}\,, \tag{2.27}$$

[3]Our second technical assumption is that not only $\Phi \to 0$ as $r \to -\infty$, but also $e^{2A}\Phi' \to 0$, so that the Φ'^2 term in (2.22) can be neglected in comparison with the ω^2 term. This can be checked given values of the parameters as in (2.18).

[4]Our third technical assumption is that Δ is not half an integer. If it is, then the expansion of $H^{(1)}_{\Delta_\Phi-1/2}$ involves a logarithm, and logarithmic scaling violations may result.

where the constant of proportionality involves $\lim_{r\to\infty} Z_x(r)$, which encodes all the physics at high scales. Plugging (2.27) into (2.24), one obtains $\mathrm{Re}\,\tilde{\sigma} \sim \omega^\delta$ for small ω, with

$$\delta = 2(\Delta_\Phi - 1)\,. \tag{2.28}$$

For the parameters indicated in (2.18), $\Delta_\Phi = \frac{1}{2} + \sqrt{\frac{101}{20}}$, resulting in $\delta \approx 3.5$.

In the high-ω limit, $\tilde{\sigma}$ should asymptote to its value in the ultraviolet AdS_4 geometry, which is constant [21]: $\tilde{\sigma}_{AdS_4} = 1$ in our conventions. Figure 2.2 shows that the behavior of $\mathrm{Re}\,\tilde{\sigma}$ is a smooth interpolation between its low- and high-frequency limits.

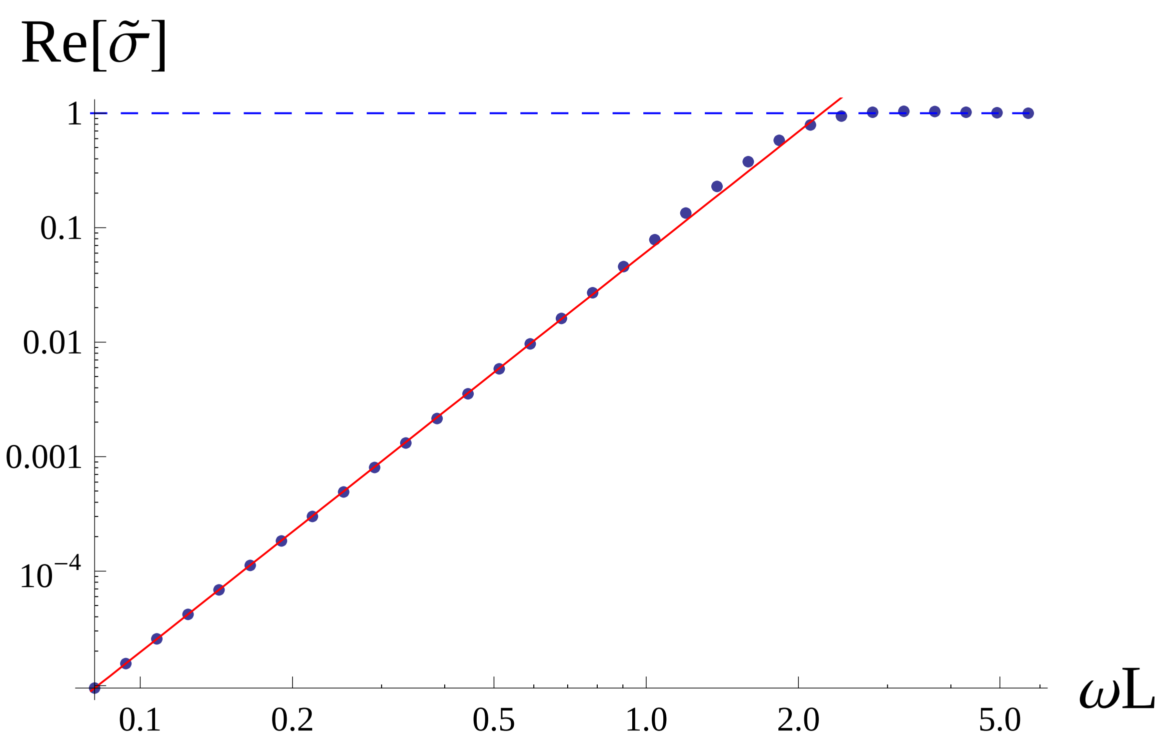

Figure 2.2: The real part of $\tilde{\sigma}$ as function of ωL for the solution displayed in figure 2.1. The dots show the result of numerical computation while the solid line is the small ω power-law behavior $\mathrm{Re}\,\tilde{\sigma} \sim \omega^\delta$ with the overall constant chosen so the line passes through the first point. The dashed line shows the high ω limit $\tilde{\sigma} = 1$. Note that there is an ambiguity in the scale of ω, as the scaling symmetries affect it. In this plot the scale is fixed by using the scaling symmetries to ensure that $h \to 1$ and $A(r) - r/L \to 0$ as $r \to +\infty$.

In conclusion: The Abelian Higgs model in AdS_4, described by the action (2.3), provides the simplest known holographic description of superconductivity or superfluidity. It is striking that this model also exhibits a zero-temperature state with relativistic conformal invariance and a critical exponent that depend continuously on the parameters of the model. Non-trivial scaling laws in the infrared probably arise for other Green's functions, for example the ones associated with the operator dual to ψ. A natural question to ask is whether these solutions are zero-temperature limits of regular black hole solutions (in the same sense that empty AdS is the limit of AdS-Schwarzschild) which are stable and thermodynamically favored over all other finite-temperature configurations. In [27], strong numerical evidence was provided that Lorentzian symmetries do emerge on the thermodynamically favored branch of superconducting black hole solutions to simple theories in AdS_4. It is not hard to produce similar numerical evidence in favor of emergent conformal symmetry when there is a symmetry-breaking minimum in the scalar potential, plausibly leading to the domain wall solutions of the previous chapter as the zero-temperature limits of the thermodynamically favored superconducting black holes.

Chapter 3

Quantum critical superconductors in string theory and M-theory

In [28, 29], explicit examples of superconducting black holes were exhibited in type IIB supergravity and M-theory, respectively. These works follow the general scheme described in section 1.4 for constructing superconducting black holes: a complex scalar charged under an abelian gauged field condenses outside the horizon when the charge of the black hole is big enough. The constructions of [28, 29] draw upon advances including [30, 31, 32, 33] in the understanding of how to embed solutions of gauged supergravity into ten- and eleven-dimensional supergravity.

To summarize the the previous chapter, we suggested that emergent conformal symmetry should emerge in the zero-temperature limit of superconducting black holes, provided the scalar potential has a symmetry-breaking minimum. We further suggested that if there was no such minimum, the zero-temperature limit should involve emergent Lorentz symmetry.

In this chapter, we apply the techniques of the previous one to the theories discussed in [28, 29] to construct domain wall geometries which are candidate ground states for finite-density matter in the gauge theories dual to the AdS_5 and AdS_4 geometries we consider. While we would like to go further and claim that the geometries we construct are the genuine ground states of the theories under consideration at finite density, such claims are difficult to establish without knowing the full spectrum of supergravity deformations.

We start in section 3.1 with the AdS_5 example, and continue in section 3.2 with the AdS_4 example. We finish in section 3.3 with a brief discussion and a conjecture about the relation between renormalization group flows and emergent conformal symmetry in finite-density systems.

The authors of [29] anticipated the quantum critical nature of the zero-temperature limit of the superconducting black holes they studied.

3.1 A string theory example

Consider the action

$$S = \frac{1}{2\kappa^2} \int d^5 x \sqrt{-g} \mathcal{L} \tag{3.1}$$

with

$$\begin{aligned} \mathcal{L} = R - \frac{1}{4} F_{\mu\nu}^2 - \frac{1}{2} \left[(\partial_\mu \eta)^2 + \sinh^2 \eta \left(\partial_\mu \theta - \frac{\sqrt{3}}{L} A_\mu \right)^2 \right] \\ + \frac{3}{L^2} \cosh^2 \frac{\eta}{2} (5 - \cosh \eta) + (\text{Chern-Simons}) \,, \end{aligned} \tag{3.2}$$

where η is the magnitude of the complex scalar and θ is its phase. The kinetic terms come from the non-linear sigma-model over the Poincaré disk, parametrized by $z = e^{i\theta} \tanh \frac{\eta}{2}$. The lift of this lagrangian to a class of solutions of type IIB supergravity, based on D3-branes at the tip of a Calabi-Yau cone, was described in [28].

As before, the domain wall geometry takes the form

$$ds^2 = e^{2A(r)} \left[-h(r) dt^2 + d\vec{x}^2 \right] + \frac{dr^2}{h(r)} \,, \tag{3.3}$$

and has non-zero gauge field $A_\mu dx^\mu = \Phi(r) dt$ and η. As we argued in the previous chapter for the four dimensional case, any such domain wall supported by matter obeying the null energy condition must have A concave down; and it also follows from the null energy condition that if h is constant in both the infrared ($r \to -\infty$) and the ultraviolet ($r \to +\infty$), then $h_{\text{IR}} < h_{\text{UV}}$.

The scalar potential in (3.2) has two extrema, $\eta = 0$ and $\eta = \eta_{\rm IR} \equiv \log(2+\sqrt{3})$, and to each of these corresponds an AdS_5 extremum of (3.2) with radius of curvature L and $L_{\rm IR} \equiv 2^{\frac{3}{2}} L/3$, respectively. The domain wall solution interpolates between these two AdS_5 geometries, similar to the one found in [34]. It differs in that we insist that as $r \to +\infty$ (the ultraviolet),

$$\eta \propto e^{-\Delta_\eta A} = e^{-3A}\,, \tag{3.4}$$

corresponding to an expectation value for the dimension 3 operator dual to η, but no deformation of the CFT lagrangian by it. Instead, denoting the conserved current dual to A_μ in the ultraviolet CFT by J_μ, we consider states with finite $\langle J_0 \rangle$ and finite chemical potential μ. In other words, we add μJ_0 to the CFT lagrangian, which does not by itself break the $U(1)$ symmetry associated with J_μ. Non-zero η does break this symmetry.

We can choose coordinates such that as $r \to -\infty$

$$A \sim \frac{r}{L_{\rm IR}}, \quad h \sim 1, \quad \eta \sim \eta_{\rm IR}, \quad \Phi \sim 0\,, \tag{3.5}$$

with exponentially suppressed corrections, which can be obtained from the equations of motion linearized around (3.5). Of particular interest are the first corrections to the scalar and gauge field,

$$\eta \approx \eta_{\rm IR} + a_\eta e^{(\Delta_{\rm IR}-4)r/L_{\rm IR}}, \quad \Phi \approx a_\Phi e^{(\Delta_\Phi-3)r/L_{\rm IR}}\,, \tag{3.6}$$

where $\Delta_{\rm IR} = 6 - \sqrt{6}$ and $\Delta_\Phi = 5$. A formal series solution for A, h, η, and Φ may be developed in the infrared, in powers of $e^{r/L_{\rm IR}}$, with all coefficients determined in terms of a_η and a_Φ.

By shifting r, we can set a_Φ to 1 without loss of generality. Such a shift adds a constant to A, but this constant can be absorbed by rescaling t and $\vec{x}$ by a common factor. To fix a_η, one must impose the ultraviolet boundary condition (3.4). There can be several values of a_η that satisfy this condition. We will consider the solution for which η has the least number of nodes, since this is the solution most likely to be stable.

By numerically integrating the equations of motion with the boundary conditions described above we find a nodeless domain wall solution for $a_\eta \approx 2.134$ (see figure 3.1). The relative speed of propagation of lightlike signals in the ultraviolet and the infrared is given by the "index of refraction" $n \equiv \sqrt{h_{\rm UV}/h_{\rm IR}}$, and for this solution we have $n \approx 2.674$.

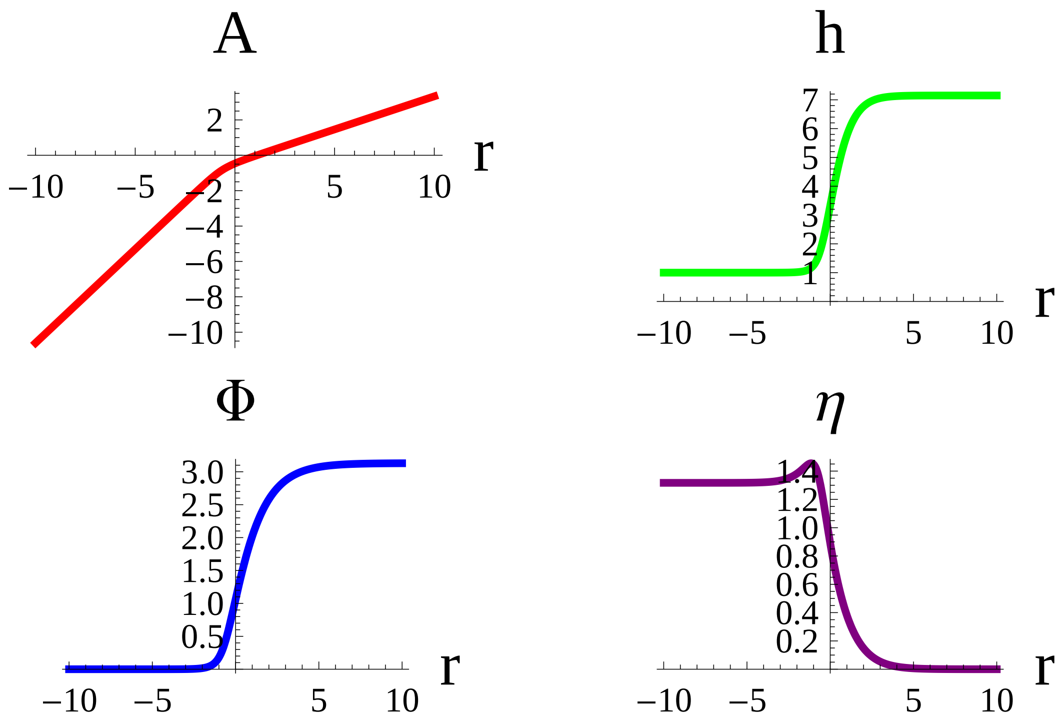

Figure 3.1: A domain wall from a string theory action.

One can define a "normalized" order parameter through the diffeomorphism invariant formula

$$\langle \hat{\mathcal{O}}_\eta \rangle \equiv \lim_{r\to\infty} \frac{\eta(r) e^{3A(r)} h(r)^{3/2}}{\Phi(r)^3} \,. \tag{3.7}$$

In terms of field theory quantities, $\langle \hat{\mathcal{O}}_\eta \rangle$ is proportional to $\langle \mathcal{O}_\eta \rangle / \mu^3$, where $\mathcal{O}_\eta$ is the operator dual to η and μ is the chemical potential. The proportionality constant depends on the precise normalization one chooses for $\mathcal{O}_\eta$ and μ. For our domain wall solution, we find $\langle \hat{\mathcal{O}}_\eta \rangle \approx 0.322$.

It is interesting to note that the ten-dimensional geometry in the far ultraviolet is AdS_5 times a Sasaki-Einstein five-manifold (SE_5), supported by five-form flux only, whereas in the far-infrared it is of the form first studied in [35], where a $U(1)$ fiber of the SE_5 has been stretched and a combination of the Neveu-Schwarz and Ramond-Ramond two-form gauge potentials have been turned on. These are not supersymmetric compactifications, so demonstrating stability is non-trivial.

Having obtained the domain wall solution, we can compute its frequency-dependent conductivity. To this end, we add a time-dependent perturbation to the gauge field, $A_x = e^{-i\omega t}a_x(r)$ and linearize its equation of motion, obtaining

$$a_x'' + \left(2A' + \frac{h'}{h}\right)a_x' + \left(\frac{\omega^2 - h\Phi'^2}{e^{2A}h^2} - \frac{3\sinh^2\eta}{h}\right)a_x = 0\,, \tag{3.8}$$

with primes denoting d/dr. If we solve (3.8), with infalling boundary conditions in the infrared, the conductivity can then be computed from the ultraviolet behavior of the perturbation. For large r,

$$a_x \approx a_x^{(0)} + a_x^{(2)}e^{-2A} + a_x^{(L)}A(r)e^{-2A}\,. \tag{3.9}$$

The Ae^{2A} term introduces some ambiguity in this computation: it gives a logarithmically divergent contribution to the conductivity [36]. However, since $a_x^{(L)}/a_x^{(2)}$ can be shown to be a real number, this issue only affects the imaginary part of the conductivity, and the real part is unambiguously given by

$$\operatorname{Re}\sigma = \frac{1}{2\kappa^2 L}\frac{2a_x^{(2)}}{i\omega a_x^{(0)}}\frac{h_{\rm UV}}{\Phi_{\rm UV}}\,. \tag{3.10}$$

Here, the factor of $h_{\rm UV}/\Phi_{\rm UV}$, where $\Phi_{\rm UV} = \Phi(+\infty)$, was introduced to render the conductivity invariant under diffeomorphisms that preserve the form of the metric (3.3). Numerical results for the real part of the conductivity are shown in figure 3.2. At large frequencies, we recover the AdS_5 behavior, $\operatorname{Re}\sigma = L\pi\omega/4\kappa^2$. At low frequencies, we can also obtain the scaling analytically, using the method of matched asymptotic expansions, as in Chapter 2.

The first step is to note that when $r \ll -L_{\rm IR}$, the corrections to (3.5) are suppressed. When they are ignored, (3.8) can be solved analytically. The infalling solution is

$$a_x^{\rm IR} = e^{-r/L_{\rm IR}}H^{(1)}_{\Delta_\Phi-2}\left(\omega L_{\rm IR}e^{-\frac{r}{L_{\rm IR}}}\right)\,, \tag{3.11}$$

where $H^{(1)}$ is a Hankel function. The next step is to note that when $r \gg L_{\rm IR}\log\omega L_{\rm IR}$, one may drop ω from (3.8) altogether. The resulting equation probably can't be solved analytically, but the point is that the solutions to (3.8) which determine the conductivity don't depend on ω in the region $r \gg L_{\rm IR} \log \omega L_{\rm IR}$, except for an overall multiplicative factor: they are given simply by the zero frequency solution. Provided $\omega L_{\rm IR} \ll 1$, there exists a window $L_{\rm IR} \log \omega L_{\rm IR} \ll r \ll -L_{\rm IR}$ where (3.11) may be matched onto the zero-frequency solution. The result of this matching is that $a_x^{(0)} \sim \omega^{-\Delta_\Phi+2}$. To extract the real part of the conductivity, first define

$$\mathcal{F} = \frac{he^{2A}}{2i} a_x \overleftrightarrow{\partial}_r a_x^* \tag{3.12}$$

and note that $\mathcal{F}$ is independent of r. Inserting (3.9) into (3.12) it follows that $\mathcal{F} = \sigma \Phi_{\rm UV} \omega \big| a_x^{(0)} \big|^2$. On the other hand, inserting (3.11) into (3.12) shows that $\mathcal{F}$ is ω-independent. So we find that

$$\operatorname{Re} \sigma \propto \omega^{2\Delta_\Phi - 5} = \omega^5 \,, \tag{3.13}$$

where in the last step we used $\Delta_\Phi = 5$. The result $\operatorname{Re} \sigma \propto \omega^{2\Delta_\Phi - 5}$ is clearly more general: it basically depends on having good control over the series expansion of the background in the infrared.

As figure 3.2 shows, numerical evaluations of the conductivity interpolate quite smoothly between the infrared and ultraviolet limits just discussed.

3.2 An M-theory example

The four-dimensional theory

$$\begin{aligned} \mathcal{L} = R - \frac{1}{4} F_{\mu\nu}^2 - \frac{1}{2} \left[(\partial_\mu \eta)^2 + \sinh^2 \eta \left(\partial_\mu \theta - \frac{1}{L} A_\mu \right)^2 \right] \\ + \frac{1}{L^2} \cosh^2 \frac{\eta}{2} (7 - \cosh \eta) \end{aligned} \tag{3.14}$$

derived as a consistent truncation of M-theory in [29, 32], clearly is nearly identical to (3.2).[1] As mentioned in [29], this truncation is consistent only when $F \wedge F = 0$.

This theory also admits a domain wall solution. The asymptotically AdS_4 geometry is of the same form as (3.3), and now the two extrema of the potential are at $\eta = 0$

[1] The notation of [29, 32] is related to ours by $\hat{A}_1 = A$ and $\hat{\chi} = \sqrt{2} e^{i\theta} \tanh \frac{\eta}{2}$.

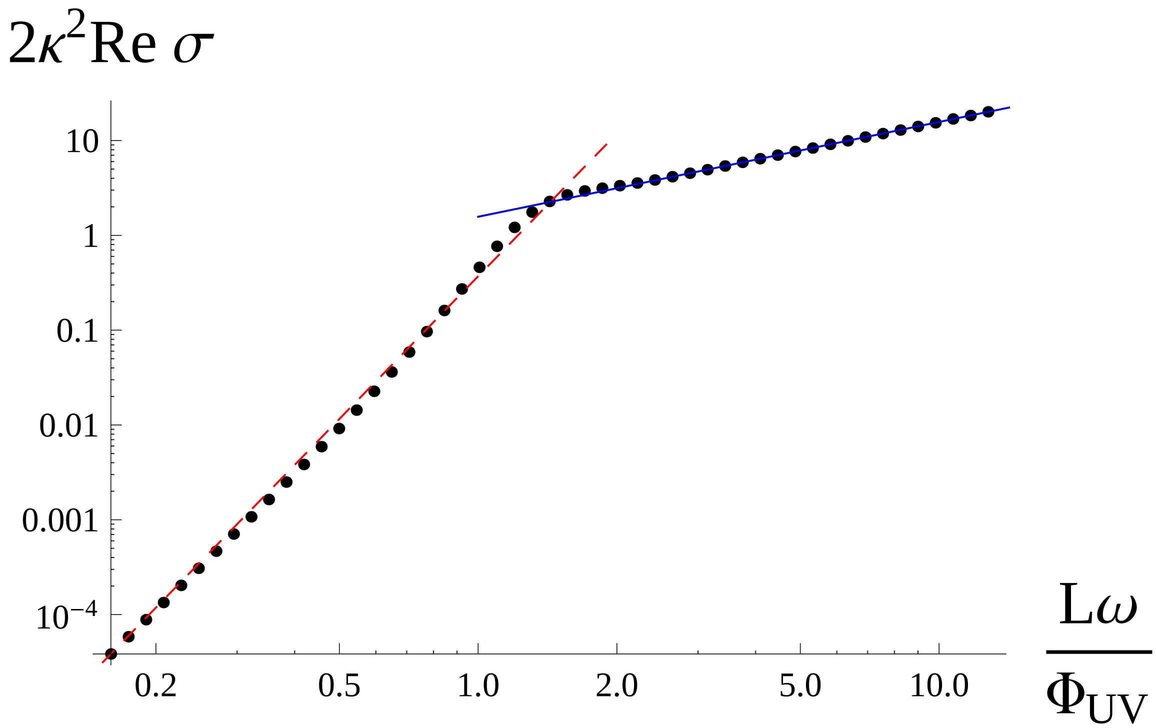

Figure 3.2: The real part of the conductivity for string theory domain wall. The dots are numerical results, the dashed line is a ω^5 power law with the coefficient chosen such that the line goes through the first dot in the plot and the solid line is the AdS_5 conductivity $\mathrm{Re}\,\sigma = \pi L\omega/4\kappa^2$.

and $\eta_{\mathrm{IR}} = \log(3 + 2^{3/2})$, corresponding to AdS_4 solutions with radii of curvature L and $L_{\mathrm{IR}} \equiv \sqrt{3}L/2$, respectively. If we assume the scalar goes to the second fixed point in the infrared, then as $r \to -\infty$,

$$\eta \approx \eta_{\mathrm{IR}} + a_\eta e^{(\Delta_{\mathrm{IR}}-3)r/L_{\mathrm{IR}}}, \quad \Phi \approx e^{(\Delta_\Phi-2)r/L_{\mathrm{IR}}}, \tag{3.15}$$

with $\Delta_{\mathrm{IR}} = (3 + \sqrt{33})/2$ and $\Delta_\Phi = 4$. Imposing no symmetry-breaking deformation of the UV CFT means demanding that

$$\eta \propto e^{-\Delta_\eta A} = e^{-2A}. \tag{3.16}$$

We numerically found a solution for $a_\eta \approx 1.256$ with index of refraction $n \approx 3.775$. The normalized order parameter analogous to (3.7) is in this case given by the diffeomorphism invariant formula

$$\langle \hat{\mathcal{O}}_\eta \rangle \equiv \lim_{r\to\infty} \frac{\eta(r) e^{2A(r)} h(r)}{\Phi(r)^2}\,, \tag{3.17}$$

and is proportional to $\langle \mathcal{O}_\eta \rangle / \mu^2$. Our domain wall solution has $\langle \hat{\mathcal{O}}_\eta \rangle \approx 0.201$.

As already noted in [29], the infrared geometry in eleven dimensions is an AdS_4 compactification of the form studied in [37, 38]. The whole geometry is non-supersymmetric, so it is difficult to definitely establish stability.

The computation of the conductivity is similar to before, so we will be brief. The main difference is that the behavior of the solutions as $r \to +\infty$ is

$$a_x \approx a_x^{(0)} + a_x^{(1)} e^{-A}\,, \tag{3.18}$$

and this time there is no ambiguity in the imaginary part, the conductivity being given by

$$\sigma = \frac{1}{2\kappa^2 L} \frac{a_x^{(1)}}{i\omega a_x^{(0)}} \sqrt{h_{\mathrm{UV}}}\,. \tag{3.19}$$

Numerical results are shown in 3.3. For high frequencies, the conductivity asymptotes to the AdS_4 value $\sigma = 1/2\kappa^2$ [21] and for low frequencies the behavior can be determined analytically with an argument similar to the one described in the previous section. As we showed in Chapter 2, in AdS_4 the scaling is $\mathrm{Re}\,\sigma \propto \omega^{2\Delta_\Phi - 4} = \omega^4$, and this agrees with the numerical results.

3.3 Discussion

The domain walls we have constructed can be fairly described as superconductors because they spontaneously break the $U(1)$ gauge symmetry associated with the field strength $F_{\mu\nu}$ in (3.1) and (3.14). According to the arguments of [13], much of the basic phenomenology of superconductors, including infinite DC conductivity, follows from this spontaneous symmetry breaking. The domain walls can fairly be characterized as quantum critical because relativistic conformal symmetry emerges in the infrared, and observables, in particular $\mathrm{Re}\,\sigma(\omega)$, have power-law scaling in the infrared with non-trivial exponents.

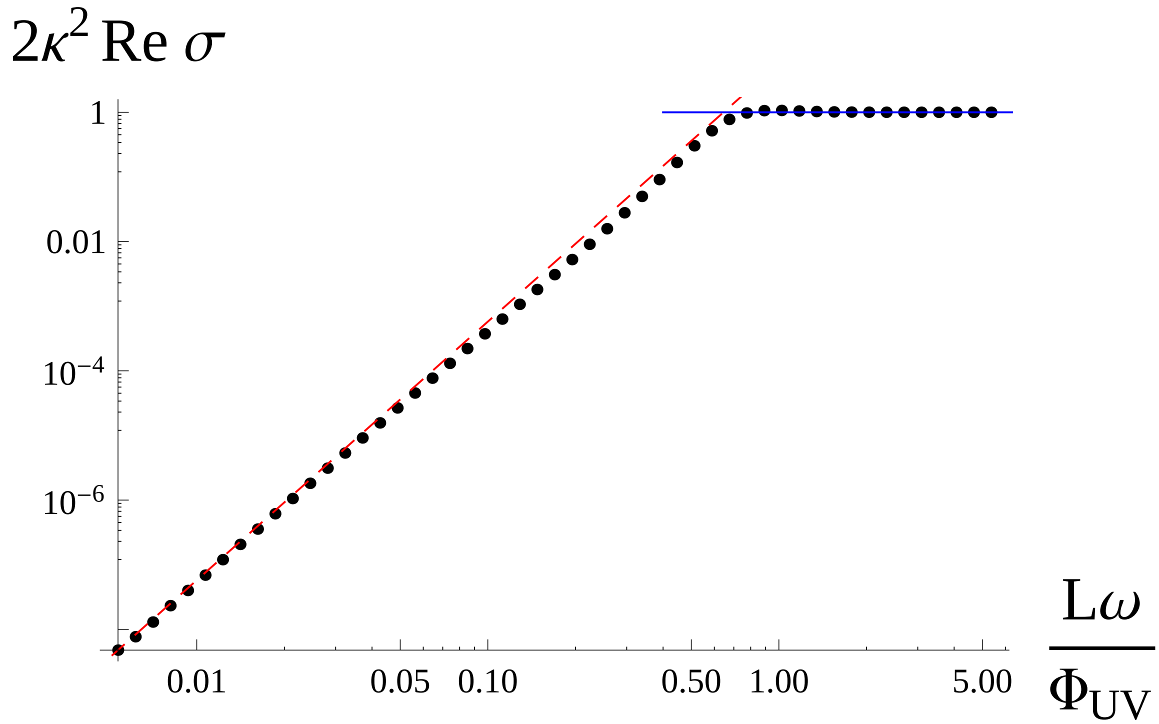

Figure 3.3: The real part of the conductivity for M-theory domain wall. The dots are numerical results, the dashed line is a ω^4 power law with the coefficient chosen such that the line goes through the first dot in the plot and the solid line is the AdS_4 conductivity $\sigma = 1/2\kappa^2$.

Clearly, the domain walls we have constructed are close relatives to holographic renormalization group flows from one conformal field theory to another. The main qualitative difference is that the breaking of the $U(1)$ symmetry was soft in the RG flows, whereas it is spontaneous in our domain walls. More explicitly: the RG flows are triggered by adding a relevant operator, dual to the scalar η in both cases, which breaks the $U(1)$ symmetry; our domain walls, on the other hand, have by design no such relevant deformation, but instead a spontaneously generated expectation value of the symmetry breaking operator.

It is natural to ask how general the relation between renormalization group flows and emergent conformal symmetry of finite-density matter might be. Here is a conjecture which makes sense to us:

- Assume that a field theory is well-defined in the ultraviolet and possesses a continuous symmetry. This ultraviolet theory need not be conformal.

- Assume also that if the ultraviolet theory is appropriately deformed, a renormalization group flow results whose infrared limit is a fixed point which breaks the continuous symmetry.

Then the conclusion is:

- The ultraviolet theory, or some deformation of it by operators which do *not* break the continuous symmetry, has a finite density, zero temperature state whose infrared behavior is governed by the same infrared fixed point. Finite density means that the time component(s) of the Noether current(s) associated with the continuous symmetry have finite expectation values.

We are aware of one way to break this conjecture [27]: it can happen that the conserved current of the ultraviolet theory flows to a relevant operator at the infrared fixed point. When that happens, it's impossible (or at least fine-tuned) for the dynamics of finite-density matter to flow to the fixed point. What we suggest as a real possibility is that relevance of current operators with expectation values in the finite-density state is the only obstacle to the conjecture as we have phrased it. Since the idea is to systematically pair an RG flow to an infrared critical point with quantum critical behavior of a finite-density state, let us refer to our suggestion as the "Criticality Pairing Conjecture," or CPC.

When applied to the gauge-string duality, the CPC implies the existence of a number of domain wall solutions interpolating among critical points of the scalar potential of gauged supergravity theories. The CPC might also be tested in situations where some non-string-theoretic approximation scheme can be found, like a large N expansion with perturbative control; or, perhaps, it could be investigated in the context of rational conformal field theories in $1 + 1$ dimensions.

Chapter 4

Interesting features of some asymptotically AdS dilatonic black holes

As we have seen in previous chapters, the AdS/CFT correspondence allows us to better understand some aspects of strongly coupled field theories by studying simple gravitational models and significant work has gone into applying this approach to the study of strongly coupled systems at finite temperature and density (see [21] for early work). The RNAdS black hole, which we describe in section 1.3, was one of the first gravity models to be considered in this context [22, 23, 39]. This black hole background is simple because it involves only the metric and a gauge field, and it is reliable in the supergravity approximation because it has curvatures that can be made everywhere small. As we have seen, the extremal RNAdS is a charged domain wall interpolating between AdS_4 in the ultraviolet and $AdS_2 \times \mathbf{R}^2$ near the horizon. The domain wall structure has been particularly important in the study [40, 41, 42] of two-point functions of an operator $\mathcal{O}_\psi$ dual to a charged fermion ψ in the bulk. These calculations (all of them relying to some degree on numerics) point to the existence of an isolated fermion normal mode at finite wave-number, call it k_F. The authors of [40, 41, 42] have argued that this normal mode signals a Fermi surface. The argument runs roughly as follows. RNAdS carries a charge under a $U(1)$ symmetry which is gauged in the bulk and global on the boundary. Fermions in the boundary theory can plausibly be assumed to be charged under this $U(1)$. The zero-temperature state at finite charge density which is dual to RNAdS is supposed to be a Fermi liquid. $\mathcal{O}_\psi$ is assumed to have some overlap with the operator which creates one fermion in the boundary field theory. If this fermion is created very near the Fermi surface, then it should have a long lifetime. So the spectral measure should have a spike at energy equal to the Fermi energy and momentum equal to the Fermi momentum. Now, the Fermi energy can reasonably be identified as the charge of the bulk fermion times the potential difference between the boundary of AdS_4 and the black hole horizon, because this is the amount of energy it takes to add one bulk fermion's worth of charge to the black hole.[1] In the conventions of [40, 42], which we also adopt, energy equal to the Fermi energy corresponds to frequency equal to zero. The spike found in the spectral measure through explicit calculations on the gravity side is indeed at zero frequency. Furthermore, it had previously been pointed out in [43, 44] that some of the thermodynamical and transport properties of near extremal RNAdS are also suggestive of a Fermi surface. So everything makes sense.

Or does it? The elephant in the room is the macroscopic zero-temperature entropy of RNAdS, which seems at odds with a description of the zero-temperature dual as a degenerate Fermi liquid. For the sake of a simple discussion, let's focus on the AdS_5 case. The dual is then a gauge theory (at least in all known constructions) for which the ranks of the gauge groups are large. Let the rank of one gauge group be N. Then the total entropy density is $N^2 k_F^3$ up to factors of order unity. More conventionally, one could express entropy density as $N^2\Omega^3$ times factors of order unity, where Ω is the chemical potential for the $U(1)$ symmetry; but k_F/Ω is $O(1)$. One way out is to suppose that the zero-point entropy owes to some unspecified dynamics of the colored degrees of freedom, while the Fermi liquid dynamics is a subleading effect in N. This seems in line with the calculations of one-loop

[1] Implicit in the argument at this step is that the boundary field theory fermion has the same $U(1)$ charge as the bulk fermion. This would be true, for example, if $\mathcal{O}_\psi = \operatorname{tr} X\lambda$ where X is a neutral scalar and λ is the boundary field theory fermion.

bulk effects in [45]. The picture that seems to emerge is that the number of fermions in the Fermi liquid (or at least, the number of fermions near the edge of the Fermi sea) is $O(1)$ rather than $O(N^2)$. Perhaps they should be thought of as color singlet bound states of an adjoint scalar and an adjoint fermion, created by an operator of the form $\operatorname{tr} X\lambda$, where X is the scalar and λ is the fermion. It is remarkable that there should be such a bound state when the entropy indicates that the theory as a whole is in a deconfined state. What seems really odd, if one subscribes to this picture, is that the spectral measure of the two-point function of $\mathcal{O}_\psi$ scales naturally as N^2. To see this without committing oneself to a definite form of $\mathcal{O}_\psi$, consider that the two-point function of the stress-tensor of the boundary field theory certainly scales as N^2, as does the two-point function of the operator dual to the dilaton: indeed, this scaling, and the agreement of the overall coefficient in certain cases, provided early hints of AdS/CFT [46, 47, 48]. Likewise the supercurrent, dual to the bulk gravitino, has two-point functions that scale as N^2, and so do all single-trace, color-singlet operators dual to bulk supergravity fields, simply because the on-shell action that defines the two-point functions naturally includes a prefactor of $1/G_5$, which is proportional to N^2. It is hard to see how this scaling squares with the picture of the spike in the spectral measure owing to quasi-particle dynamics of a color-singlet bound state: the magnitude of the spike itself scales as N^2. In summary, the picture of $O(1)$ Fermi liquid phenomena resting on top of deconfined $O(N^2)$ dynamics of colored degrees of freedom presents some serious puzzles, and pending a resolution of them—including a microscopic account of the zero-point entropy with coefficients that agree or almost agree between field theory and gravity—one should feel entitled to some doubt about the whole picture.

Matters would be simpler if the zero-point entropy weren't there. Better yet would be if the $O(N^2)$ thermodynamics also exhibited linear specific heat, as one expects for a Fermi liquid. If such a setup could be found, with a normal mode similar to the one that exists for RNAdS, then one could plausibly advance the interpretation that adjoint fermions in the field theory are in a Fermi liquid state at zero temperature; that the normal mode (with magnitude scaling as N^2) signals the existence of $O(N^2)$ quasi-particle excitations (adjoint or bifundamentally charged fermions in quiver theories) at the edge of the Fermi surface; and that the specific heat at low temperatures (also scaling as N^2) is the specific heat of the Fermi liquid.

So, can a suitable black hole be constructed in an asymptotically AdS_5 geometry? The answer is "Yes." In fact one can even concoct a theory where the black hole solution is analytically known. The simplest such theory (at least, the simplest one we know) is

$$\mathcal{L} = \frac{1}{2\kappa^2}\left[R - \frac{1}{4}e^{4\alpha}F_{\mu\nu}^2 - 12(\partial_\mu\alpha)^2 + \frac{1}{L^2}(8e^{2\alpha} + 4e^{-4\alpha})\right] , \tag{4.1}$$

and the spatially uniform, electrically charged solution is

$$\begin{aligned} & ds^2 = e^{2A}(-h\,dt^2 + d\vec{x}^2) + \frac{e^{2B}}{h}dr^2 \qquad A_\mu dx^\mu = \Phi dt \\ & A = \log\frac{r}{L} + \frac{1}{3}\log\left(1 + \frac{Q^2}{r^2}\right) \qquad B = -\log\frac{r}{L} - \frac{2}{3}\log\left(1 + \frac{Q^2}{r^2}\right) \\ & h = 1 - \frac{\mu L^2}{(r^2 + Q^2)^2} \qquad \Phi = \frac{Q\sqrt{2\mu}}{r^2 + Q^2} - \frac{Q\sqrt{2\mu}}{r_H^2 + Q^2} \\ & \alpha = \frac{1}{6}\log\left(1 + \frac{Q^2}{r^2}\right) . \end{aligned} \tag{4.2}$$

This black hole is extremal if $r_H = 0$, which implies $\mu L^2 = Q^4$. The extremal solution has a naked singularity at $r = 0$, which we will say more about in section 4.3. The neutral scalar α plays the role of a dilaton because it controls the physical gauge coupling.

The thermodynamics of the charged dilatonic black hole (4.2) is most easily expressed in the microcanonical ensemble in terms of a rescaled energy density, entropy density, and charge density:

$$\hat{\epsilon} \equiv \frac{\kappa^2}{4\pi^2 L^3}\epsilon = \frac{3\mu}{8\pi^2 L^6} \qquad \hat{s} \equiv \frac{\kappa^2}{4\pi^2 L^3}s = \frac{r_H\sqrt{\mu}}{2\pi L^5} \qquad \hat{\rho} \equiv \frac{\kappa^2}{4\pi^2 L^3}\rho = \frac{Q\sqrt{2\mu}}{4\pi^2 L^5} . \tag{4.3}$$

From (4.3) together with the condition $h(r_H) = 0$, one may straightforwardly verify the micro-canonical equation of state:

$$\hat{\epsilon} = \frac{3}{2^{5/3}\pi^{2/3}}\left(\hat{s}^2 + 2\pi^2\hat{\rho}^2\right)^{2/3} . \tag{4.4}$$

The temperature and chemical potential can be found by differentiation:

$$T = \left(\frac{\partial\hat{\epsilon}}{\partial\hat{s}}\right)_{\hat{\rho}} \qquad \Omega = \left(\frac{\partial\hat{\epsilon}}{\partial\hat{\rho}}\right)_{\hat{s}} . \tag{4.5}$$

One easily finds

$$\hat{s} = \pi\sqrt{\frac{2\hat{\epsilon}}{3}}\,T \approx (\pi^2\hat{\rho})^{2/3}\,T \approx \frac{\Omega^2}{4}T\,, \tag{4.6}$$

where the approximate equalities hold in the low-temperature limit. The rescaled specific heats at constant charge density and constant chemical potential,

$$\hat{C}_{\hat{\rho}} = T\left(\frac{\partial \hat{s}}{\partial T}\right)_{\hat{\rho}} \qquad \hat{C}_{\Omega} = T\left(\frac{\partial \hat{s}}{\partial T}\right)_{\Omega} \tag{4.7}$$

coincide with each other and with the rescaled entropy density $\hat{s}$ in this limit.

With a black hole in hand whose low-temperature thermodynamics lends itself to the claim that the dual is a Fermi liquid, the next obvious question is whether it supports isolated fermionic normal modes similar to the ones found in RNAdS. We will show by example in section 4.1 that it does. Next one might inquire whether one can embed this black hole in string theory. Indeed one can. In fact, (4.1) is a consistent truncation of maximal gauged supergravity in five dimensions [49], and the solution (4.2) is the black hole solution in this theory where two of the three commuting $U(1)$ gauge groups carry equal charge, and the third carries no charge. Thus it can be immediately lifted to a ten-dimensional geometry, asymptotic to $AdS_5 \times S^5$, which describes the near-horizon limit of D3-branes which have equal spin in two of the three orthogonal transverse planes, and zero spin in the third plane [50]. By way of comparison, RNAdS_5 can be lifted to the near-horizon limit of D3-branes with equal spin in all three orthogonal transverse planes.

When (4.2) is lifted to an asymptotically $AdS_5 \times S^5$ solution to type IIB supergravity, its field theory dual must be $\mathcal{N} = 4$ super-Yang-Mills theory (hereafter $\mathcal{N} = 4$ SYM), which has massless scalars charged under the $U(1)$ symmetry dual to A_μ, as well as massless charged fermions. It is hard to see how these charged scalars would fail to take over the dynamics at low temperatures and finite chemical potential: in particular, one would expect that they condense, spontaneously breaking the $U(1)$ symmetry that is gauged in the bulk theory (4.1). This indeed happens, as can be seen from studying the dynamics of bulk scalars in the 20 of $SO(6)$ in the background (4.2) [51]. In section 4.2 we note another, simpler instability: There is a negative thermodynamic susceptibility below a critical temperature which leads to the spontaneous breaking of an $SU(2)$ symmetry as well as translational invariance. This negative susceptibility is a well studied [52, 53] example of the Gregory-Laflamme instability [54, 55], although its interpretation here in terms of breaking an $SU(2)$ symmetry is new as far as we know.

While the lift to an asymptotically $AdS_5 \times S^5$ geometry does not particularly encourage the view that the dual physics is a Fermi liquid, it does provide an interesting explanation of the linear specific heat: there is an AdS_3 factor in the near horizon geometry, which takes two of its dimensions from the AdS_5 factor and one from the S^5. In section 4.3, we explain the appearance of this AdS_3 factor heuristically in terms of an effective string built from intersecting giant gravitons, along the lines of [56]. It is tempting to speculate that the non-chiral conformal invariance associated with the AdS_3 geometry is a more general feature of embeddings of black holes with linear specific heat in string theory and M-theory. The question naturally arises: Could there be an embedding where there is a Fermi liquid in the dual field theory which somehow explicitly realizes the non-chiral conformal symmetry?

The spinning D3-branes construction has a well-known M-theory analogue. In section 4.4, we find that it can reproduce many of the features we found appealing in the string theory construction. Namely, it has a four-dimensional reduction consisting of a charged dilatonic black hole that supports an isolated fermion normal mode at finite k at zero temperature and has linear specific heat at low temperatures.

Once one has achieved a detailed understanding of a charged dilatonic black hole with linear specific heat at low temperature, a natural follow-up question is whether the theory (4.1) can be modified in a simple way to accommodate other behaviors for the specific heat. We explore this question in section 4.5, exhibiting some further exactly solvable examples and summarizing their thermodynamic properties.

We end with a summary of our findings in section 4.6.

4.1 Fermion normal modes

Let us now consider fermions in the zero temperature limit of the charged dilatonic black hole (4.2). We will take the fermionic action to be

$$S_f = i \int d^5x\, \bar{\psi}(\Gamma^\mu D_\mu - m)\psi + S_{\text{bdy}} \tag{4.8}$$

where $D_\mu \psi = \left(\partial_\mu + \frac{1}{4}\omega_\mu{}^{\underline{\rho\sigma}}\Gamma_{\underline{\rho\sigma}} - iqA_\mu\right)\psi$ and $\omega_\mu{}^{\underline{\rho\sigma}}$ is the spin connection. S_{bdy} is a boundary term necessary to have well defined variational problem [57] and does not affect the equations of motion. We will specify it below. We denote curved space indices by μ and tangent space indices by $\underline{\mu}$. It is convenient to chose a basis for the Γ matrices where $\Gamma^{\underline{r}}$ is diagonal, and we choose

$$\begin{gathered}
\Gamma^{\underline{0}} = i\begin{pmatrix} \sigma_2 & 0 \\ 0 & \sigma_2 \end{pmatrix}, \quad \Gamma^{\underline{1}} = \begin{pmatrix} 0 & \sigma_1 \\ \sigma_1 & 0 \end{pmatrix}, \quad \Gamma^{\underline{2}} = \begin{pmatrix} 0 & \sigma_3 \\ \sigma_3 & 0 \end{pmatrix}, \\
\Gamma^{\underline{3}} = i\begin{pmatrix} 0 & -1 \\ 1 & 0 \end{pmatrix}, \quad \Gamma^{\underline{r}} = \begin{pmatrix} 1 & 0 \\ 0 & -1 \end{pmatrix},
\end{gathered} \tag{4.9}$$

where σ_1, σ_2, and σ_3 are the Pauli matrices. The matrices $\Gamma^{\underline{0}}, \ldots, \Gamma^{\underline{3}}$ are then four-dimensional Γ matrices with $\Gamma^5 = \Gamma^{\underline{r}}$.

The action (4.8) is *ad hoc* in the sense that we do not derive it from supergravity or from an embedding of the black hole solution (4.2) in string theory. We will explain such an embedding in sections 4.2 and 4.3, and in principle we could replace S_f by the quadratic fermion action of maximally supersymmetric gauged supergravity in five dimensions. However, this action is complicated, involving mixing between spin-3/2 fields and spin-1/2 field through the super-Higgs mechanism, Yukawa couplings, and also couplings between the gauge field strength $F_{\mu\nu}$ and bulk fermion bilinears. So it seems to be quite a challenge to diagonalize the action. Also, we do not want to commit ourselves to the embedding of (4.1) into maximal gauged supergravity as the only potentially interesting one. Altogether it seems worthwhile to start with the fermionic action (4.8).

We will only consider $m \geq 0$. Noting the translation symmetry in the t, x^i directions, we take the fermion wave-function to be of the form

$$\psi(t,x^i,r) = e^{-i\omega t+ikx^1}u(r) = e^{-i\omega t+ikx^1}\begin{pmatrix} u_1^+(r) \\ u_2^+(r) \\ u_1^-(r) \\ u_2^-(r) \end{pmatrix}. \tag{4.10}$$

Because of rotational invariance in the $\vec{x}$ direction, we can assume that the momentum is in the $+x^1$ direction: that is, $k>0$. With this ansatz, Dirac's equation can be written as

$$\left[e^{-B}\sqrt{h}\Gamma^{\underline{r}}\partial_r + ie^{-A}\left(k\Gamma^{\underline{1}} - \frac{\omega+q\Phi}{\sqrt{h}}\Gamma^{\underline{0}}\right) + \frac{8hA'+h'}{4\sqrt{h}e^B}\Gamma^{\underline{r}} - m\right]u = 0\,. \tag{4.11}$$

To find fermion normal modes we need to solve (4.11) with the appropriate boundary conditions at $r=0$ and look for values of the parameters for which u grows more slowly as $r\to+\infty$ than the generic solution.

To decide on the boundary conditions at $r=0$, we can solve (4.11) near $r=0$ using series expansions. The form of the expansion depends crucially on whether ω is zero or non-zero. We expect normal modes only at $\omega=0$, since for $\omega\neq 0$ the solutions exhibit a non-zero flux in the r direction, so let us consider the zero frequency case. The series expansion are then of the form

$$u = Ur^{-\frac{7}{6}+\frac{|k|}{|\Omega|}}\left(1+O\big(r^{1/3}\big)\right) + Vr^{-\frac{7}{6}-\frac{|k|}{|\Omega|}}\left(1+O\big(r^{1/3}\big)\right) \qquad (\omega=0)\,, \tag{4.12}$$

where $\Omega=\sqrt{2}Q/L^2$ is the chemical potential at zero temperature. The subleading terms have series expansions in integer powers of $r^{1/3}$ that can easily be found. The equation of motion also allows us to write the $3,4$ components of the constant spinors U and V algebraically in terms of their $1,2$ components, but the exact form of that relationship won't be important. The boundary condition that we will impose is to set V, the coefficient of the most divergent solution, to zero. This amounts to requiring that $\sqrt{-g}\bar{\psi}\psi$ be finite at $r=0$, a property shared by the purely infalling solutions for $\omega\neq 0$. We found numerically that purely infalling solutions for $\omega\neq 0$ approach the zero frequency solutions with $V=0$ as you take $\omega\to 0$.

Let us now consider the behavior of the solutions near the boundary, i.e., as $r \to +\infty$. In this limit, the geometry is AdS_5 with radius of curvature L and the gauge field Φ is a constant, so we can solve (4.11) , obtaining

$$u_a^{\pm} = C_a^{\pm} e^{-\frac{5}{2}A} X_{\mp\frac{1}{2}-mL}\left(\kappa e^{-A}\right) + D_a^{\pm} e^{-\frac{5}{2}A} X_{\pm\frac{1}{2}+mL}\left(\kappa e^{-A}\right) \tag{4.13}$$

where

$$\kappa^2 \equiv L\sqrt{k^2 - (q\Phi + \omega)^2}\,, \tag{4.14}$$

and X_ν is an appropriate Bessel function. If $\kappa^2 > 0$, we should take for κ the positive square root and set $X_\nu = I_\nu$, the modified Bessel function. If $\kappa^2 < 0$, we can either take $\kappa = i\sqrt{(q\Phi + \omega)^2 - k^2}$ or, equivalently, replace κ by $|\kappa|$ in (4.13) and set $X_\nu = J_\nu$.[2] Similarly to what happened for $r = 0$, we can use the equation motion to write C_a^- and D_a^- algebraically in terms of C_a^+ and D_a^+, and are left with 4 independent constants of integration.

Expanding (4.13) at large r, we see that $u_a^+ \propto C_a^+ r^{-2+mL}$, and we therefore identify normal modes with solutions of (4.11) with $V = 0$ for which $C_1^+ = C_2^+ = 0$, i.e., for which the coefficient of the most divergent solution near the boundary is zero. Note that the structure of (4.11) means that u_1^+ only couples to u_2^- and u_2^+ only to u_1^-, so it is consistent to set $u_2^+ = u_1^- = 0$ (or $u_1^+ = u_2^- = 0$) and look simply for zeros of C_1^+ (or, resp. C_2^+). These normal modes correspond to poles of the retarded Green's function [57], with normal modes with nonzero u_1^+ (or nonzero u_2^+) corresponding to poles of G_{11} (or poles of G_{22}, resp.). More concretely, if we choose the boundary term in the action (4.8) to be

$$S_{\text{bdy}} = -i \int\limits_{r=1/\varepsilon} d^4x\,\sqrt{-gg^{rr}}\,\bar{\psi}_+\psi_-\,, \qquad \psi_\pm \equiv \frac{1}{2}\left(1 \pm \Gamma^{\underline{r}}\right)\psi\,, \tag{4.15}$$

where ε is a positive quantity to be taken to zero after functional derivatives are taken, then

[2] We are assuming that $\nu \notin \mathbb{Z}$, so that J_ν and $J_{-\nu}$ are linearly independent. For $\nu \in \mathbb{Z}$, the X_ν should be built out of J_ν and Y_ν.

ψ is dual to a positive chirality Weyl spinor[3] and the retarded Green's function is given by

$$G_R = \left(\frac{\kappa}{2}\right)^{2mL} \frac{\Gamma\left(\frac{1}{2} - mL\right)}{\Gamma\left(\frac{1}{2} + mL\right)} \begin{pmatrix} -i\frac{D_2^-}{C_1^+} & 0 \\ 0 & i\frac{D_1^-}{C_2^+} \end{pmatrix} . \tag{4.16}$$

Before giving a concrete example of a normal mode, let's consider two heuristic constraints on suitable values of k. First, we expect that $\kappa^2 < 0$, which for $\omega = 0$ reduces to

$$|k| < k_{\text{max}} \equiv L|q\Omega| \,. \tag{4.17}$$

We arrive at this condition by noting that if $\kappa^2 > 0$, then for a normal mode at large r, $u_a^+ \propto e^{-\frac{5}{2}A} I_{\frac{1}{2}+mL}\left(\kappa e^{-A}\right)$, and so u_a^+ increases monotonically (and eventually exponentially in e^{-A}) as one goes down into AdS_5. It is hard to see how this asymptotic behavior would match onto a solution that is normalizable at $r = 0$. On the other hand, if $\kappa^2 < 0$, $u_a^+ \propto e^{-\frac{5}{2}A} J_{\frac{1}{2}+mL}\left(|\kappa| e^{-A}\right)$ at large r, which is oscillatory and there is no apparent obstruction to the matching. Because the asymptotic behaviors we described are only approximations to u, one cannot take the bound (4.17) as rigorous.

Second, we prefer to investigate wave-numbers k such that the leading power in (4.12) is positive, i.e. obeying

$$|k| > k_{\text{min}} \equiv \frac{7}{6}|\Omega| \,. \tag{4.18}$$

This condition simply ensures that ψ does not diverge at $r = 0$. While this is not strictly necessary, it is convenient numerically and helps ensure the absence of back-reaction. Conditions (4.18) and (4.17) have nonzero intersection only if $q > q_{\text{min}} \equiv \frac{7}{6L}$. So, as a specific example, we consider the following choice of parameters:

$$L = 1 \qquad m = 0 \qquad Q = 1 \qquad q = 2 \,. \tag{4.19}$$

$L = 1$ is a choice of units. $Q = 1$ corresponds to $\Omega = \sqrt{2}$, and $q = 2$ satisfies the bound $q > q_{\text{min}}$.

[3]We could have made a different choice for S_{bdy}, with $\psi_+ \leftrightarrow \psi_-$. With this choice, ψ is dual to a negative chirality Weyl spinor, and the formula for the Green's function is slightly different.

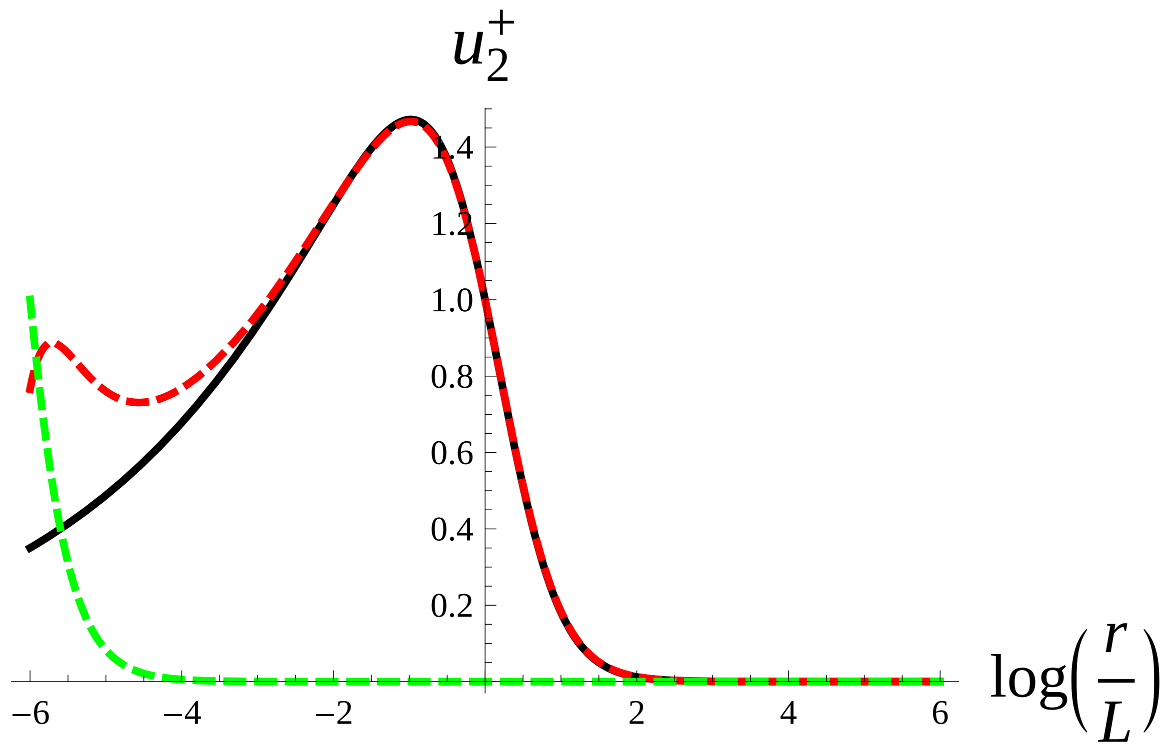

Figure 4.1: A normal mode with u_2^+ nonzero (corresponding to a pole in G_{22}) for $m = 0$, $Q/L = 1$, $q/L = 2$ and $k/\Omega = 3/2$. The solid line corresponds to u_2^+, which is purely real. For this normal mode u_1^+ and u_2^- are exactly zero and u_1^- is purely imaginary (the analytical forms are given in (4.20)). The dashed lines show the real (Red) and imaginary (Green) parts of the purely infalling solution for $L\omega = 10^{-3}$. Note that they match away from $r = 0$ and differ for small r, where the terms proportional to ω in (4.11) become dominant.

To find a normal mode with this choice of parameters, our approach was to numerically integrate (4.11) with initial conditions given by the $r = 0$ series expansion (with first term given by (4.12) with $V = 0$) at some small but finite r. The near boundary coefficients C_a^+ where then extracted by evaluating the Wronskian of the numerical solution with the boundary solution (4.13) and k was varied until a zero was found. The range allowed by (4.17) and (4.18) is $\frac{7}{6} \leq \frac{k}{\Omega} \leq 2$. We found a normal mode with u_2^+ nonzero in this range and were even able to write it down in closed form! The normal mode occurs for $k/\Omega = 3/2$

(see Fig. 4.1), and is given by

$$
\begin{aligned}
u_2^+ &= \frac{2r^{\frac{1}{3}}}{(1+r^2)^{\frac{1}{6}}(2+r^2)^{\frac{5}{4}}}\left(\sqrt{2+r^2}-r\right)^{\frac{1}{2}} \\
u_1^- &= \sqrt{2}i\frac{2r^{\frac{1}{3}}}{(1+r^2)^{\frac{1}{6}}(2+r^2)^{\frac{5}{4}}}\left(\sqrt{2+r^2}-r\right)^{-\frac{1}{2}} ,
\end{aligned}
\tag{4.20}
$$

and $u_1^+ = u_2^- = 0$. It is easy to verify this is a solution of (4.11), and expanding it at small r we obtain $u_2^+ = r^{\frac{1}{3}} + O(r^{\frac{4}{3}})$, which shows that $V = 0$ (cf. (4.12)). If we expand it at large r, we find $u_2^+ = 2r^{-3} + O(r^{-4})$, and this shows that $C_2^+ = 0$ (if it were nonzero, there would be a term proportional to r^{-2}) and so that (4.20) is in fact a normal mode.

One can understand the simple analytic form of the charged dilatonic black hole solution (4.2) as a consequence of its relation to spinning D3-branes. The analytic form of the normal mode (4.20) is more mysterious, since neither the action (4.8) nor the choice of parameters (4.19) was drawn from string theory.

4.2 A thermodynamic instability

Now let us turn to the question of embedding (4.1) and the solution (4.2) into string theory. We will treat this embedding in two steps. First, in this section, we will discuss embedding of (4.1) in maximal gauged supergravity. From this embedding, one can already see the thermodynamic instability mentioned in the beginning of this chapter. Then in section 4.3 we will consider the lift to ten dimensions. We note in advance that only a small fraction of this section and the next is original. The rest is a compilation of results from the literature, in particular [58, 59, 53, 50, 56].

The $SO(6)_R$ symmetry of $\mathcal{N} = 4$ SYM corresponds to the rotation group in directions transverse to the D3-branes: that is, rotations of the S^5 factor in $AdS_5 \times S^5$. The Cartan subalgebra of $SO(6)$ is $U(1)^3$. Translationally-invariant states of $\mathcal{N} = 4$ SYM can have three independent commuting R-charge densities corresponding to these three $U(1)$'s. Let's denote these R-charge densities in the field theory as ρ_i. As before, let ϵ and s be the energy and entropy densities in the field theory, and let us define rescaled quantities

$$\hat{\epsilon} \equiv \frac{\epsilon}{N^2} \qquad \hat{s} \equiv \frac{s}{N^2} \qquad \hat{\rho}_i = \frac{\rho_i}{N^2} \,. \tag{4.21}$$

Because of the relation

$$\frac{L^3}{\kappa^2} = \frac{N^2}{4\pi^2} \tag{4.22}$$

for $SU(N)$ $\mathcal{N} = 4$ SYM, the definitions of $\hat{\epsilon}$ and $\hat{s}$ agree with the ones given in (4.3).

The $SO(6)_R$ symmetry of $\mathcal{N} = 4$ SYM is the gauge group of maximal gauged supergravity in five dimensions. The lagrangian of this theory is quite complicated, but a simple truncation of it that includes the $U(1)^3$ Cartan subalgebra is the STU model [58],

$$\mathcal{L} = \frac{1}{2\kappa^2}\left[R - \frac{1}{2}G_{ij}F^i_{\mu\nu}F^{\mu\nu j} - G_{ij}\partial_\mu X^i \partial^\mu X^j - V(X) + \text{Chern-Simons}\right] . \tag{4.23}$$

The Chern-Simons term will not matter for the calculations of this paper. The index i runs from 1 to 3, and the scalars X^i are constrained to satisfy $X^1X^2X^3 = 1$. The target space metric and potential are given by

$$G_{ij} = \frac{1}{2}\,\text{diag}\left\{\frac{1}{(X^1)^2}, \frac{1}{(X^2)^2}, \frac{1}{(X^3)^2}\right\} \qquad V = -\frac{4}{L^2}\sum_{i=1}^{3}\frac{1}{X^i} \,. \tag{4.24}$$

The general translationally invariant black brane solution with unequal electric charges is

$$\begin{aligned}
ds^2 &= -\frac{f}{H^{2/3}}dt^2 + \frac{H^{1/3}}{f}dr^2 + H^{1/3}\frac{r^2}{L^2}d\vec{x}^2 \\
\Phi_i &= \frac{Q_i\sqrt{\mu}}{r^2+Q_i^2} - \frac{Q_i\sqrt{\mu}}{r_H^2+Q_i^2} \qquad X^i = \frac{H^{1/3}}{H_i} \\
f &= -\frac{\mu}{r^2} + \frac{r^2}{L^2}H \qquad H = H_1H_2H_3 \qquad H_i = 1 + \frac{Q_i^2}{r^2}
\end{aligned} \tag{4.25}$$

The horizon radius r_H is determined as the largest root of f. One straightforwardly finds

$$\hat{\epsilon} = \frac{3\mu}{8\pi^2L^6} \qquad \hat{s} = \frac{r_H\sqrt{\mu}}{2\pi L^5} \qquad \hat{\rho}_i = \frac{Q_i\sqrt{\mu}}{4\pi^2L^5} \,. \tag{4.26}$$

To recover (4.1) from (4.23), we set

$$A^3_\mu = 0 \qquad A^1_\mu = A^2_\mu = A_\mu/\sqrt{2} \qquad X^1 = X^2 = e^{-2\alpha} \qquad X^3 = e^{4\alpha} \,. \tag{4.27}$$

It is now easy to check that the solution (4.2) and its thermodynamics (4.3) are recovered from (4.25) and (4.26) by setting

$$Q_3 = 0 \qquad Q_1 = Q_2 = Q \qquad \hat{\rho}_3 = 0 \qquad \hat{\rho}_1 = \hat{\rho}_2 = \frac{\hat{\rho}}{\sqrt{2}} \,. \tag{4.28}$$

It may seem odd that there is no factor of $\sqrt{2}$ between Q_1 and Q. This can be understood as a convention on the normalization of the Q_i. Q and the Q_i are really length scales in the five-dimensional geometries, not charge densities per se, so their normalization is essentially arbitrary.

The relations (4.26) parametrize the equation of state. Following [53], one may make this parameterization more efficient by defining

$$y = \frac{r}{\sqrt[4]{\mu L^2}} \qquad y_H = \frac{r_H}{\sqrt[4]{\mu L^2}} = \frac{3^{3/4}}{2^{5/4}\sqrt{\pi}} \frac{\hat{s}}{\hat{\epsilon}^{3/4}} \qquad y_i = \frac{Q_i}{\sqrt[4]{\mu L^2}} = \frac{3^{3/4}\sqrt{\pi}}{2^{1/4}} \frac{\hat{\rho}_i}{\hat{\epsilon}^{3/4}} \,. \tag{4.29}$$

Then the condition that $f = 0$ at $r = r_H$ becomes

$$(y_1^2 + y_H^2)(y_2^2 + y_H^2)(y_3^2 + y_H^2) - y_H^2 = 0 \,. \tag{4.30}$$

The equation (4.30) is a relation among the dimensionless ratios $\hat{s}/\hat{\epsilon}^{3/4}$ and $\hat{\rho}_i/\hat{\epsilon}^{3/4}$, and as such it is all the scale-invariant information available about the equation of state. One can solve it explicitly for y_H, and from that solution extract an expression for $\hat{s}$ in terms of $\hat{\epsilon}$ and $\hat{\rho}_i$. This expression is quite complicated because it involves solving a general cubic equation. A considerably easier procedure is to define new variables

$$x_i \equiv \frac{y_i}{y_H} = 2\pi \frac{\hat{\rho}_i}{\hat{s}} \tag{4.31}$$

and note that (4.30) becomes

$$\frac{1}{y_H^4} = (1 + x_1^2)(1 + x_2^2)(1 + x_3^2) \,. \tag{4.32}$$

This can be converted immediately into a simple expression for $\hat{\epsilon}$ in terms of $\hat{s}$ and $\hat{\rho}_i$. For the two charge case, this expression is

$$\begin{aligned} \hat{\epsilon} &= \frac{3}{2^{5/3}\pi^{2/3}} \sqrt[3]{(\hat{s}^2 + 4\pi^2\hat{\rho}_1^2)(\hat{s}^2 + 4\pi^2\hat{\rho}_2^2)} \\ &\approx \frac{3\pi^{2/3}}{2^{1/3}} (\hat{\rho}_1\hat{\rho}_2)^{2/3} \left[1 + \left(\frac{1}{\hat{\rho}_1^2} + \frac{1}{\hat{\rho}_2^2} \right) \frac{\hat{s}^2}{12\pi^2} + O(s^4) \right] \,, \end{aligned} \tag{4.33}$$

where in the second line we have passed to the near-extremal limit, where the entropy density is much smaller than the charge densities. From the fact that the leading dependence of $\hat{\epsilon}$ on $\hat{s}$ near extremality is quadratic, it follows immediately that the entropy density is linear in the temperature close to extremality. More explicitly, one can solve $T = \partial\hat{\epsilon}/\partial\hat{s}$ for $\hat{s}$ to find

$$\hat{s} \approx (2\pi)^{4/3} \frac{(\hat{\rho}_1\hat{\rho}_2)^{4/3}}{\hat{\rho}_1^2 + \hat{\rho}_2^2} T \qquad \text{for low } T. \tag{4.34}$$

(4.34) generalizes (4.6) to the case of unequal charges.

The equation of state (4.33) encodes a thermodynamic instability, which is a special case of the Gregory-Laflamme type instabilities found in [53]. To see it in a simple way, let us rewrite (4.33) as

$$\hat{\epsilon} = \frac{3}{2^{5/3}\pi^{2/3}} \sqrt[3]{(\hat{s}^2 + 2\pi^2(\hat{\rho} - \hat{\rho}_z)^2)(\hat{s}^2 + 2\pi^2(\hat{\rho} + \hat{\rho}_z)^2)}\,, \tag{4.35}$$

where we have defined

$$\begin{pmatrix} \hat{\rho} \\ \hat{\rho}_z \end{pmatrix} = \frac{1}{\sqrt{2}} \begin{pmatrix} 1 & 1 \\ -1 & 1 \end{pmatrix} \begin{pmatrix} \hat{\rho}_1 \\ \hat{\rho}_2 \end{pmatrix}. \tag{4.36}$$

Local thermodynamic stability is the condition that $\hat{\epsilon}$ is concave up as a function of the extensive thermodynamic variables $\hat{s}$ and $\hat{\rho}_i$. One therefore calculates the Hessian matrix

$$\frac{\partial^2\hat{\epsilon}}{\partial(\hat{s},\hat{\rho},\hat{\rho}_z)^2} \equiv \begin{pmatrix} \frac{\partial^2\hat{\epsilon}}{\partial\hat{s}^2} & \frac{\partial^2\hat{\epsilon}}{\partial\hat{s}\partial\hat{\rho}} & \frac{\partial^2\hat{\epsilon}}{\partial\hat{s}\partial\hat{\rho}_z} \\ \frac{\partial^2\hat{\epsilon}}{\partial\hat{\rho}\partial\hat{s}} & \frac{\partial^2\hat{\epsilon}}{\partial\hat{\rho}^2} & \frac{\partial^2\hat{\epsilon}}{\partial\hat{\rho}\partial\hat{\rho}_z} \\ \frac{\partial^2\hat{\epsilon}}{\partial\hat{\rho}_z\partial\hat{s}} & \frac{\partial^2\hat{\epsilon}}{\partial\hat{\rho}_z\partial\hat{\rho}} & \frac{\partial^2\hat{\epsilon}}{\partial\hat{\rho}_z^2} \end{pmatrix} = \frac{3}{8}\left(\frac{\hat{s}}{\hat{\epsilon}}\right)^2 \begin{pmatrix} \frac{2+3x_\rho^2}{2\pi^2} & -\frac{2x_\rho}{\pi} & 0 \\ -\frac{2x_\rho}{\pi} & 6 + x_\rho^2 & 0 \\ 0 & 0 & 6 - 3x_\rho^2 \end{pmatrix}, \tag{4.37}$$

where the last expression is valid only for $\hat{\rho}_z = 0$, and we have defined

$$x_\rho \equiv 2\pi\frac{\hat{\rho}}{\hat{s}}\,. \tag{4.38}$$

The $(\hat{s},\hat{\rho})$ block of the Hessian matrix is positive definite for all values of x_ρ, but evidently $\partial^2\hat{\epsilon}/\partial\hat{\rho}_z^2$ goes smoothly from positive to negative values as x_ρ increases through the value $\sqrt{2}$. Thus $x_\rho = \sqrt{2}$ is the boundary of thermodynamic stability, and the instability arises on the low temperature, high charge density side of it. Correspondingly, if one defines conjugate variables Ω and Ω_z dual to $\hat{\rho}$ and $\hat{\rho}_z$, and also a rescaled free energy density

$$\hat{f} = \hat{\epsilon} - T\hat{s} - \Omega\hat{\rho} - \Omega_z\hat{\rho}_z\,, \tag{4.39}$$

then the matrix of susceptibilities $\partial^2 \hat{f}/\partial(T,\Omega,\Omega_z)^2$ is minus the inverse of $\partial^2\hat{\epsilon}/\partial(\hat{s},\hat{\rho},\hat{\rho}_z)^2$. In particular, the $\hat{\rho}_z$ susceptibility is

$$\hat{\chi}_z \equiv -\frac{\partial^2 \hat{f}}{\partial \Omega_z^2} = \frac{1}{\partial^2\hat{\epsilon}/\partial\hat{\rho}_z^2} = \frac{8}{9}\left(\frac{\hat{\epsilon}}{\hat{s}}\right)^2 \frac{1}{2-x_\rho^2} = \frac{4}{9}\frac{\hat{\epsilon}^2}{\hat{s}^2 - 2\pi^2\hat{\rho}^2} \approx \frac{\sqrt{2}\,\hat{\rho}/3\pi}{T-T_c}\,, \tag{4.40}$$

where

$$T_c = \frac{\Omega}{\sqrt{2}\,\pi}\,. \tag{4.41}$$

The approximate equality in (4.40) is accurate near T_c. The behavior of $\hat{\chi}_z$ is reminiscent of mean-field ferromagnetism.

It is worth remarking that the off-diagonal charge $\hat{\rho}_z$ is actually one component of an $SU(2)$ triplet of charges, call them $(\hat{\rho}_x,\hat{\rho}_y,\hat{\rho}_z)$. To see this, recall first that that $U(1)^3$ charges $(\hat{\rho}_1,\hat{\rho}_2,\hat{\rho}_3)$ are embedded in $SU(4)_R \approx SO(6)_R$ as the Cartan subalgebra. When all of them are non-zero and equal (i.e. for RNAdS_5), a symmetry $U(3) \subset SU(4)_R$ is preserved. This $U(3)$ is the one which acts on the three complex scalars of $\mathcal{N}=4$ SYM as a triplet. When one sets $\hat{\rho}_3 = 0$, this $U(3)$ is broken to $U(2)\times U(1)$. The $U(1)$ inside $U(2)$ (that is, its center) corresponds to the charge $\hat{\rho}$, while the J_z generator of $SU(2)$ (in a conventional Pauli basis) corresponds to $\hat{\rho}_z$. The other generators of $SU(2)$ correspond to $\hat{\rho}_x$ and $\hat{\rho}_y$. Note that the $SU(2)$ under discussion is a global flavor symmetry in the boundary theory, making it more similar to isospin than to intrinsic angular momentum of particles. The susceptibilities $\hat{\chi}_x$ and $\hat{\chi}_y$ are identical to $\hat{\chi}_z$ when $\hat{\rho}_x = \hat{\rho}_y = \hat{\rho}_z = 0$. So the instability (4.40) involves a spontaneous breaking of the $SU(2)$ symmetry. One should expect the typical state to involve non-zero $(\hat{\rho}_x,\hat{\rho}_y,\hat{\rho}_z)$ pointing in different directions in different parts of space. Topological defects may even be possible. The main difficulty is that there is little to no understanding about the endpoint of evolution of the thermodynamic instability. At linear order, in a region where only $\hat{\rho}_z$ becomes non-zero, what is happening is that $\hat{\rho}_1$ and $\hat{\rho}_2$ become slightly unequal without otherwise changing the thermodynamics.

As explained in [60, 61], thermodynamic instabilities correspond to dynamical instabilities in the real-time geometry. In the present case, where the instability relates (at linear order) only to the development of an $SU(2)$ charge and not to a spatial modulation of the entropy density, the dynamical instability should involve only matter fields in the bulk, not the metric. The pertinent matter fields should be the $SU(2)$ gauge field and certain scalars that couple to it through its kinetic term. In the case of the instability toward developing non-zero $\hat{\rho}_z$, the only gauge field involved is $A^1_\mu - A^2_\mu$, and the only scalar involved is X^1/X^2. Because the instability relates to thermodynamics, it should be present at arbitrarily small wave-number. Presumably it ceases to exist at a critical wave-number, $k_{\rm GL}$, comparable to the chemical potential Ω.

4.3 A ten-dimensional lift

As we have already remarked, the charged dilatonic black hole has a naked singularity at $r = 0$. We should study the ten-dimensional lift via maximal gauged supergravity to find out if this singularity has an obvious resolution. This lift is well known [50]: for the general three-charge black hole (4.25), it is

$$
\begin{gathered}
ds_{10}^2 = \sqrt{\Delta}\left[-\frac{f}{H}dt^2 + \frac{dr^2}{f} + \frac{r^2}{L^2}d\vec{x}^2\right] + \frac{1}{\sqrt{\Delta}}\sum_{i=1}^{3} H_i\left(L^2 d\mu_i^2 + \mu_i^2\left[L d\phi_i + \frac{\sqrt{\mu}}{Q_i}\left(\frac{1}{H_i} - 1\right)dt\right]^2\right) \\
F_5 = G_5 + *G_5 \qquad G_5 = dB_4 \qquad B_4 = -\frac{r^4}{L^4}\Delta dt\wedge d^3x - \sum_{i=1}^{3}\frac{Q_i\sqrt{\mu}}{L}\mu_i^2 d\phi_i \wedge d^3x\,.
\end{gathered}
\tag{4.42}
$$

In addition to the functions f, H, and H_i appearing in (4.25), we have defined

$$
\Delta = H\sum_{i=1}^{3}\frac{\mu_i^2}{H_i} \qquad \mu_1 = \cos\theta_1\cos\theta_2 \qquad \mu_2 = \cos\theta_1\sin\theta_2 \qquad \mu_3 = \sin\theta_1\,. \tag{4.43}
$$

Evidently, $\mu_1^2 + \mu_2^2 + \mu_3^2 = 1$, so (θ_1, θ_2) are coordinates on S^2. The S^5, parametrized by $(\theta_1, \theta_2, \phi_1, \phi_2, \phi_3)$, is thus regarded as a T^3 fibration over S^2. If we set $Q_1 = Q_2 = Q$, $Q_3 = 0$, and $\mu = Q^4/L^2$ (the last corresponding to the extremal limit) and approach the horizon at $r = 0$, the solution takes the following form:

$$\begin{aligned} ds^2_{10,\text{near}} &= |\mu_3| \left(-\frac{2r^2}{L^2} dt^2 + \frac{L^2}{2r^2} dr^2 + \frac{r^2 L^2}{Q^2} d\phi_3^2 \right) + |\mu_3| \frac{Q^2}{L^2} d\vec{x}^2 \\ &\quad + \frac{1}{|\mu_3|} \left[L^2 d\mu_1^2 + L^2 d\mu_2^2 + \mu_1^2 \left(L d\phi_1 - \frac{Q}{L} dt \right)^2 + \mu_2^2 \left(L d\phi_2 - \frac{Q}{L} dt \right)^2 \right] \\ B_{4,\text{near}} &= -\frac{Q^3}{L^3} \left[\mu_1^2 \left(L d\phi_1 - \frac{Q}{L} dt \right) + \mu_2^2 \left(L d\phi_2 - \frac{Q}{L} dt \right) \right] \wedge d^3 x \,. \end{aligned} \tag{4.44}$$

Intriguingly, the metric has an AdS_3 factor, suggesting that the infrared dynamics is controlled by a 1+1-dimensional conformal field theory. The rest of the metric, on any given time slice, is a sum of two conformally flat pieces, where the conformal factors, $|\mu_3| = \sqrt{1 - \mu_1^2 - \mu_2^2}$ or its reciprocal, are finite and non-zero only on the interior of the unit disk in the μ_1-μ_2 plane. The locus of points where $\mu_3 = 0$, and where the metric (4.44) is ill-defined, corresponds to the equator of S^2, and to an equatorial S^3 of S^5. The geometry (4.44) in fact splits into two identical pieces, joined along this S^3. Each is a warped product of AdS_3, $\mathbf{R}^3$, and the unit ball in $\mathbf{R}^4$, where the unit ball spins rigidly and equally in the two independent planes of $\mathbf{R}^4$.

It is not entirely surprising to find an AdS_3 factor in the near-horizon geometry. Following [62], we note that angular momentum in the S^5 directions can be carried by D3-branes wrapped on various three-spheres in that S^5. These wrapped D3-branes, called "giant gravitons," have as their field theory dual operators which are determinants or sub-determinants of one of the three complex adjoint scalar fields of $\mathcal{N} = 4$ SYM [63], which we will denote Z_1, Z_2, and Z_3. More specifically: $\det Z_i$ corresponds to a D3-brane wrapped on the equatorial S^3 of S^5 found by intersecting the hyperplane $z_i = 0$ with the sphere $\sum_{j=1}^3 |z_j|^2 = L^2$ in $\mathbf{C}^3$. It was suggested in [64] that a large enough number of giant gravitons of one type (say, the type associated with Z_1) could be described by an $AdS_5 \times S^5$ geometry that they create around themselves. Now consider a configuration with both $\det Z_1$ and $\det Z_2$ giant gravitons. They intersect along an equatorial S^1 of S^5, defined by intersecting $z_1 = z_2 = 0$ with $\sum_{i=1}^3 |z_i|^2 = L^2$. The low-energy dynamics at the intersection is plausibly a 1+1-dimensional CFT whose central charge is proportional to the product of the number of giant gravitons of each type, in analogy to how D3-branes on orthogonal cycles of T^4 intersect over the "effective string" of [65, 66]. This CFT, we presume, is dual to the AdS_3 factor in (4.44).

The full story is presumably somewhat more complicated than the intersecting equatorial D3-branes described in the previous paragraph. In particular, it is known [67] that a singular, supersymmetric relative of the solutions (4.42) can be understood in terms of three orthogonal sets of giant gravitons with a distribution of sizes. Moreover, in the treatment of [67], black holes with horizons have finite μ, and so are finitely far from the supersymmetric case, where $\mu = 0$.

The presence of an AdS_3 factor fits nicely with the linear specific heat, since all $1+1$-dimensional CFT's have linear specific heat: that's simply on account of the fact that entropy density, as a dimension one object, must scale linearly with the only available energy scale, namely temperature. On the gravity side, the near-extremal generalization of (4.44) involves the AdS_3-Schwarzschild geometry:

$$\begin{aligned} ds^2_{10,\text{near}} = |\mu_3| \left(-\frac{2(r^2 - r_H^2)}{L^2} dt^2 + \frac{L^2}{2(r^2 - r_H^2)} dr^2 + \frac{r^2 L^2}{Q^2} d\phi_3^2 \right) + |\mu_3| \frac{Q^2}{L^2} d\vec{x}^2 \\ + \frac{1}{|\mu_3|} \left[L^2 d\mu_1^2 + L^2 d\mu_2^2 + \mu_1^2 \left(L d\phi_1 - \frac{Q}{L} dt \right)^2 + \mu_2^2 \left(L d\phi_2 - \frac{Q}{L} dt \right)^2 \right] , \end{aligned} \tag{4.45}$$

with B_4 unchanged from (4.44). Like (4.44), (4.45) is not only a limiting form of a solution of the equations of motion of type IIB supergravity; it is by itself a solution of those equations, away from $\mu_3 = 0$.

From the $1+1$-dimensional CFT perspective, the ground state entropy of the three-charge black hole in AdS_5 arises from partitioning a specified amount of momentum along the effective string into excitations of one chiral half of the theory, while leaving the other chiral half in its vacuum state. The Virasoro algebra acting on the AdS_2 factor of the near-horizon RNAdS_5 geometry is probably the same as the one from the chiral half of the effective string CFT that remained in its ground state.

In our discussion of ten-dimensional lifts, we seem to have committed ourselves to the maximally supersymmetric case, which seems unlikely to have much to do with Fermi liquids given that there are massless charged scalars in the gauge theory. Other lifts to ten dimensions may be possible, with reduced supersymmetry, as in [28]; and some of these lifts could be dual to a CFT with no charged scalars, or no gauge-invariant operators built from charged scalars that can condense. However, a fermionic field theory description may be closer to hand than it appears in the maximally supersymmetric case: at least in the case of a single charge, one can show [68] that BPS solutions are classified in terms of free fermions. Our limiting solution (4.44) is fairly similar to the ansatz of [68]. It is tempting to think it preserves some fraction of supersymmetry, and that there might be an analogous fermionic description. If there is such a description, the fermions probably emerge from the dynamics of eigenvalues of large N matrices, as in the $c = 1$ matrix model.

4.4 An AdS_4 example

An obvious extension of the ideas discussed in the previous section to the case of $AdS_4 \times S^7$ is to consider three mutually orthogonal groups of M5-brane giant gravitons, each on an equatorial S^5 in S^7. The triple intersection of M5-branes from each group is an equatorial S^1 in S^7. This intersection is similar to the effective string of [69], and plausibly the low-energy dynamics is a 1+1-dimensional CFT. So one expects in the eleven-dimensional lift of the extremal three-charge AdS_4 black hole to find an AdS_3 factor similar to the form (4.44). One also expects linear specific heat at low temperature. This last expectation is easy to check using just the thermodynamic formulas of [53]—and it is true. Let us consider the general eleven-dimensional geometry, given by [50]

$$\begin{aligned} ds_{11}^2 &= \tilde{\Delta}^{\frac{2}{3}} \left[-\frac{\tilde{f}}{\sqrt{\tilde{H}}} dt^2 + \frac{\tilde{r}^2}{4L^2} \frac{\sqrt{\tilde{H}}}{f} d\tilde{r}^2 + \frac{r^4}{4L^4} \sqrt{\tilde{H}} d\vec{x}^2 \right] \\ &\quad + \frac{4}{\tilde{\Delta}^{\frac{1}{3}} \tilde{H}^{\frac{1}{4}}} \sum_{i=1}^{4} \tilde{H}_i \left(L^2 d\mu_i^2 + \mu_i^2 \left[L d\phi_i - \sqrt{\frac{\mu}{4Q_i}} \left(\frac{1}{H_i} - 1 \right) dt \right]^2 \right) \\ F_4 &= dA_3 \qquad A_3 = -\frac{r^6}{(2L)^6} \tilde{H}^{\frac{3}{4}} \tilde{\Delta} dt \wedge d^2x + \sum_{i=1}^{4} 2\sqrt{\mu Q_i}\, \mu_i^2 d\phi_i \wedge d^2x \,. \end{aligned} \tag{4.46}$$

Here, the μ_i parametrize an S^3, i.e., $\mu_1^2 + \mu_2^2 + \mu_3^2 + \mu_4^2 = 1$, while the ϕ_i parametrize a T^4. Together, these coordinates cover an S^7, regarded as a T^4 fibration over S^3. We introduced the functions

$$\tilde{H}_i = 1 + \frac{4LQ_i}{\tilde{r}^2} \qquad \tilde{H} = \tilde{H}_1\tilde{H}_2\tilde{H}_3\tilde{H}_4 \qquad \tilde{\Delta} = \tilde{H}^{1/4}\sum_{i=1}^{4}\frac{1}{\tilde{H}_i} \qquad \tilde{f} = -\frac{\tilde{\mu}}{\tilde{r}} + \frac{\tilde{r}^2}{L^2}\tilde{H}\,. \quad (4.47)$$

Note that (4.46) approaches $AdS_4 \times S^7$ for large $\tilde{r}$, and this is most easily seen by using the radial coordinate $r = \frac{\tilde{r}^2}{2L}$. We are most interested in the three-equal-charge case $Q_1 = Q_2 = Q_3 = Q$ and $Q = 0$. The extremal limit then corresponds to taking $\tilde{\mu} = \frac{Q^6}{2L^5}$, and near horizon limit of the resulting geometry is given by

$$\begin{aligned} ds^2_{11,\text{near}} &= |\mu_4|^{4/3}\left(-\frac{3Q\tilde{r}^2}{4L^3}dt^2 + \frac{4L^2}{3r^2}dr^2 + \frac{Lr^2}{Q}d\phi_4^2\right) + |\mu_4|^{4/3}\frac{Q^2}{L^2}d\vec{x}^2 \\ &\quad + \frac{4}{|\mu_4|^{2/3}}\left[\sum_{i=1}^{3} L^2 d\mu_i^2 + \mu_i^2\left(Ld\phi_i + \frac{Q}{2L}dt\right)^2\right] \\ A_{3,\text{near}} &= \frac{Q^3}{L^3 s}\sum_{i=1}^{3}\mu_i^2\left[dt + \frac{2L^2}{Q}d\phi_i\right] \wedge d^2x\,, \end{aligned} \qquad (4.48)$$

where we emphasize that the sums extend to $i = 3$ only. As expected, we find an AdS_3 factor.

When reduced to four dimensions, the geometry (4.46) gives rise to multiply charged black holes. The minimal four dimensional lagrangian that has the three-equal-charge black hole we are interested in as a solution is [61]

$$\mathcal{L} = \frac{1}{2\kappa^2}\left[R - \frac{1}{4}e^{\alpha}F_{\mu\nu}^2 - \frac{3}{2}(\partial_\mu\alpha)^2 + \frac{6}{L^2}\cosh\alpha\right]\,, \qquad (4.49)$$

and the four dimensional geometry is given by

$$\begin{aligned} ds^2 &= e^{2A}(-hdt^2 + d\vec{x}^2) + \frac{e^{2B}}{h}dr^2 \qquad F = dA \qquad A_\mu dx^\mu = \Phi dt \\ A &= \log\frac{r}{L} + \frac{3}{4}\log\left(1 + \frac{Q}{r}\right) \qquad B = -A \qquad h = 1 - \frac{\mu L^2}{(Q+r)^3} \\ \alpha &= \frac{1}{2}\log\left(1 + \frac{Q}{r}\right) \qquad \Phi = \frac{\sqrt{3Q\mu}}{Q+r} - \frac{\sqrt{3Q}\mu^{\frac{1}{6}}}{L^{\frac{2}{3}}}\,. \end{aligned} \qquad (4.50)$$

The extremal limit of (4.50) now corresponds to taking $\mu = Q^3/L^2$. If we consider a four dimensional Dirac fermion in the extremal limit of(4.50), and with action given by the four dimensional analogue of (4.8), we again find an isolated normal mode. With the conventions of [57] for the Γ matrices and the ansatz (4.10) for ψ, Dirac's equation can be written

$$\left[e^{-B}\sqrt{h}\Gamma^{\underline{r}}\partial_r + ie^{-A}\left(k\Gamma^{\underline{1}} - \frac{\omega+q\Phi}{\sqrt{h}}\Gamma^{\underline{0}}\right) + \frac{6hA'+h'}{4\sqrt{h}e^B}\Gamma^{\underline{r}} - m\right]u = 0\,. \tag{4.51}$$

It is useful to define the chemical potential $\tilde{\Omega} \equiv \sqrt{3}Q/L^2 = -\Phi(+\infty)/L$. For $\omega = 0$, the solutions of (4.51) are approximated near $r = 0$ by

$$u = Ur^{-\frac{5}{8}+\frac{|k|}{|\tilde{\Omega}|}}\left(1+O\big(r^{1/4}\big)\right) + Vr^{-\frac{5}{8}-\frac{|k|}{|\tilde{\Omega}|}}\left(1+O\big(r^{1/4}\big)\right) \qquad (\omega=0)\,, \tag{4.52}$$

and as before, we impose the boundary condition $V = 0$. Near the boundary, we now have

$$u_a^{\pm} = C_a^{\pm}e^{-2A}X_{\mp\frac{1}{2}-mL}\left(\kappa e^{-A}\right) + D_a^{\pm}e^{-2A}X_{\pm\frac{1}{2}+mL}\left(\kappa e^{-A}\right), \tag{4.53}$$

with κ and X_ν the same as in the five dimensional case. Normal modes are then solutions of (4.51) with $V = 0$ and $C_a^+ = 0$, and correspond to poles of the Green's function. They can easily be found numerically, for example, in units where $L = 1$, we take $m = 0$, $Q = 1$ (corresponding to $\tilde{\Omega} = \sqrt{3}$) and $q = 2$ and find a normal mode with u_2^+ nonzero for $k/\tilde{\Omega} \approx 1.26746$.

4.5 Scaling solutions

Truncations of supergravity actions to abelian gauge fields plus neutral scalars often take the form

$$\mathcal{L} = \frac{1}{2\kappa^2}\left[R - \frac{1}{4}\sum_a f_a(\vec{\phi})(F^a_{\mu\nu})^2 - \frac{1}{2}\partial_\mu\vec{\phi}\cdot\partial^\mu\vec{\phi} - V(\vec{\phi})\right], \tag{4.54}$$

where the functions $f_a(\vec{\phi})$ and $V(\vec{\phi})$ are linear combinations of exponentials of the form $e^{\vec{\beta}\cdot\vec{\phi}}$, where $\vec{\beta}$ is a vector of constants. Examples involving only scalars were explored in some depth in [70]. There it was argued that in typical near-extremal solutions, the scalars run away in a definite direction where one term in $V(\vec{\phi})$ dominates, or where several terms dominate over all others and stand in fixed ratio with themselves. In other words, to understand typical near-extremal dynamics, it is enough to consider a single canonically normalized real scalar, call it ϕ, with a potential

$$V(\phi) = V_0 e^{\eta\phi}\,, \tag{4.55}$$

where η is a positive constant and V_0 is negative, and ϕ is assumed to diverge to $+\infty$ in the extremal solution. It was argued there that the entropy density scales at low temperature as T^χ, where $\chi = 6/(2-3\eta^2)$ when the bulk geometry is five-dimensional. In this section, we will study charged black holes solutions to the lagrangian

$$\mathcal{L} = \frac{1}{2\kappa^2}\left[R - \frac{f(\phi)}{4}F_{\mu\nu}^2 - \frac{1}{2}(\partial\phi)^2 - V(\phi)\right], \tag{4.56}$$

where $V(\phi)$ is chosen as in (4.55), and

$$f(\phi) = e^{\gamma\phi} \tag{4.57}$$

for some constant γ. We again assume that the bulk is five-dimensional. The large α behavior of the theory (4.1) that we started with corresponds to $\eta = 1/\sqrt{6}$ and $\gamma = \sqrt{2/3}$. Because η and γ are defined in reference to a canonically normalized scalar, their values would change if the scalar kinetic term changes. Renormalization of scalar kinetic terms is commonplace in theories without a high degree of supersymmetry. So it makes sense to work out what happens for arbitrary η and γ.

We start with an ansatz closely related to (4.2):

$$ds^2 = L^2\left[e^{2A}\left(-h\,dt^2 + d\vec{x}^2\right) + \frac{dr^2}{h}\right] \qquad A_\mu dx^\mu = L\Phi\,dt\,, \tag{4.58}$$

where it is assumed that A, h, Φ, and ϕ depend only on r. L is, at this stage, an arbitrary length scale, present in order to render the coordinates $(t, \vec{x}, r)$ dimensionless. Following [71], one can construct a Noether charge

$$\mathcal{Q} \equiv e^{2A}\left(e^{2A}h' - f(\phi)\Phi\Phi'\right). \tag{4.59}$$

$\mathcal{Q}$ is independent of r when the equations of motion are obeyed. Moreover, evaluating $\mathcal{Q}$ at the horizon, where Φ is required to vanish, shows that $\mathcal{Q} = 2\kappa^2 Ts$. So $\mathcal{Q} = 0$ is an extremality condition.

The Maxwell equation can be solved directly, leading to

$$\Phi' = \frac{\rho}{e^{2A}f(\phi)}, \tag{4.60}$$

where ρ is a dimensionless version of charge density. The result (4.60) holds for any choice of $f(\phi)$. When we make the simple choices (4.55) and (4.57), the following solutions to the equations of motion can be found by inspection:

$$\begin{aligned} A &= \frac{1}{6}(\gamma+\eta)^2 \log r \\ \phi &= -(\gamma+\eta)\log r \\ \Phi &= \frac{\rho}{\zeta}(r^\zeta - r_H^\zeta) \\ h &= -\frac{2L^2 V_0}{\zeta(2+\gamma^2+\gamma\eta)} r^{1-2(\gamma+\eta)^2/3}(r^\zeta - r_H^\zeta)\,, \end{aligned} \tag{4.61}$$

where we impose the relations

$$\zeta = 1 + \frac{2\gamma^2+\gamma\eta-\eta^2}{3} \qquad \rho = \sqrt{-2V_0 L^2 \frac{2-\gamma\eta-\eta^2}{2+\gamma^2+\gamma\eta}}\,. \tag{4.62}$$

It is easy to check that the solution (4.61) is extremal, in the sense of having $\mathcal{Q}=0$, precisely when $r_H = 0$. When it is non-extremal, one can obtain the following expressions for the horizon entropy density (measured with respect to the dimensionless coordinates $\vec{x}$) and the temperature (measured with respect to the dimensionless time t):

$$s = \frac{2\pi L^3}{\kappa^2} r_H^{(\gamma+\eta)^2/2} \qquad T = -\frac{L^2 V_0}{2\pi} \frac{r_H^{1+(\gamma-5\eta)(\gamma+\eta)/6}}{2+\gamma^2+\gamma\eta}\,. \tag{4.63}$$

Evidently, we have the scaling behavior

$$s \propto T^\chi \qquad \text{where} \qquad \chi = \frac{(\gamma+\eta)^2}{2+(\gamma-5\eta)(\gamma+\eta)/3}\,. \tag{4.64}$$

It is easy to check that plugging in $\eta = 1/\sqrt{6}$ and $\gamma = \sqrt{2/3}$ gives $\chi = 1$. It should be possible to get a wide range of dependences of s on T by choosing more general $V(\phi)$ and $f(\phi)$. For example, one can probably get log-corrected power-law scaling of s on T by altering $V(\phi)$ and/or $f(\phi)$ by powers of ϕ.

The solutions (4.61) are not asymptotically AdS_5. In fact, their asymptotics for large r can be rather peculiar, with h growing faster than e^{2A}. But if a term is added to $V(\phi)$ which makes $\phi = 0$ its global maximum, we expect that asymptotically AdS_5 charged dilatonic black hole solutions will exist whose entropy scales as we have found in (4.64) near extremality. Probably a wide range of such black holes support fermion normal modes similar to the one described in sections 4.1 and 4.4, and so are candidates for holographic duals of generalized Fermi liquids.

4.6 Summary

Let's summarize the properties of the charged dilatonic black hole in AdS_5, given explicitly by (4.2):

- It has linear specific heat at low temperature, like a Fermi gas does.
- It supports a fermion normal mode of the type previously argued to be associated with a Fermi surface. For the choice of parameters we made at the end of section 4.1, the wave-function for the normal mode has a simple closed form.
- Its embedding in $d = 5$ maximal gauged supergravity has a thermodynamic instability toward the development of an $SU(2)$ charge, with a susceptibility that has a singularity like the Curie-Weiss law at finite temperature. This instability is of the Gregory-Laflamme type, and the endpoint of its evolution is unknown.
- The five-dimensional solution has a naked singularity.
- The lift to ten dimensions based on $d = 5$ maximal supergravity describes spinning D3-branes with two of the independent spins equal and the third zero.
- The ten-dimensional geometry near extremality has an AdS_3-Schwarzschild factor which accounts for the linear specific heat and suggests invariance of the infrared dynamics under a non-chiral Virasoro algebra.
- There is an obvious generalization to AdS_4 which realizes most of the same properties.
- An analysis of scaling solutions indicates that power-law behaviors $s \propto T^\chi$ with continuously variable χ can be arranged through simple modifications of the theory on which our original example was based.

The solution (4.2) is non-supersymmetric, except when $\mu = 0$, which is finitely below the extremal limit. The simple form of the near-horizon limit of the 10-dimensional lift suggests that some supersymmetry (perhaps a quarter) may be recovered in this limit. If so, the infrared dynamics would be controlled by a $1+1$-dimensional superconformal field theory. We hope that a better understanding of the dual field theory in the asymptotically $AdS_5 \times S^5$ case can be achieved by studying states with two large commuting R-charges. In a more general setting, the hope is that an explicit construction could be found where the $U(1)$ charge of the black hole is carried only by fermions in the field theory dual. It would be particularly interesting if the exact expression (4.20) we found for the normal mode generalizes to an exact two-point function, because then one would have some analytic control over excitations of a strongly interacting degenerate Fermi liquid in four spacetime dimensions.

Chapter 5

Normalizable fermion modes in a holographic superconductor

As we have discussed in Chapter 3, the Abelian Higgs model in anti-de Sitter space is the most straightforward way to realize superconducting black holes in string theory. Already in [14] it was suggested that the complex scalar should be the dual of an operator which destroys a Cooper pair. However, the dual field theory typically involves both fermions and bosons. For example, in the construction of [28], the dual of the complex scalar is a sum of a fermion bilinear and a scalar trilinear. One might imagine a case where the field theory has no scalars (or, at least, none charged under the global symmetry dual to the $U(1)$ gauge symmetry of the bulk that gets spontaneously broken). Although no such example has been exhibited explicitly, there also isn't any argument we know of that there can't be one.

With fermions in the field theory, one can certainly consider color singlet operators dual to fermions in the bulk: for example, operators schematically of the form $\operatorname{tr} X^n \lambda$ with $n \geq 1$ could be dual to spin-1/2 fermions, and $\operatorname{tr} X^n \lambda\lambda\lambda$ with $n \geq 0$ could be dual to either spin-1/2 or spin-3/2 fermions, depending on how indices are contracted. (More properly, one must anticipate that bulk fermions are dual to a linear combination of operators with an odd number of field theory fermions.) It's difficult to have a bulk fermion dual to an operator with one field theory fermion and nothing else, because it's individual fermions in the field theory aren't gauge singlets. Calculations with fermions [40, 41, 42, 72] have focused on an properties of the two-point function of fermionic operators in the background of a RNAdS black hole, in particular a singularity at finite momentum which has been argued to be evidence of non-Fermi liquid behavior. In the previous Chapter, we extended these studies to different non-superconducting black hole backgrounds.

In this chapter, we wish to study the behavior of spin-1/2 bulk fermions in response to the superconducting AdS_4 domain wall solution discussed in Chapter 3, a zero-temperature geometry whose finite- and low-temperature limits were previously studied in [29]. This domain wall solution has two advantages over the four-dimensional RNAdS solution: 1) RNAdS is unstable toward superconducting instabilities, and the domain wall solution is plausibly the endpoint of the evolution of one such instability; 2) RNAdS has macroscopic entropy at zero temperature which has not found a satisfactory explanation, but the domain wall solution has no entropy at all, at least in the classical supergravity approximation. A technical disadvantage of the domain wall solution is that it is known only numerically, so to study fermions we will have to solve differential equations whose coefficients are known only numerically. According to Chapters 2 and 3 and also based on studies including [27, 71, 73], we expect that domain wall solutions with at least Lorentz invariance in the infrared are fairly generic ground states of the Abelian Higgs model, although Lifshitz scaling in the infrared is another possibility. Domain walls with conformal invariance in both the ultraviolet (UV) and infrared (IR) are under the best theoretical control, since curvatures can be made small everywhere. But we anticipate that arguments presented here could be extended to more general domain wall solutions, and the conclusions might be fairly similar when there is emergent Lorentz symmetry in the infrared.

Ideally, the fermions we should study in the AdS_4 domain wall should be the ones present in maximal $d = 4$ supergravity (or some consistent truncation thereof). There are two reasons we do not do this. The first is simplicity: The quadratic actions for fermions in these theories are complicated, and there appears to be significant mixing between the gravitini and spin-1/2 fermions. The second is flexibility: We will consider different values of the charge and mass of the fermion, and we will see that the final results significantly depend on the choice of these parameters.

The remainder of this chapter is structured as follows. In section 5.1 we briefly review the domain wall background. In section 5.2 we present a semi-classical argument which focuses attention on a compact region of phase space and suggests that the normal modes will lie approximately along segments of hyperbolas. In section 5.3 we numerically solve the Dirac equation for a charged fermion in the AdS_4 domain wall solution, finding one or more bands of fermion normal modes. We conclude with a discussion in section 5.4.

5.1 The bosonic background

The bosonic lagrangian that is the basis for the domain wall background is the four dimensional case discussed in Chapter 3, which we reproduce here for the reader's convenience

$$\begin{aligned}\mathcal{L} = R - \frac{1}{4}F_{\mu\nu}^2 - \frac{1}{2}\left[(\partial_\mu\eta)^2 + \sinh^2\eta\left(\partial_\mu\theta - \frac{1}{L}A_\mu\right)^2\right] \\ + \frac{1}{L^2}\cosh^2\frac{\eta}{2}(7-\cosh\eta)\end{aligned} \tag{5.1}$$

where η is a real scalar, θ is a real pseudoscalar, and we use mostly plus metric conventions. We remind the reader that the domain wall geometry takes the form

$$ds^2 = e^{2A(r)}\left[-h(r)dt^2 + d\vec{x}^2\right] + \frac{e^{2B(r)}dr^2}{h(r)}, \tag{5.2}$$

and has non-zero $\eta(r)$ and gauge field $A_\mu dx^\mu = \Phi(r)dt$. We can always choose coordinates where $B = 0$, and will make this choice in numerical computations but will keep B general in formulae. The scalar potential in (5.1) has two extrema, at $\eta = 0$ and $\eta_{\rm IR} \equiv \log(3+2^{3/2})$, and associated to these are AdS_4 solutions with radii of curvature $L_{\rm UV} = L$ and $L_{\rm IR} = \sqrt{3}L/2$, respectively. The domain wall interpolates between these two AdS geometries. We can choose coordinates such that as $r \to -\infty$

$$A \sim \frac{r}{L_{\rm IR}} \qquad h \sim 1 \qquad \eta \sim \eta_{\rm IR} \qquad \Phi \sim 0\,, \tag{5.3}$$

while as $r \to +\infty$,

$$A \sim \frac{r}{\sqrt{h_{\rm UV}}L_{\rm UV}} \qquad h \sim h_{\rm UV} \qquad \eta \sim 0 \qquad \Phi \sim \Phi_{\rm UV}\,, \tag{5.4}$$

where $h_{\rm UV}$ and $\Phi_{\rm UV}$ can only be determined numerically and are given by $h_{\rm UV} \approx 14.249$ and $\Phi_{\rm UV} = 9.328$. The solution is shown in Fig. 5.1. At a constant r slice the metric is, up to a constant rescaling, the Minkowski metric with an effective "speed of light" given by $v(r) = \sqrt{h(r)}$. The value of $v(r)$ can be changed by a redefinition of the t and x coordinates, but ratios of v at different values of r are invariant. In our choice of coordinates, $v_{\rm IR} \equiv v(-\infty) = 1$ and $v_{\rm UV} \equiv v(+\infty) = 3.775$.

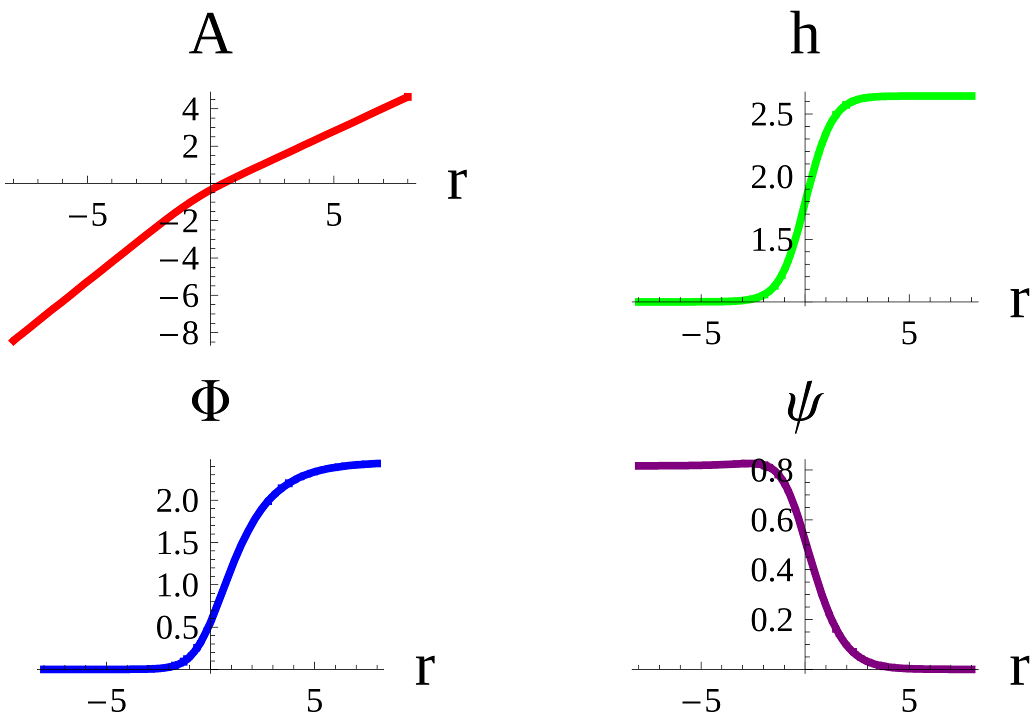

Figure 5.1: The metric, gauge field and scalar field for the domain wall solution in M-theory.

5.2 A semi-classical argument

The fermionic lagrangian that we will consider is

$$\mathcal{L}_f = i\bar{\psi}(\Gamma^\mu D_\mu - m)\psi\,, \tag{5.5}$$

where $D_\mu\psi = \left(\partial_\mu + \frac{1}{4}\omega_\mu{}^{\underline{\rho\sigma}}\Gamma_{\underline{\rho\sigma}} - iqA_\mu\right)\psi$ and $\omega_\mu{}^{\underline{\rho\sigma}}$ is the spin connection. We employ the same conventions on fermions in AdS_4 as in [40], except that we use μ for a curved space index and $\underline{\mu}$ for a tangent space index. We always assume $m \geq 0$.

Much can be learned from the asymptotics of solutions to the Dirac equation following from (5.5) in the UV and IR asymptotic regions. These asymptotics are simple because all one is describing is a free fermion propagating in empty anti-de Sitter space with a constant electrostatic potential Φ. Our discussion here will be somewhat heuristic, relying on replacing the Dirac equation by an on-shell relation which is only justified in a geometric optics limit. We will give a more precise treatment in section 5.3.

The on-shell constraint implied by the Dirac equation is

$$g^{\mu\nu}(k_\mu - qA_\mu)(k_\nu - qA_\nu) + m_{\text{eff}}^2 = 0\,. \tag{5.6}$$

Here $A_\mu = (\Phi, 0, 0, 0)$ and $k_\mu = (-\omega, k_1, k_2, k_r)$. Without loss of generality one can use the rotational symmetry in the x^1-x^2 directions to set $k_2 = 0$ and $k_1 = k \geq 0$. The frequency ω and the momentum k are definite real numbers when we choose the wave-function to take the form $e^{-i\omega t + ikx^1}$ times some function of r. The radial momentum varies as a function of r. The effective mass m_{eff}^2 is the bare mass m^2 plus some contributions from the spin connection and curvatures. In components, (5.6) becomes

$$-\frac{(\omega + q\Phi)^2}{h} + k^2 + e^{2(A-B)}k_r^2 + e^{2A}m_{\text{eff}}^2 = 0\,. \tag{5.7}$$

We next observe that the last term is suppressed in the infrared compared to that first two, unless m_{eff}^2 increases quickly in the infrared. This is impossible if the infrared geometry is anti-de Sitter space: indeed, in that case, m_{eff}^2 is constant in the infrared. In geometries where only Lorentz symmetry is recovered in the infrared, it is possible that m_{eff}^2 does increase very quickly, either because of the contributions from the spin connection and curvatures, or from a dependence of m on some scalar field which diverges as one passes to the extreme infrared. Barring such a circumstance, we see that the sign of k_r^2 is the same in the infrared as the sign of $(\omega + q\Phi)^2/h_{\text{IR}} - k^2$. Limiting ourselves now to the case where $\Phi \to 0$, we see that k_r^2 is non-positive when

$$\frac{|\omega|}{v_{\text{IR}}} \leq k \qquad \text{where} \qquad v_{\text{IR}} = \sqrt{h_{\text{IR}}}\,. \tag{5.8}$$

Now, if k_r were real an non-zero, then its value would be essentially the radial momentum of the fermion. As an extension of standard boundary conditions at a black hole horizon, one may reasonably require this momentum to be infalling (that is, toward the infrared). But it makes no sense for the fermion to be falling down ever further into the infrared when its state is a normal mode. Instead, k_r should be either 0 or imaginary, so that the wave-function of the fermion can decay as one passes further into the infrared. If the infrared geometry is anti-de Sitter, then the decay is very rapid: exponential in $|k_r|e^{-A}$, or power-like in e^{-A} if $k_r = 0$. In a more general setting, the right requirement is for the fermion wave-function to be normalizable in the infrared, which presumably rules out oscillatory and singular behavior while allowing a more regular solution similar to the exponentially damped solution in anti-de Sitter space. The upshot of this discussion is that (5.8) is one requirement that a normal mode must satisfy.

The requirement that $\omega = 0$ for a fermionic normal mode in RNAdS comes from reasoning rather similar to what we just went through: only for this value of ω can one avoid oscillatory behavior in the infrared indicating that the fermion is falling into the black hole. In fact, since $h \to 0$ at the horizon of the RNAdS geometry, one has $v_{\rm IR} = 0$, so one can still use $\omega \leq v_{\rm IR}|k|$ as the condition that restricts the possible values of ω and k based on the infrared dynamics.

In the extreme ultraviolet, the last term of (5.7) dominates over the first two, so one can conclude that k_r^2 has the sign opposite $m_{\rm eff}^2$, namely negative. So oscillatory behavior is impossible. Though our reasoning here is non-rigorous, the conclusion that solutions are non-oscillatory is correct: all components of the fermion wave-function must have power-law behavior in e^{-A}, no matter what ω and k are. Now, it is hard to see how one would find a normal mode if k_r^2 were always negative, because then either the wave-function of the fermion would tend to increase monotonically toward the ultraviolet or else monotonically toward the infrared, neither of which would be consistent with normalizable behavior. So, as a necessary condition beyond (5.8), it is reasonable to expect that

$$\sup_r k_r^2 = \sup_r \left\{ \frac{(\omega + q\Phi)^2}{h} - k^2 - e^{2A} m_{\rm eff}^2 \right\} > 0 \,. \tag{5.9}$$

In principle, knowing a bosonic background, one can use (5.9) to obtain an upper bound on values of k where normal modes can exist, as a function of ω. In practice this is laborious.

We prefer to use instead the related condition:

$$\frac{|\omega + q\Phi_{\rm UV}|}{v_{\rm UV}} > k\,, \tag{5.10}$$

where $v_{\rm UV} = \sqrt{h_{\rm UV}}$. (5.9) and (5.10) are equivalent in the limit where $\omega/v_{\rm UV}$ and k are large compared to $m_{\rm eff}$. So (5.10), which is simple to apply, is really the large frequency, large wave-number limit of the better justified condition (5.9).

To summarize: A heuristic and inexact treatment of asymptotics in the UV and IR regions of a domain wall geometry leads to the expectations that normal modes will be confined to what we will term the "preferred wedge," namely

$$\frac{|\omega|}{v_{\rm IR}} \leq k < \frac{|\omega + q\Phi|}{v_{\rm UV}}\,. \tag{5.11}$$

In other words, the projection of the gauge-invariant momentum $k_\mu - qA_\mu$ onto boundary directions should be timelike in the ultraviolet, in order to produce non-monotonic dependence on r, and spacelike in the infrared, in order to ensure that the fermions aren't falling into the far infrared. The first inequality in (5.11) (from the infrared constraint) can be expected to be more reliable than the second inequality (from the ultraviolet behavior). The preferred wedge is compact, as figure 5.2 shows.

Having established our expectations for the region of the ω-k plane where normal modes may appear, the next obvious question is what the pattern of normal modes will be in this region. First, if there are normal modes at all, it is reasonable to think that they form one-dimensional families. The reason is that individual components of the Dirac spinor satisfy a second-order differential equation, so there are two linearly independent solutions. Demanding that the one that is normalizable in the infrared is also normalizable in the ultraviolet amounts to a single real condition on the two real parameters ω and k. So indeed one expects one-dimensional families.

A Bohr-Sommerfeld estimate of the location of normal modes takes the schematic form

$$\int\limits_{r_{\rm IR}(\omega,k)}^{r_{\rm UV}(\omega,k)} dr\, k_r = \pi(n+\nu)\,. \tag{5.12}$$

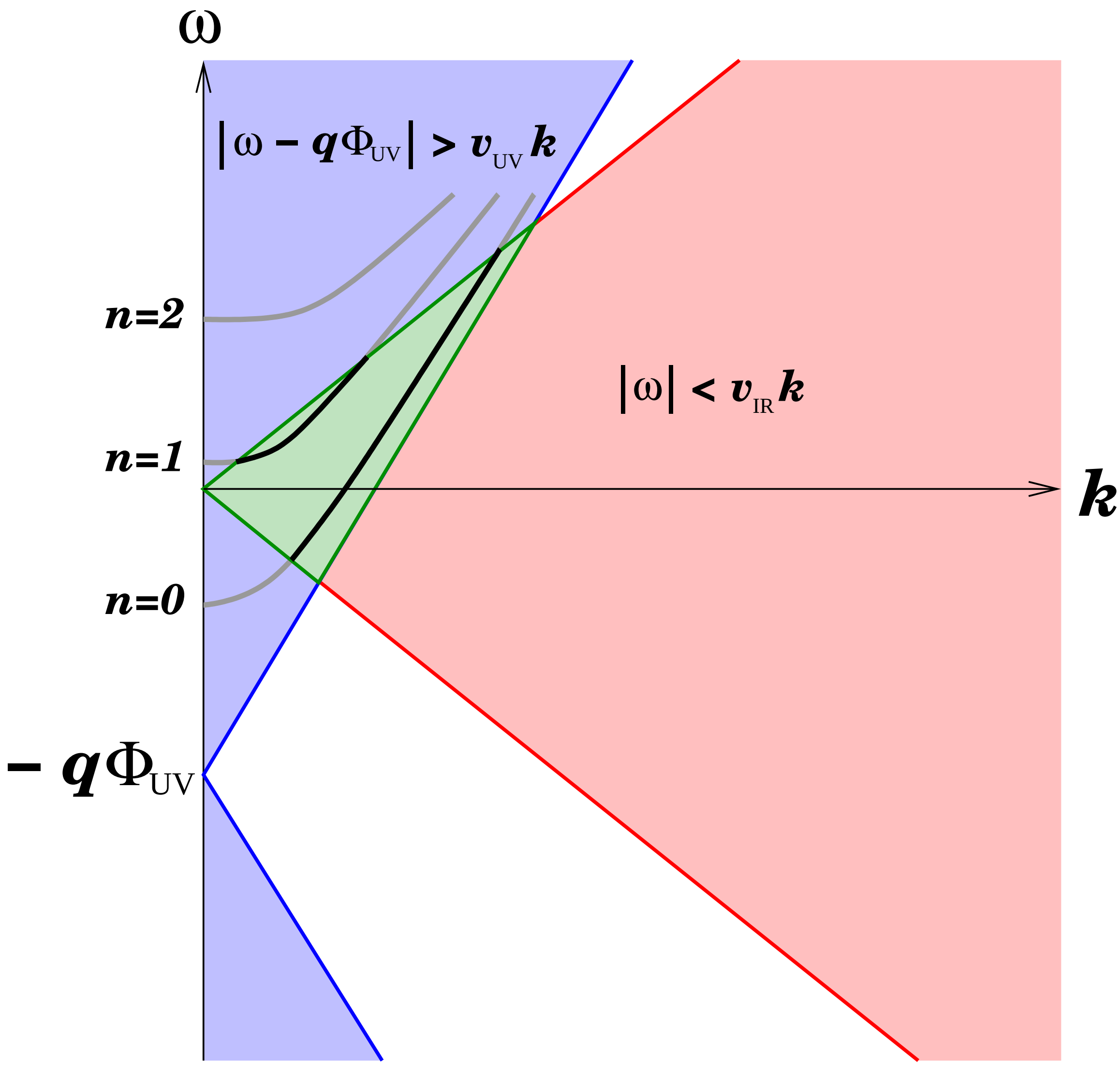

Figure 5.2: The green wedge is where (5.11) holds. This is the region where our heuristic geometric optics arguments indicate that one might find fermion normal modes. The grey and black curves are an approximate depiction of the hyperbolas (5.13), representing an approximate WKB treatment of where normal modes lie. Only the black parts of the curve correspond to actual normal modes; the grey parts are where normal modes might have been if the green wedge had been larger.

Here r_{UV} and r_{IR} are the radii where $k_r = 0$ is a solution to (5.7); k_r is the positive root of (5.7) for $r_{\mathrm{IR}} < r < r_{\mathrm{UV}}$; n is a non-positive integer; and a standard expectation for ν (the Keller-Maslov index) is 1/2. Passing to a further approximation, one can consider the case where the integral (5.12) is dominated by radii where the geometry is approximately

$AdS_{\rm UV}$ and the gauge potential is approximately $\Phi_{\rm UV}$. Then the integral (5.12) should be roughly proportional to $\sqrt{\frac{(\omega+q\Phi)^2}{h} - k^2}$, with a constant of proportionality that depends on details of the bosonic background and so cannot readily be computed. Using (5.12), we are led to an approximate condition

$$\frac{(\omega + q\Phi_{\rm UV})^2}{v_{\rm UV}^2} - k^2 = (Y_1 n + Y_2)^2 \tag{5.13}$$

for the position of the $n^{\rm th}$ band of normal modes. Y_1 and Y_2 are constants and n is again a non-positive integer, which is the number of nodes in the fermion wave-function. (Different components of the Dirac spinor could have bands of normal modes described by (5.13) with different Y_2 but the same Y_1. Associating n with the number of nodes can only be expected to work when one is focusing on the normal modes involving a particular component.) Evidently, we should expect only finitely many bands of normal modes, because the hyperbola (5.13) doesn't intersect the region $|\omega| < v_{\rm IR} k$ when n is large.

Since the hyperbolas (5.13) do not intersect the UV boundary $|\omega - q\Phi_{\rm UV}| = v_{\rm UV} k$ of the preferred wedge region for normal modes, the topological prediction we get out is that the bands begin and end on the IR boundary, $|\omega| = v_{\rm IR} k$. It is possible for a band to both begin and end on the upper branch of the IR boundary, i.e. the one with $\omega > 0$. Herein lies an interesting possibility: for such a band, there would be a minimum energy required to add a fermion belonging to it (unless the band dipped below the $\omega = 0$ axis and then rose back up). This is obviously an attractive feature if one is to make contact between these holographic models of superconductors and real-world superconductors. However, we are obliged to add that it is equally possible for bands of normal modes to cross the $\omega = 0$ axis one or more times. Then the natural configuration to consider is the one where the $\omega < 0$ normal modes are populated, while the $\omega > 0$ modes aren't. This results in a Fermi surface in the bulk, and apparently a gapless state for the fermions. Two considerations might change this state of affairs: 1) The fermions interact gravitationally and so presumably have an attractive channel that causes them to superconduct in the bulk through the usual mechanism of forming Cooper pairs; and 2) The gas of fermions back-reacts on the bulk, as in [74].

In the next section, we will exhibit a case where most bands cross the $\omega = 0$ surface at least once, and another case where there is a single band that does not cross the $\omega = 0$ axis and therefore has a gap in the sense explained in the previous paragraph. It is interesting indeed to inquire what behavior the fermions of maximal gauged supergravity exhibit in the domain wall geometry summarized in section 5.1: gapped or ungapped?

As a final aside, it is easy to imagine cases where there are no normal modes: the condition (5.7) could be impossible to satisfy, or it could be that Y_2 in (5.13) is too large for any of the would-be normal modes to intersect with permitted infrared boundary conditions. This doesn't seem quite to be a situation meriting the term "gapped behavior," because there isn't a definite energy that one can add to the system to obtain a long-lived fermionic quasi-particle. But perhaps it is reasonable to expect that in a strongly interacting superconductor at zero temperature, unpaired fermions can never be stable. Normal modes could be altogether absent in ground states with emergent conformal or Lorentz symmetry, where the preferred wedge is (modulo caveats already discussed) really a triangular wedge as shown in figure 5.2; or they could be altogether absent in ground states with Lifshitz symmetry, where $v_{\rm IR} = 0$ and the preferred wedge shrinks to a line segment along the $\omega = 0$ axis; or, indeed, they could be altogether absent in an RNAdS vacuum: this happens if q is too small. It would be interesting to study the spectral measure of the fermion two-point function in situations where there are no normal modes. It could be that a ridge similar to the one found, for example, in [40], would remain, suggestive of unstable fermionic quasi-particles.

5.3 Bands of fermion normal modes in AdS_4

Let us now describe the numerical computation of the normal modes in more detail. We use the conventions of the previous chapter, which we reproduce here for convenience. It is convenient to choose a basis of Γ matrices such that $\Gamma^{\underline{r}}$ is diagonal, such as

$$\Gamma^{\underline{r}} = \begin{pmatrix} 1 & 0 \\ 0 & -1 \end{pmatrix} , \qquad \Gamma^{\underline{i}} = \begin{pmatrix} 0 & \gamma^i \\ \gamma^i & 0 \end{pmatrix} \qquad i = 0, 1, 2 \,, \tag{5.14}$$

where γ^i are gamma matrices in three dimensions given by $\gamma^0 = i\sigma_2$, $\gamma^1 = \sigma_1$, and $\gamma^2 = \sigma_3$. As argued above, symmetry allows us to take the spinor to be of the following form:

$$\psi(t, \vec{x}, r) = e^{-i\omega t + ikx^1} u(r) = e^{-i\omega t + ikx^1} \begin{pmatrix} u_1^+(r) \\ u_2^+(r) \\ u_1^-(r) \\ u_2^-(r) \end{pmatrix} . \tag{5.15}$$

The Dirac equation can then be written as

$$\left[\sqrt{h}\Gamma^{\underline{r}}\partial_r + ie^{-A}\left(k\Gamma^{\underline{1}} - \frac{\omega + q\Phi}{\sqrt{h}}\Gamma^{\underline{0}}\right) + \frac{6hA' + h'}{4\sqrt{h}}\Gamma^{\underline{r}} - m\right] u = 0 \, . \tag{5.16}$$

Let us now consider the asymptotic behavior of solutions to (5.16). We are interested in regular and purely infalling solutions, which implies that in the infrared (corresponding to $r \to -\infty$),

$$u_a^\pm(r) \approx U_a^\pm e^{-2A} K_{\frac{1}{2} \pm mL_{\mathrm{IR}}}\left(\kappa_{\mathrm{IR}} e^{-A}\right) \qquad \kappa_{\mathrm{IR}} \equiv L_{\mathrm{IR}}\sqrt{k_1^2 - \omega^2} \, . \tag{5.17}$$

Here $a = 1, 2$, K_ν is a modified Bessel function, and the $U_a^\pm$ are constants that satisfy

$$\frac{U_2^-}{U_1^+} = -\frac{U_2^+}{U_1^-} = i\sqrt{\frac{k_1 + \omega}{k_1 - \omega}} \tag{5.18}$$

and are otherwise arbitrary. In what follows, we will set $U_1^+ = U_2^+ = 1$.

In the ultraviolet, corresponding to $r \to +\infty$, the most general solution is of the form

$$u_a^\pm = C_a^\pm e^{-2A} I_{\mp\frac{1}{2} - mL_{\mathrm{UV}}}\left(\kappa_{\mathrm{UV}} e^{-A}\right) + D_a^\pm e^{-2A} I_{\pm\frac{1}{2} + mL_{\mathrm{UV}}}\left(\kappa_{\mathrm{UV}} e^{-A}\right) , \tag{5.19}$$

where $\kappa_{\mathrm{UV}}^2 \equiv k_1^2 - \frac{(\omega + q\Phi_{\mathrm{UV}})^2}{h_{\mathrm{UV}}}$ and I_ν is a modified Bessel function. As before, (5.16) allows you to solve for C_a^-, D_a^- algebraically in terms of C_a^+, D_a^+, but the exact form of this relation will not be important.

Expanding (5.19) at large r, we see that

$$u_a^+ \approx C_a^+ \left(\frac{\kappa_{\mathrm{UV}}}{2}\right)^{-\frac{1}{2} - mL_{\mathrm{UV}}} \frac{e^{\left(-\frac{3}{2} + mL_{\mathrm{UV}}\right)A}}{\Gamma\left(\frac{1}{2} - mL_{\mathrm{UV}}\right)} + D_a^+ \left(\frac{\kappa_{\mathrm{UV}}}{2}\right)^{\frac{1}{2} + mL_{\mathrm{UV}}} \frac{e^{\left(-\frac{5}{2} - mL_{\mathrm{UV}}\right)A}}{\Gamma\left(\frac{3}{2} - mL_{\mathrm{UV}}\right)} . \tag{5.20}$$

According to the standard AdS/CFT prescription, we identify C_a^+ with the source and D_a^+ with the response of a boundary fermionic operator with conformal dimension $\Delta = \frac{3}{2} + mL_{\rm UV}$.[1]

Normal modes are then solutions of (5.16) that in the infrared satisfy (5.17) and have $C_a^+ = 0$. They correspond to poles of the retarded Green's function. To make this connection more explicit, consider the full fermionic action

$$S_f = i \int d^5x\, \bar{\psi}(\Gamma^\mu D_\mu - m)\psi + S_{\rm bdy} \tag{5.21}$$

where $S_{\rm bdy}$, which we neglected up to now, is a boundary term that does not contribute to the equations of motion. It is necessary to have a well posed variational problem and gives the only nonzero contribution to the onshell action. We choose

$$S_{\rm bdy} = -i \int\limits_{r=1/\varepsilon} d^4x\, \sqrt{-gg^{rr}}\, \bar{\psi}_+ \psi_- \,, \qquad \psi_\pm \equiv \frac{1}{2}\left(1 \pm \Gamma^{\underline{r}}\right)\psi \,, \tag{5.22}$$

where ε is a positive quantity to be taken to zero after functional derivatives are taken. By taking the appropriate functional derivatives of (5.21), we obtain the retarded Green's function [57]

$$G_R = \left(\frac{\kappa_{\rm UV}}{2}\right)^{mL_{\rm UV}} \frac{\Gamma\left(\frac{1}{2} - mL_{\rm UV}\right)}{\Gamma\left(\frac{1}{2} + mL_{\rm UV}\right)} \begin{pmatrix} -i\frac{D_1^-}{C_2^+} & 0 \\ 0 & i\frac{D_2^-}{C_1^+} \end{pmatrix} , \tag{5.23}$$

and we see that zeros of C_2^+ are poles of G_{11} while zeros of C_1^+ are poles of G_{22}. From (5.16) and the form of the Γ matrices (5.14) it is clear that the four components of the spinor u couple to each other only in pairs: u_1^+ and u_2^- mix, and so do u_2^+ and u_1^-. This means we are free to consider only u_1^+ and u_2^- nonzero and look for zeros of C_1^+ or consider only u_2^+ and u_1^- nonzero and look for zeros of C_2^+.

Before discussing our numerical results let us comment on the meaning of the "preferred wedge" (5.11). It is clear that (5.8) translates[2] to $\kappa_{\rm IR}^2 > 0$ which implies that u is *not* oscillatory in the IR. Condition (5.10) on the other hand, translates to $\kappa_{\rm UV}^2 < 0$ which

[1] For $0 \leq m < 1/2$, it is also legitimate to identify D_a^+ with the source and C_a^+ with the response, but we will in this paper stick with the identification valid for all m.

[2] Remember we are using units where $v_{\rm IR} = 1$.

implies that u *is* oscillatory in the UV. This is in agreement with the geometrical optics arguments that led us to formulate these conditions in section 5.2.

We now have the necessary ingredients to find normal modes numerically: we can solve (5.16) with initial conditions given by (5.17) for some large negative r. We can then determine the C_a^+ coefficients by fitting the numerical results to (5.19) for large positive r and vary the parameters until we find zeros of the C_a^+. As expected, we find a continuous set of normal modes inside the "preferred wedge". As you increase q, the "preferred wedge" grows and accommodates more bands.

As a specific example consider $m = 0$ and $qL_{\rm UV} = 10$, for which the bands are shown in Fig. 5.3. We find an abundance of normal modes, with poles of G_{22} alternating with poles of G_{11}. The number of nodes in the wave functions (some of which are shown in Fig. 5.4) is greater for bands that are closer to the origin. The bands are well approximated by hyperbola, although (5.13) does not seem to capture their shape very well. Generalizing (5.13), we can fit the bands to

$$\frac{(\omega + q\Phi)^2}{v^2} - k^2 = m_{\rm eff}^2 \,, \tag{5.24}$$

where we treat $m_{\rm eff}$ as an arbitrary fitting parameter. We can either use the extreme UV values of Φ and v and do one-parameter fits (shown as gray dot-dashed lines in Fig 5.3) or treat Φ and v as arbitrary fitting parameters also and do three-parameter fits (shown as black dashed lines in Fig 5.3). In the former case, we find that $m_{\rm eff}$ increases as a small power of the band number. In the latter case (unsurprisingly) we obtain better fits, and we note that the best fit values of Φ and v approach the expected UV values when you consider bands farther from the origin.

In Fig. 5.3, all the bands cross the $\omega = 0$ line and are therefore ungapped. As you decrease q, the "preferred wedge" shrinks and fewer bands are present, but for $m = 0$ at least one of them always seems to intersect the $\omega = 0$ line. We can argue that this is always the case if we note that for small enough ω and k, the Green's function should approach its

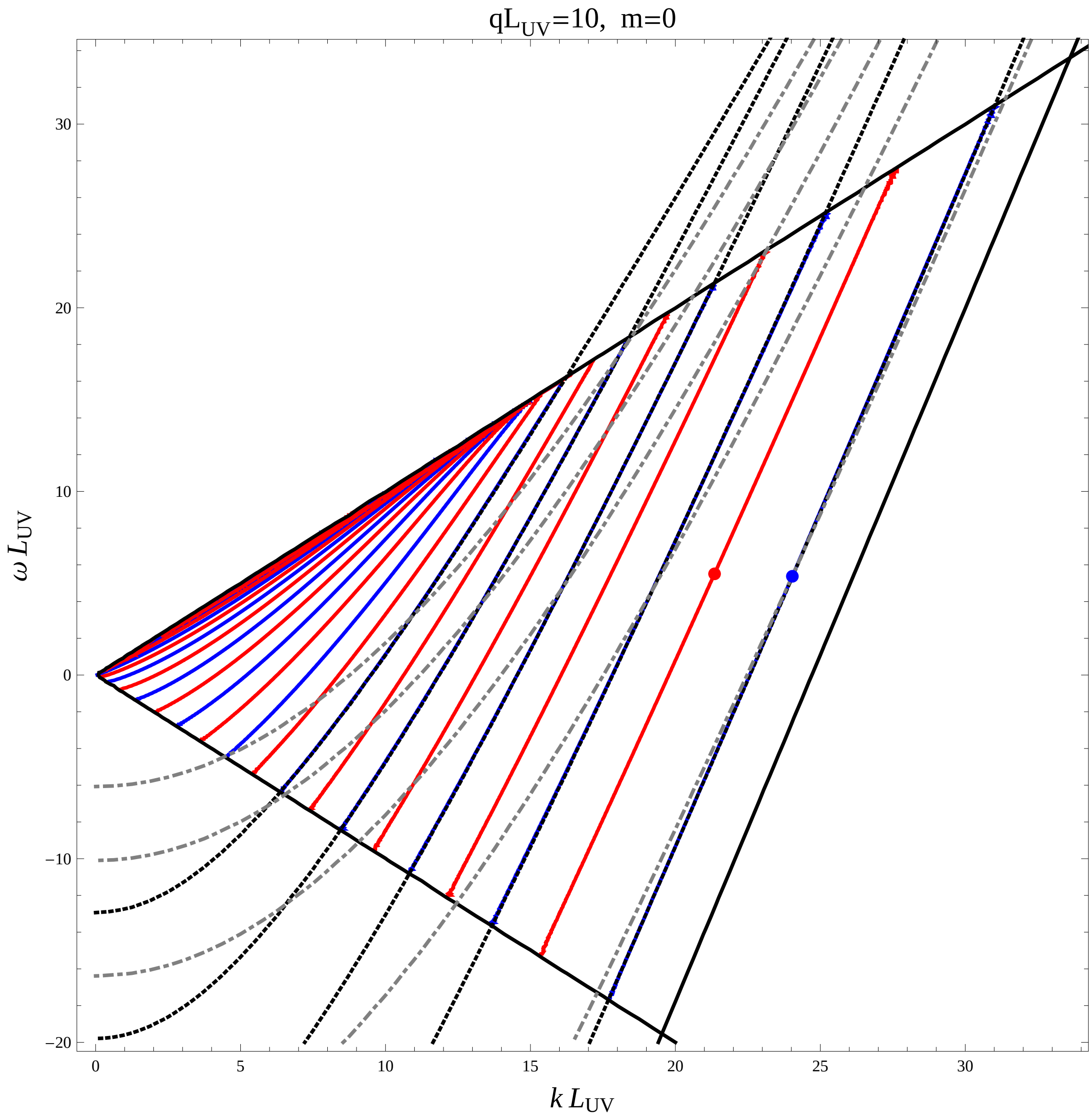

Figure 5.3: Fermion normal modes in the AdS_4 domain wall for $m = 0$ and $qL_{\rm UV} = 10$. The black lines mark the boundary of the “preferred wedge” (5.11). The red lines correspond to normal modes where u_1^+ and u_2^- are nonzero (poles in G_{22}) while the blue lines correspond to normal modes where the u_2^+ and u_1^- are nonzero (poles in G_{11}). The gray dot-dashed lines are one parameter fits and the black dashed lines are three parameter fits to hyperbola. The red and blue dots mark the location of the normal modes shown in Fig. 5.4.

AdS value [57]

$$G_R = f\left(mL_{\rm IR}\right)\kappa^{2mL_{\rm IR}-1}\gamma\cdot k \propto \kappa^{2mL_{\rm IR}}\begin{pmatrix} -\sqrt{\frac{k-\omega}{k+\omega}} & 0 \\ 0 & \sqrt{\frac{k+\omega}{k-\omega}} \end{pmatrix}\,, \tag{5.25}$$

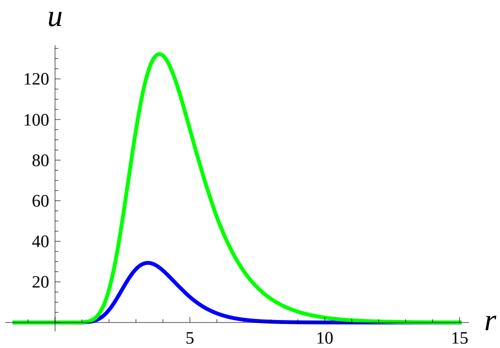

Figure 5.4: The wave functions for two fermion normal modes of the AdS_4 domain wall for $m = 0$ and $qL_{\rm UV} = 10$. We note that in the $\kappa_{\rm IR} > 0$ region, we can always choose the u_a^+ to be purely real, in which case it follows that the u_a^- are purely imaginary. The plot on the left shows the real part of u_1^+ (blue) and the imaginary part of u_2^- (green) corresponding to the blue dot in Fig. 5.3. The plot on the right shows the real part of u_2^+ (red) and the imaginary part of u_1^- (cyan) corresponding to the red dot in Fig. 5.3.

where $\kappa^2 = k^2 - \omega^2$ and $f(mL_{\rm IR})$ is some unimportant constant. Thus, for $m = 0$, there is always a divergence at the origin that signals a normal mode with $(\omega, k) = 0$ and at least one of the bands is ungapped. For positive m however, this divergence is gone and we expect the possibility of gapped bands. In fact, for $qL_{\rm UV} = 3/2$ and $mL_{\rm IR} = 1$, we find a single gapped band (see Fig. 5.5).

Finally, we note that it is also possible to choose the parameters in such a way that there are no normal modes at all. If $qL_{\rm UV}$ is small enough, this seems to be the generic behavior. For instance, taking $m = 0$ and $qL_{\rm UV} = 1/8$, we find no normal modes.

5.4 Discussion

We studied charged Dirac fermions in an AdS_4 domain wall solution and found that generically they exhibit continuous bands of normal modes. This is in stark contrast to fermions in RNAdS, which exhibit one or more isolated normal modes at $\omega = 0$ and finite k [40, 41, 42, 72]. However, we note that the same semiclassical argument that led us to expect continuous bands in the domain wall geometry can be used to argue for isolated nor-

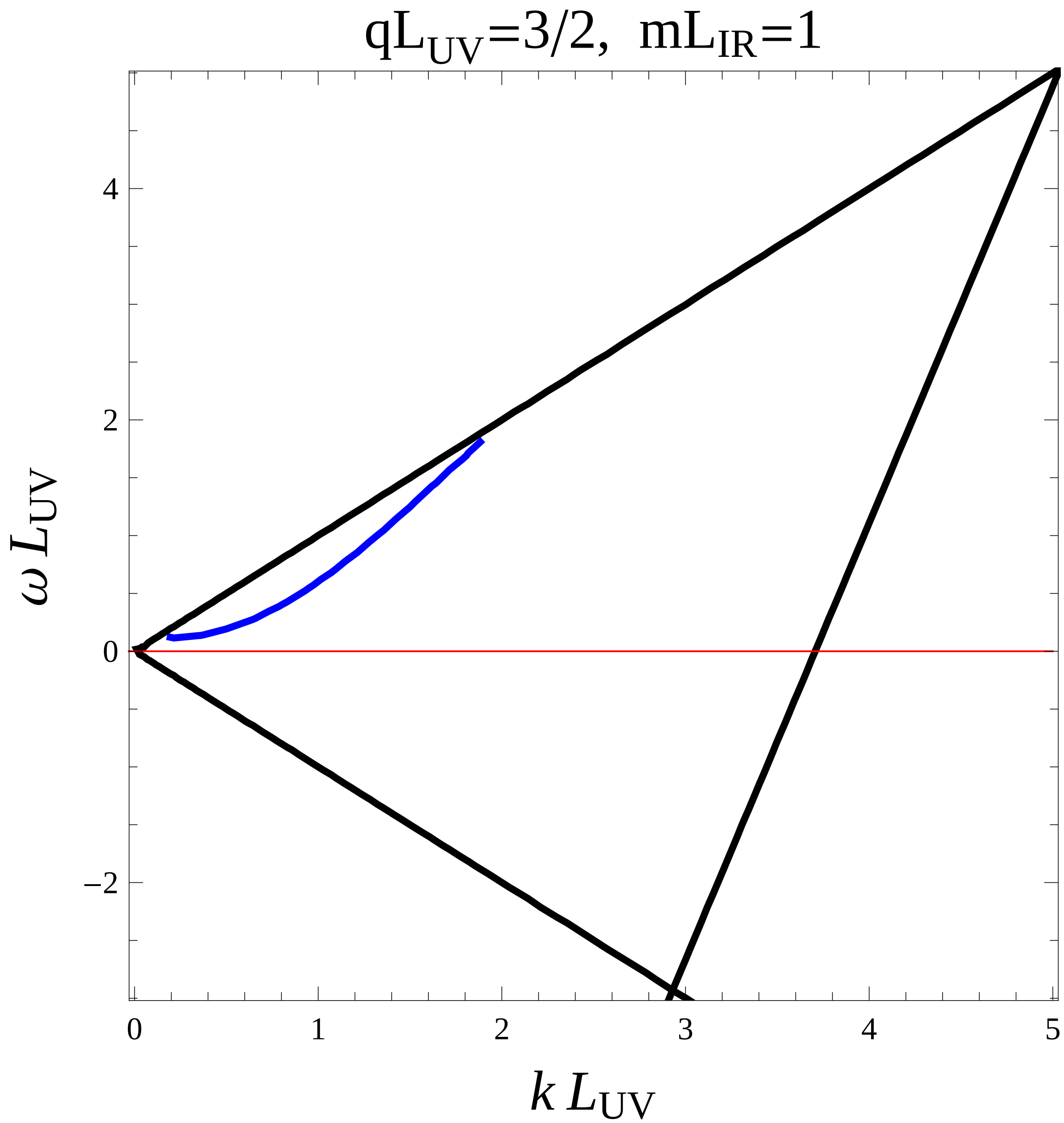

Figure 5.5: Fermion normal modes of the AdS_4 domain wall for $mL_{\rm IR} = 1$ and $qL_{\rm UV} = 3/2$. The black lines mark the boundary of the "preferred wedge" (5.11). The blue line corresponds to normal modes where the u_2^+ and u_1^- are nonzero (poles in G_{11}). Notice it never intersects the $\omega = 0$ line (red). So this is a gapped band.

mal modes in RNAdS. In fact, since RNAdS has an horizon at which the metric function h vanishes, it can in some sense be thought of as degenerate domain wall for which $v_{\rm IR} = 0$. The condition on the location of the normal modes given by(5.8) then degenerates to $\omega = 0$

and, choosing units where $v_{\mathrm{UV}} = 1$, the remaining condition (5.10) becomes $|q\Phi_{\mathrm{UV}}| > k$. The "preferred wedge" thus becomes a "preferred segment" and the same parameter counting that led us to expect continuous bands for the domain wall geometry tells us that we should find a discrete set of normal modes at $\omega = 0$, which is precisely what happens for RNAdS.

Since in our conventions, energy equal to the Fermi energy is equivalent to frequency equal to zero, the natural zero temperature configuration is one where the normal modes with $\omega \leq 0$ are occupied and those with $\omega > 0$ are unoccupied. Therefore, a particularly important feature of the bands is whether they cross the $\omega = 0$ axis. We found this feature depends on the choice of the charge and mass of the fermion. For zero mass fermions, the bands seem to always cross the $\omega = 0$ axis and the resulting configuration would seem to have a Fermi surface. However, to better understand this Fermi surface it would be necessary to consider the back-reaction of the fermions on the bulk geometry, which might conceivably destroy the Fermi surface. For positive mass fermions, with a suitable choice of the charge, we found an example of a single band that does not touch the $\omega = 0$ axis, i.e., the band is gapped. Such a feature is desirable in making comparisons with real-world superconductors at zero temperature, and it may be fairly generally achievable when there is at least emergent Lorentz symmetry in the infrared.

Because our bosonic background is embeddable in M-theory [29, 28], it would be interesting to redo our calculations using the quadratic fermion action of maximal gauged $d = 4$ supergravity. It appears to be non-trivial to diagonalize this quadratic action, but the advantage is that one should in principle be able to understand the operators dual to the fermions. It would also be interesting to redo our calculations in AdS_5, where we expect qualitatively similar results, simply because the semi-classical arguments of section 5.2 don't depend on dimension. Preliminary numerical studies yielded results in agreement with these expectations.

Chapter 6

Fermion correlators in non-abelian holographic superconductors

In Chapter 1 we introduced a simple class of holographic superconductors in which the symmetry breaking order parameter was a charged scalar. These are therefore s-wave holographic superconductors. In this chapter we will be concerned with some properties of holographic superconductors with a vector order parameter, the so called p-wave superconductors. Early studies of these non-Abelian superconductors include [75, 76, 77].

Consider as an example a dual field theory which is four-dimensional and includes chiral fermions λ_α and $\bar{\kappa}^{\dot{\alpha}}$, both transforming in the complexified adjoint of an $SU(N)$ gauge group, and both carrying charge $-e$ under the $U(1)$ symmetry that gets spontaneously broken. Then the symmetry breaking order parameter could be $\langle \operatorname{tr} \lambda^\alpha \lambda_\alpha \rangle$ in the case of an s-wave holographic superconductor, or $\langle \operatorname{tr} \lambda^\alpha \sigma^1_{\alpha\dot{\beta}} \bar{\kappa}^{\dot{\beta}} \rangle$ in the case of a p-wave superconductor, where σ^1 is the first Pauli matrix. There is no lattice structure in the dual field theory; thus the breaking of rotational invariance by the p-wave condensate is spontaneous. The holographic treatment of both the s-wave and p-wave cases is typically at the level of mean field theory in that one solves classical equations of motion in the bulk without inquiring about the role of fluctuations. This is justified on the field theory side if one is restricting attention to leading order effects in a large N expansion, where N is the rank of the gauge group.[1]

One useful probe of the electronic structure of high-T_c superconductors is the angle resolved photoemission experiments (ARPES) which essentially rely on the photoelectric effect and measure the energy of the electrons emitted from the sample. ARPES experiments demonstrate some interesting properties of high T_c superconductors. These properties include a gap with $d_{x^2-y^2}$ symmetry, deformed Dirac cones whose apexes are the nodes of the superconducting gap, Fermi arcs whose zero temperature limits are the nodes in the gap, and a peak-dip-hump structure of the emission intensity as a function of frequency at fixed wave-number. A review of ARPES measurements can be found in [81].

Holographic superconductors differ from high-T_c superconductors in several respects: Most notably, they are symmetry-breaking states of large N gauge theories, and they have no underlying lattice structure. Nevertheless, it is interesting to ask whether or not the properties of the fermionic spectral function in high T_c superconductors are shared by their holographic counterparts. In both [82, 83] and also as we discussed in Chapter 5, following [84, 41, 40], an analysis of fermion correlation functions was carried out for the holographic s-wave superconductors introduced in [14, 26]. In this work, after elucidating some details of the phase diagram of the holographic p-wave superconductors in AdS$_4$, we discuss some properties of its fermionic correlation functions. Along the way we introduce a variant of the holographic p-wave construction, based on an $SO(4)$ gauge group.

This work is organized as follows. In section 6.1 we review the construction of a p-wave superconductor in AdS$_4$ and study its phase diagram. An interesting property of the p-wave superconductor, first observed in [85], is that the bulk geometry is a domain wall interpolating between infrared and ultraviolet limits which are each AdS$_4$ with an asymptotically flat gauge connection.[2] In section 6.2 we discuss in detail scalar, fermion, and vector correlation functions in the asymptotic regions of such backgrounds, starting

[1] In [78, 79, 80] non mean field theory behavior was exhibited by arranging for a particular bulk lagrangian for the scalar field.

[2] To be precise, the gauge connection has a field strength whose stress tensor becomes insignificant near the boundary compared to the negative cosmological constant. It is in this sense that the ultraviolet geometry can be approximated by AdS$_4$ with a flat gauge connection.

from a general gauge group. In section 6.3 we explain how to compute the fermion spectral function in the full, zero-temperature, domain-wall, p-wave background and described some of its properties. The numerical results of the computation can be found in section 6.4. In section 6.5 we discuss the results in the context of ARPES experiments on high T_c superconductors.

6.1 The p-wave holographic superconductor

The simplest example of a non-abelian holographic superconductor is the p-wave superconductor first introduced in [76] (following earlier work [75]) and further studied in [77, 85] and [86, 87, 88, 89]. The bulk action for the p-wave superconductor is given by

$$S = \int_M d^4x \sqrt{-g} \left(R + \frac{6}{L^2} - \frac{1}{2} \operatorname{tr} F_{\mu\nu}^2 \right) . \tag{6.1}$$

In what follows we will set $L = 1$. Here $F_{\mu\nu}$ is the field strength of an $SU(2)$ gauge potential:

$$F_{\mu\nu} = \partial_\mu A_\nu - \partial_\nu A_\mu - i g_{\mathrm{YM}} [A_\mu, A_\nu] \, , \tag{6.2}$$

and

$$A_\mu = A_\mu^a \tau^a \, , \tag{6.3}$$

and $\tau^a = \frac{1}{2}\sigma^a$, where σ^a are the Pauli matrices. Consider a configuration in which the gauge field takes the form:

$$A = \Phi(r)\tau^3 dt + W(r)\tau^1 dx. \tag{6.4}$$

Based on the general arguments in [75, 76], one expects that apart from the Reissner-Nordstrom solution for which $W = 0$, there exist other solutions where $W \neq 0$, corresponding to a non-zero expectation value of the boundary current J_x^1. This expectation value spontaneously breaks both the $SU(2)$ gauge symmetry and rotational invariance. Symmetry breaking solutions of this type have been studied in the limit where $g_{\mathrm{YM}} \to \infty$ in [76] and in a conjectured zero temperature configuration in [85]. In [88], five dimensional, non-zero temperature and finite gauge coupling geometries were studied. The purpose of this section is to fill a gap in the literature by studying the AdS$_4$ p-wave superconductor geometry for finite temperature and coupling. Through this numerical study we will confirm that the domain wall geometries of [85] are indeed the zero-temperature limits of symmetry-breaking black holes.

Parametrizing the line element by

$$ds^2 = -r^2\gamma(r)e^{-\chi(r)}dt^2 + \frac{dr^2}{r^2\gamma(r)} + r^2(c(r)^2dx^2 + dy^2)\,, \tag{6.5}$$

we find that the equations of motion for the gauge field and the metric are

$$\begin{aligned}
\frac{1}{2}rW'\left(2r\gamma' - \frac{2rc'\gamma}{c} - r\chi'\gamma + 4\gamma\right) + \frac{g_{\rm YM}^2 W\Phi^2 e^{\chi}}{r^2\gamma} + r^2\gamma W'' &= 0\\
\frac{1}{2}r^2\gamma\Phi'\left(\frac{2c'}{c} + \chi' + \frac{4}{r}\right) - \frac{g_{\rm YM}^2 W^2\Phi}{r^2c^2} + r^2\gamma\Phi'' &= 0\\
\frac{c'}{c}\left(\frac{\gamma'}{\gamma} - \chi' + \frac{2}{r}\right) - \frac{g_{\rm YM}^2 W^2\Phi^2 e^{\chi}}{r^6c^2\gamma^2} - \frac{\chi'}{r} &= 0\\
-\frac{r^2\gamma c''}{c} - \frac{rc'\left(r\gamma' + 8\gamma\right)}{2c} - \frac{g_{\rm YM}^2 W^2\Phi^2 e^{\chi}}{4r^4c^2\gamma} + \gamma\left(-\frac{W'^2}{4c^2} - 3\right) - r\gamma' - \frac{1}{4}e^{\chi}\Phi'^2 + 3 &= 0\\
cc'' + c'c\left(\frac{\gamma'}{\gamma} + \frac{4}{r} - \frac{1}{2}\chi'\right) - \frac{g_{\rm YM}^2 W^2\Phi^2 e^{\chi}}{2r^6\gamma^2} + \frac{W'^2}{2r^2} &= 0\,.
\end{aligned} \tag{6.6}$$

We have omitted an additional equation of motion which is automatically satisfied once the gauge fields and metric components solve (6.6). In the limit where $g_{\rm YM} \to \infty$, the matter content of the theory decouples from gravity and the equations of motion reduce to gauge fields in an AdS$_4$-Schwarzschild or AdS$_4$ background. This is the probe limit, initially studied in [76], following earlier work [26] on a similar limit of the holographic Abelian Higgs model. In the following subsection we will solve the equations of motion numerically and discuss some of the features of the solution. We will revisit the probe limit in section 6.1.2.

6.1.1 Numerics and phase diagram

The equations for W, Φ and c are second order while the equations for γ and χ are first order. Thus, to obtain a solution, we need to specify eight integration constants. In the deep infrared (IR), located at $r = 0$, we set $\Phi \underset{\rm IR}{\longrightarrow} 0$, $W \underset{\rm IR}{\longrightarrow}$ finite, $\gamma \underset{\rm IR}{\longrightarrow}$ finite and $c \underset{\rm IR}{\longrightarrow}$ finite. (If we are looking for finite temperature solutions then we should require that γ vanishes at the horizon $r = r_{\rm H}$, and if we are looking for zero temperature solutions we should require that γ is finite in the deep IR). Near the boundary, located at $r \to \infty$, we require that $W \underset{\text{UV}}{\longrightarrow} 0$ and that $\Phi \underset{\text{UV}}{\longrightarrow} \mu$, μ being the chemical potential of the boundary theory. The remaining two integration constants can be thought of as the values of χ and c at the boundary, and these can be gauged to 0 and 1, respectively, by rescaling the t and x coordinates. In practice, we've looked for solutions by using a standard shooting algorithm from the horizon to the boundary.

To analyze the stability of the solutions with $W \neq 0$ we compute the boundary theory grand canonical potential Ω (per unit volume) of these configurations and compare it to the grand canonical potential of the Reissner-Nordstrom black hole. The computation of Ω is carried out by computing the on-shell Euclidean action $\Omega = -TS_{\text{E}}/V$. We refer the reader to [88] for the details of a similar computation in AdS_5. We find that solutions with a non-vanishing condensate, $W \neq 0$, are stable only below a critical temperature T_c, which varies with the charge g_{YM}. Above T_c the canonical potential for the AdS Reissner-Nordstrom black hole is lower, and it is the preferred solution (see figure 6.1). We find that the phase transition from the RN solution to the condensed solution is second order if $g_{\text{YM}} > 1.14 \pm 0.01$, and is first order if $g_{\text{YM}} < 1.14 \pm 0.01$. When $g_{\text{YM}} < 0.710 \pm 0.001$ the condensed solution no longer exists.[3]

In [85] it was conjectured that the zero temperature limit of the condensed phase is a domain wall geometry similar to the one described in Chapter 2: The infrared and ultraviolet geometries are both asymptotically AdS but with different speeds of light. The condensate W, the gauge field Φ and the metric components χ and c interpolate between their infrared values $W_{\text{IR}} > 0$, $c_{\text{IR}} > 1$, $\chi_{\text{IR}} \neq 0$ and $\Phi_{\text{IR}} = 0$ in the infrared to their UV values $W_{\text{UV}} = 0$, $c_{\text{UV}} = 1$, $\chi_{\text{UV}} = 1$ and $\Phi_{\text{UV}} = \mu > 0$. γ approaches 1 both in the UV and in the IR. Note that since c differs in the UV and IR, the appropriate speeds of light differ in the x and y directions. This anisotropy is a new and distinctive feature of the domain wall of [85]. Another interesting feature is that the AdS radius is the same in the ultraviolet and infrared: indeed, both limits are just empty AdS_4 with a flat $SU(2)$ gauge connection.

[3] With 20 digits of working precision, the lowest value of q for which Mathematica's NDSolve algorithm could obtain a solution was $q = 0.7103$.

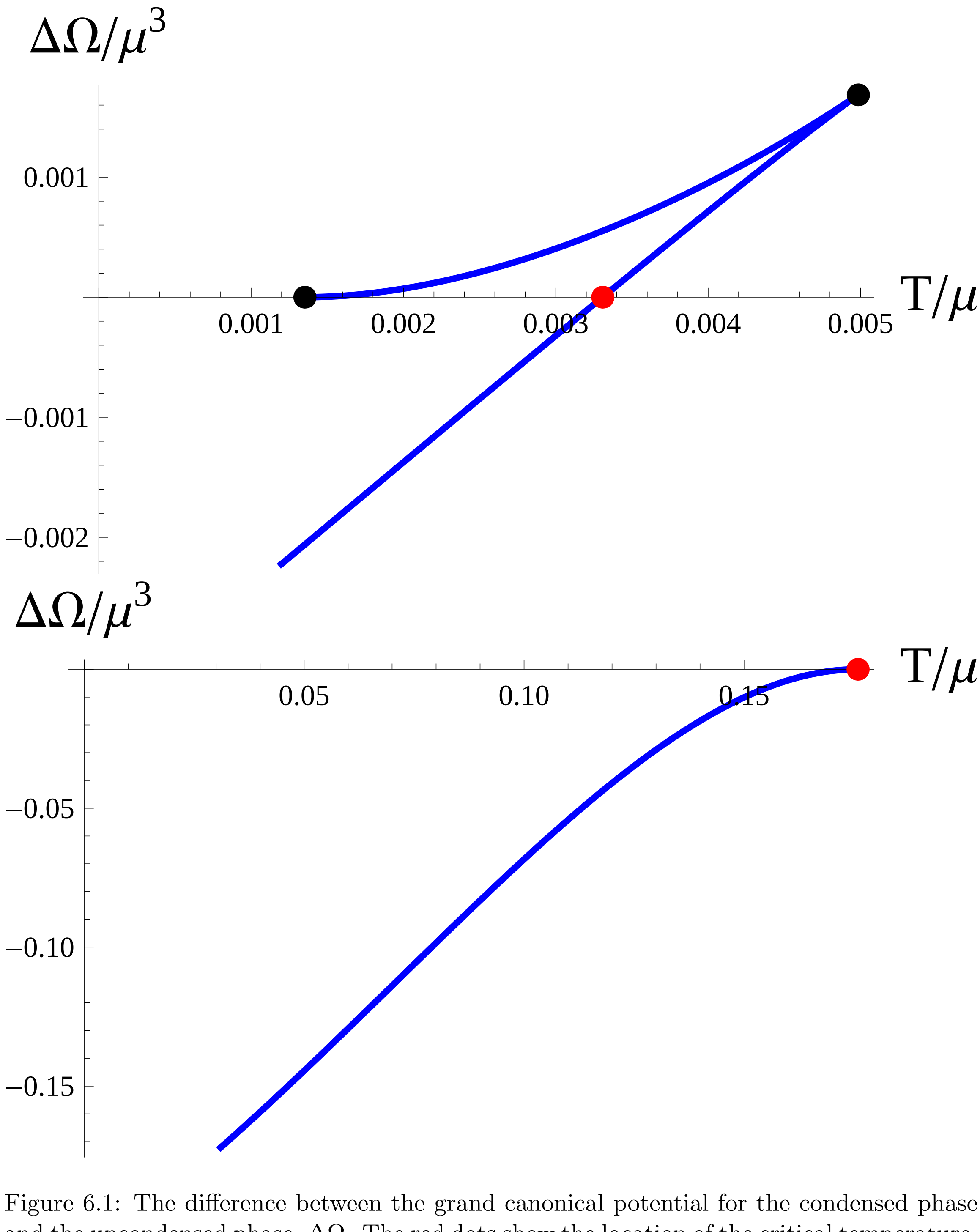

Figure 6.1: The difference between the grand canonical potential for the condensed phase and the uncondensed phase, $\Delta\Omega$. The red dots show the location of the critical temperature, and the black dots the location of the spinodal points. The left plot corresponds to $g_{\rm YM} = 0.79$ and the right one to $g_{\rm YM} = 3$.

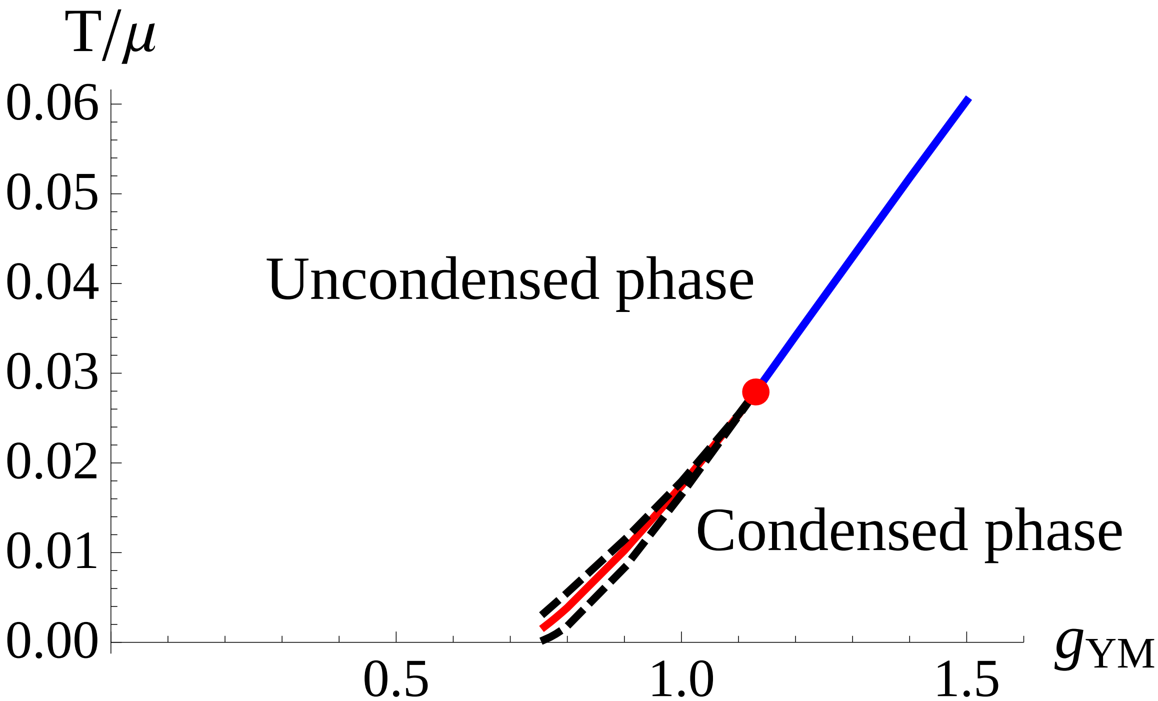

Figure 6.2: The phase diagram for the p-wave superconductor. The blue curve indicates a second order transition and the red line a first order phase transition. The dashed black lines are spinodal curves and the red dot marks a tricritical point.

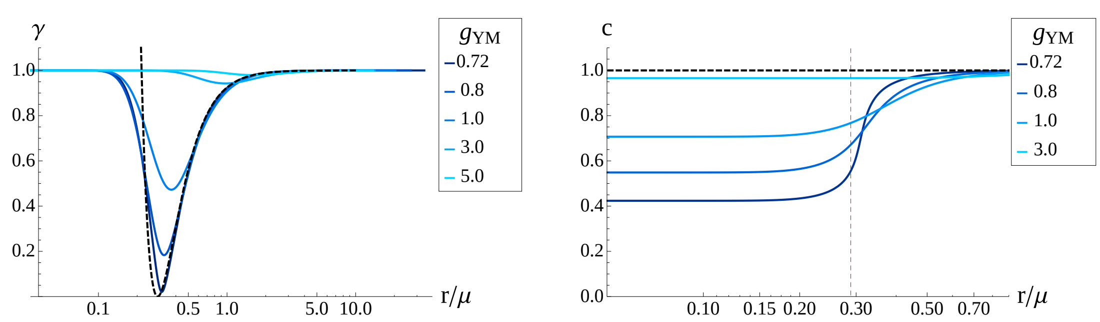

Figure 6.3: Plots of the metric components γ and c at zero temperature as a function of the the charge. As the charge approaches its critical value, the black hole hair gets pushed further into the IR, conforming to an extremal Reissner-Nordstrom black hole in the UV. The dashed black line corresponds to the extremal Reissner-Nordstrom solution. The dashed vertical red line on the right plot signifies the location of the extremal RN horizon where $\gamma = 0$.

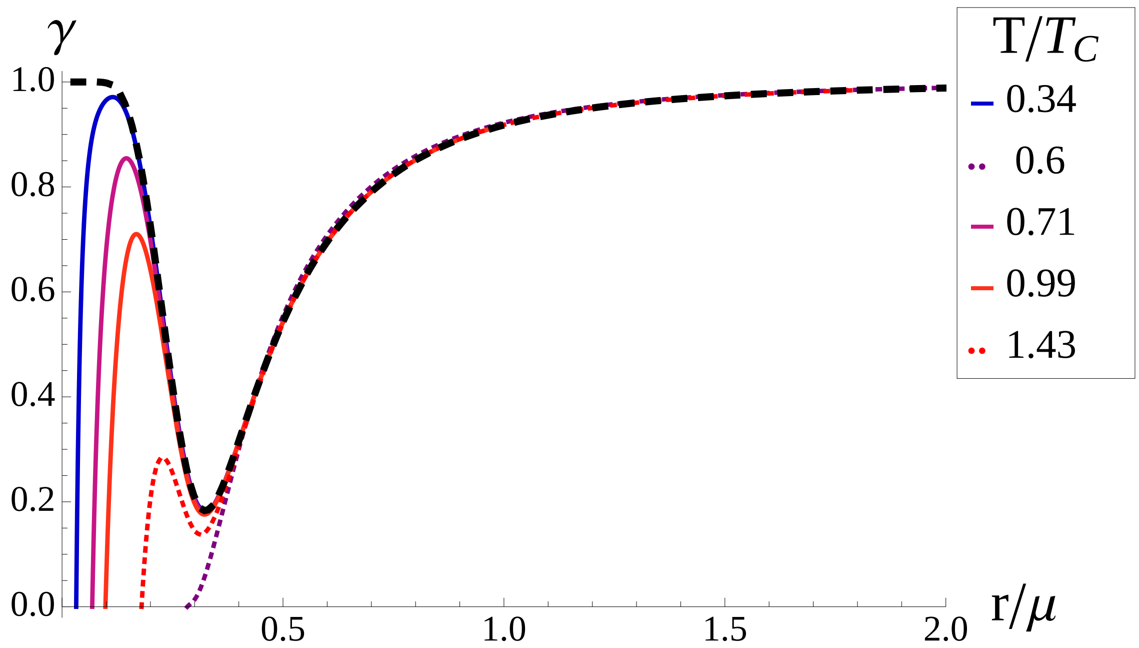

Figure 6.4: Plots of γ as a function of the temperature for $q = 0.8$. The curves are color coded according to the temperature of the solution. The dashed line shows the domain wall solution and the dotted lines correspond to superheated or supercooled solutions.

By following the branch of symmetry-breaking solutions from the region where W is perturbatively small to the region where it is larger, we were able to verify that the domain wall geometries described in the previous paragraph are indeed the zero temperature limits of solutions with regular, finite-temperature horizons. See figure 6.4. From the phase diagram of the $SU(2)$ superconductor, depicted in figure 6.3, and by comparing the domain wall geometry of the condensed phase with subsequently small $g_{\rm YM}$ to that of the extremal RN solution (figure 6.3), it appears that crossing $g_{\rm YM} = 0.710 \pm 0.001$ at $T = 0$ results in a phase transition from the condensed solution to the extremal RN solution.

6.1.2 The probe limit

As discussed earlier, in the probe limit the matter content of the theory decouples from the metric and the equations of motion (6.6) reduce to the Yang-Mills equation in a fixed background geometry. For convenience we rescale the gauge field to get rid of all the factors of $g_{\rm YM}$ in the equations of motion: that is, $\Phi \to \Phi/g_{\rm YM}$ and $W \to W/g_{\rm YM}$. This has the same effect as setting $g_{\rm YM} = 1$ in the Yang-Mills equations—but we should bear in mind that the probe approximation is justified precisely by taking $g_{\rm YM}$ large. An additional simplification is possible at zero temperature: we recall that AdS_4 is conformally flat, and that the classical Yang-Mills equations in four dimensions are conformally invariant. Explicitly, if the metric is expressed as

$$ds^2 = \frac{L^2}{z^2}(-dt^2 + dx^2 + dy^2 + dz^2)\,, \tag{6.7}$$

then systematically dropping the overall prefactor L^2/z^2 has no effect on the Yang-Mills equations. With the ansatz (6.4), they take the form

$$\Phi'' = W^2\Phi \qquad W'' = -\Phi^2 W\,, \tag{6.8}$$

where primes denote d/dz. The boundary conditions appropriate for describing the type of domain wall solution we are interested in are

$$\begin{aligned} &\Phi \to 0 \quad \text{and} \quad W \to W_{\rm IR} && \text{at } z = 0 \\ &\Phi \to \mu \quad \text{and} \quad W \to 0 && \text{as } z \to +\infty\ , \end{aligned} \tag{6.9}$$

where $W_{\rm IR}$ and μ are finite. Even though one can find one conserved charge for this system [90] (namely the Hamiltonian associated with radial translations), the equations of (6.8) do not appear to be integrable. A closely related system studied in [91] is known to exhibit strongly chaotic behavior.

We find it convenient to change variables and make the field redefinitions as follows:

$$\Phi(z) = W_{\rm IR}\tilde{\Phi}(\zeta) \qquad W(z) = W_{\rm IR}\tilde{W}(\zeta)\,, \tag{6.10}$$

where

$$\zeta = e^{-W_{\rm IR} z}\zeta_0\,, \tag{6.11}$$

and ζ_0 is a constant yet to be determined. Large z now corresponds to $\zeta = 0$, and we can reformulate the boundary value problem by requiring that at $\zeta = 0$,

$$\tilde{W}(0) = 1 \qquad \tilde{\Phi}(0) = 0 \qquad \tilde{\Phi}'(0) = 1 \qquad \tilde{W}'(0) = 0\,. \tag{6.12}$$

The UV is located at $\zeta = \zeta_0$ and ζ_0 is the smallest ζ for which

$$\tilde{W}(\zeta) = 0. \tag{6.13}$$

The equation for $X = \tilde{W} + i\tilde{\Phi}$ is

$$\zeta^2 \partial_\zeta^2 X + \zeta \partial_\zeta X + \frac{1}{4} X((X^*)^2 - X^2) = 0 \tag{6.14}$$

which we can solve by Taylor expanding around $\zeta = 0$. Defining

$$X = \sum_{n=0}^{\infty} i^n \alpha_n \zeta^n\,, \tag{6.15}$$

we find that the α_n's satisfy:

$$n^2 \alpha_n = \sum_{k=0}^{\left[\frac{n-1}{2}\right]} \sum_{p=0}^{k} \alpha_{n-(2k+1)} \alpha_{2k+1-p} \alpha_p \tag{6.16}$$

where $[(n-1)/2]$ means the largest integer that is smaller or equal to $(n-1)/2$. Equation (6.16) can be solved recursively once we are given $\alpha_0 = 1$ and $\alpha_1 = 1$. The first few terms in the expansion are

$$\tilde{W}(\zeta) + i\tilde{\Phi}(\zeta) = 1 + i\zeta - \frac{1}{4}\zeta^2 - \frac{i}{16}\zeta^3 + \frac{3}{128}\zeta^4 + \frac{3i}{512}\zeta^5 - \frac{1}{512}\zeta^6 - \ldots \tag{6.17}$$

and we note that the quantities $4^n\, n!\, n!!\, \alpha_n$ are positive integers at least to $n = 100$. Once again, by considering the first 100 terms of the series, we approximate the radius of convergence of the Taylor series expansions for X to be 3.38. Between 0 and 3.38, $\tilde{W}$ has a zero (meaning the phase of X is $i\pi/2$) that appears to be unique. It is at

$$\zeta_0 \approx 2.5918\,. \tag{6.18}$$

See Fig. 6.5.

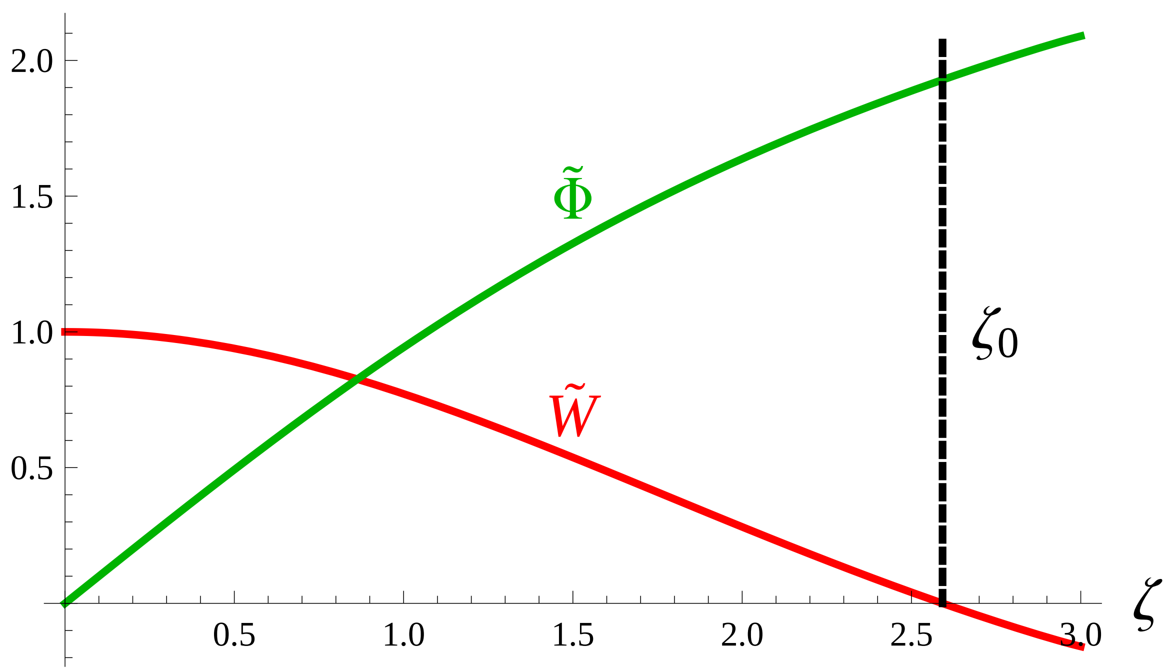

Figure 6.5: The approximate functions $\tilde{\Phi}(\zeta)$ and $\tilde{W}(\zeta)$ evaluated from (6.15) with $n = 40$, with the positive root of $\tilde{W}$ shown.

One may now extract $\mu = \tilde{\Phi}(\zeta_0) W_{\rm IR} \approx 1.9285 W_{\rm IR}$. Note that the range of ζ corresponding to $0 < z < \infty$ is $\zeta_0 > \zeta > 0$. It is convenient that the radius of convergence of the Taylor series (6.17) is significantly larger than ζ_0: because of this, we can get uniformly good accuracy for $\tilde{\Phi}$ and $\tilde{W}$ on the interval of interest from the Taylor series expansion. In practice we terminated the series (6.17) at $n = 100$. In section 6.4 we will approximate this $T = 0$ background with a sharp domain wall solution depicted in figure 6.5.

6.2 Two-point functions from conformally flat backgrounds

With zero-temperature and finite-temperature backgrounds in hand, an obvious next step is to compute Green's functions associated with interesting physical phenomena, such as conductivity and photoemission. Such computations typically rely heavily on numerics, because even the coefficients in the differential equations to be solved are known only numerically. It turns out, however, that some of the features of the final answer can be understood qualitatively in terms of the Green's functions one would get for the ultraviolet and infrared AdS_4 geometries alone. These asymptotic forms can be obtained analytically. This section is devoted to a general study of such Green's functions for more general gauge groups and even for slightly more general gravitational backgrounds than AdS_4. The backgrounds we study are conformally flat, and we require that the gauge connection is also flat: that is, there is no Yang-Mills field strength. In the context of AdS/CFT, the flat Yang-Mills connection in the bulk implies that the field theory lagrangian on the boundary has been explicitly deformed by components of conserved currents associated with continuous symmetries, and that all the deformations commute both with each other and the original Hamiltonian. As explained earlier, our motivation for carrying out this analysis is to get a better understanding of the infrared and ultraviolet behavior of the domain wall geometries of the non-abelian holographic superconductors described in the previous subsection. Our analysis is, however, more general. We will see that we can understand not only the fermion correlators, but also the UV and IR limits of scalar and vector correlation functions for a generic non-abelian gauge group.

The calculations in this section, though slightly abstract when expressed in terms of an arbitrary semi-simple Lie algebra and arbitrary unitary representations thereof, are in essence formal elaborations of the simplest calculations possible in AdS/CFT. We have even avoided the use of curved geometries by restricting attention to the conformally coupled scalar, the massless Dirac fermion, and non-abelian gauge fields with a Yang-Mills action. The equations we solve can be understood as describing the free propagation of massless fields in flat space—with a few mild modifications dictated by the bulk gauge symmetries. Thus, this section is relatively self-contained and may serve as a useful introduction to holographic Green's functions for formally inclined readers.

Readers wishing to pass over the technical details but understand the qualitative features may wish to skip straight to section 6.2.5.

6.2.1 The action

Consider the following action for gravity, a Yang-Mills field of a simple gauge group with Lie algebra $\mathbf{g}$, a complex scalar field Σ in the unitary representation $\mathbf{r}_\Sigma$ of $\mathbf{g}$, a Dirac fermion Ψ in the unitary representation $\mathbf{r}_\Psi$ of $\mathbf{g}$ and a real singlet scalar ϕ:

$$S = \int_M d^4x \sqrt{-g} \left[\left(1 - \frac{1}{6}|\Sigma|^2\right) R - \frac{1}{2} \operatorname{tr} F_{\mu\nu}^2 - i\bar{\Psi}\Gamma^\mu D_\mu \Psi - \frac{1}{2}(\partial\phi)^2 - |D_\mu\Sigma|^2 - V(\phi) \right] + S_{\text{bdy}} \,. \tag{6.19}$$

Ordinarily there is a prefactor $1/2\kappa^2 = 1/16\pi G_N$ multiplying S, but we drop this factor. We normalize the trace tr in (6.19) so that $\operatorname{tr} t^a t^b = \frac{1}{2}\delta^{ab}$, where the t^a are generators of $\mathbf{g}$. Since the gauge group is simple, the field strength is given by

$$F_{\mu\nu} = \partial_\mu A_\nu - \partial_\nu A_\mu - ig_{\text{YM}}[A_\mu, A_\nu] \,, \tag{6.20}$$

and we have defined

$$\begin{aligned} D_\mu \Sigma &= (\partial_\mu - ig_{\text{YM}} A^a t^a_{\mathbf{r}_\Sigma})\Sigma \\ D_\mu \Psi &= \left(\partial_\mu + \frac{1}{4}\omega_\mu{}^{\underline{\rho\sigma}}\Gamma_{\underline{\rho\sigma}} - ig_{\text{YM}} A^a_\mu t^a_{\mathbf{r}_\Psi}\right)\Psi \,. \end{aligned} \tag{6.21}$$

Here $t^a_{\mathbf{r}}$ are the generators of $\mathbf{g}$ in the representation $\mathbf{r}$, $\omega_\mu{}^{\underline{\rho\sigma}}$ is the spin connection, and underlined Greek indices are tangent space indices. When there is no risk of confusion, we will omit the subscript on representation matrices like $t^a_{\mathbf{r}_\Sigma}$: so, for example, $t^a\Sigma = t^a_{\mathbf{r}_\Sigma}\Sigma$. We define gamma matrices so that $\Gamma^{\underline{0}}$ is anti-hermitian, while the other $\Gamma^{\underline{\mu}}$ are hermitian, and so that $\{\Gamma^{\underline{\mu}}, \Gamma^{\underline{\nu}}\} = 2\eta^{\underline{\mu\nu}}$ where $\eta^{\underline{\mu\nu}} = \text{diag}\{-1, 1, \ldots, 1\}$. Also, we define $\bar{\Psi} = \Psi^\dagger\Gamma^{\underline{t}}$. The terms in the action S_{bdy} includes boundary terms which do not affect the equations of motion but render the on-shell action finite.

There are several simple ways in which we could generalize (6.19)—but typically will not for the purposes of this section. First, we could generalize to gauge group that are semi-simple or that contain abelian factors. The main difference is that then one has multiple independent gauge couplings. Second, we could introduce an explicit mass term for Σ, and/or other Σ dependence in V. Third, we could introduce a Dirac mass for Ψ, and in the case of a real representation for fermions, also a Majorana mass. And fourth, depending on the choice of representations $\mathbf{r}_\Sigma$ and $\mathbf{r}_\Psi$, we could introduce some Yukawa interactions.

The action (6.19) is similar to what one typically finds for the gauged supergravity truncations of the near-horizon dynamics of D- and M-brane constructions. It was chosen for purposes of producing simple illustrations of the Green's function computations that we want to do. The biggest difference between (6.19) and supergravity actions is that in supergravity, there are spin-3/2 fields (the gravitini) in addition to $g_{\mu\nu}$, A_μ, Ψ, Σ, and ϕ. Further differences are that in gauged supergravity, one would typically redefine the metric through a scalar-dependent Weyl transformation so that the Einstein-Hilbert term has no prefactor; and that in supergravity, the kinetic terms of the other fields would typically involve interesting functions of the scalars.

6.2.2 Conformally flat backgrounds

The simplest class of solutions to (6.19) is

$$ds^2 = \mathrm{e}_0(z)^2(-dt^2 + dx^2 + dy^2 + dz^2) \qquad\qquad \phi = \phi(z)\,, \tag{6.22}$$

with all other fields set to 0. For example, if $V(\phi) = -6/L^2$, then

$$\mathrm{e}_0(z) = L/z \qquad\qquad \phi(z) = 0 \tag{6.23}$$

provide a solution to the equations of motion. An solution (6.23) is the Poincaré patch of AdS_4, dual to a conformal field theory (CFT) in $2+1$ dimensions. In the coordinate system used in (6.22) and (6.23), z runs from 0, which is the boundary of AdS_4, to infinity. Typically the CFT is a large N gauge theory, and the large N approximation justifies the classical treatment of the bulk dynamics. The large N gauge groups of the boundary theory have nothing to do with the bulk gauge group $\mathbf{g}$. Rather, $\mathbf{g}$ is the algebra of continuous global symmetries of the boundary theory. We will denote the Noether currents associated with these symmetries by J_m^a, where a is an index for the adjoint of $\mathbf{g}$ and m runs over the three boundary directions.

There are more general solutions to the equations of motion following from (6.19). In what follows we will be interested in solutions of the form (6.19) where e_0 and ϕ are defined for $z > 0$, and where e_0 is a monotonically decreasing function of z which diverges at $z = 0$. Such solutions can frequently be related to vacua of conformal field theories deformed by an operator $\mathcal{O}_\phi$ dual to ϕ. When such a relation exists, the solutions are termed holographic renormalization group (RG) flows. True to this name, these geometries break conformal invariance. However, they manifestly preserve the Lorentz invariance of $\mathbf{R}^{2,1}$. They also preserve the full gauge invariance under $\mathbf{g}$, because ϕ is (by assumption) a gauge singlet.

What we want particularly to note is that the solution (6.22) (even when it's not AdS_4) is unaltered upon the introduction of non-zero gauge field A_μ, provided the field strength $F_{\mu\nu}$ vanishes. More particularly, we are interested in configurations where $A_z = 0$ and A_m is constant for $m = 0, 1, 2$. In order to be a flat connection, A_m must take values in a Cartan subalgebra $\mathbf{h}$ of $\mathbf{g}$:

$$A_m = A_m^a t^a \in \mathbf{h} \,. \tag{6.24}$$

Through an appropriate choice of basis, we can insist that all the t^a occurring in the sum (6.24) belong to $\mathbf{h}$. We will refer to the flat gauge connection (6.24) as a Wilson line. This would be more strictly appropriate if we compactified the x and y directions into a torus and formed the integrals $\int_\gamma A$ over closed curves γ wrapping the torus.

The gauge fields (6.24) explicitly break some or all of the gauge and Lorentz invariance, while preserving translation invariance. In the context of AdS/CFT, if the lagrangian of the field theory dual to the holographic RG flow (6.22) is $\mathcal{L}_0$, then the lagrangian with the gauge fields (6.24) turned on is

$$\mathcal{L} = \mathcal{L}_0 + A_m^a J^{ma} \,. \tag{6.25}$$

Two-point functions of operators which are singlets under $\mathbf{g}$, such as $\mathcal{O}_\phi$ and the stress tensor T_{mn}, respect the Lorentz invariance of the background (6.22), at least to leading order in N, because the free propagation of singlet fields, such as perturbations of ϕ and $g_{\mu\nu}$, do not respond to the Wilson lines (6.24). On the other hand, correlation functions of the operators $\mathcal{O}_\Sigma$ and $\mathcal{O}_\Psi$ dual to Σ and Ψ, and also of the Noether currents J_m^a, must be sensitive to the Wilson line. The main goal of this whole section is to describe that dependence.

The key to making the calculation of the two-point functions of $\mathcal{O}_\Sigma$, $\mathcal{O}_\Psi$, and J_m^a tractable is that the action simplifies greatly upon the conformal transformations

$$\Sigma = \frac{\sigma}{\mathrm{e}_0} \qquad \Psi = \frac{\psi}{\mathrm{e}_0^{3/2}} \,. \tag{6.26}$$

The parts of the action (6.19) involving A_μ, Σ, and Ψ can now be expressed as

$$S_{\text{flat}} = \int_M d^4x \left[-\frac{1}{2} \operatorname{tr} F_{\mu\nu}^2 - i\bar{\psi}\Gamma^{\underline{\mu}} D_\mu \psi - |D_\mu \sigma|^2 \right] - \int_{\partial M} d^3x \, i\bar{\psi}\Gamma_- \psi \,, \tag{6.27}$$

where we have now written S_{bdy} for the fermions explicitly in terms of the projection matrix Γ_-, and we have defined

$$\Gamma_\pm = \frac{1 \mp \Gamma^{\underline{z}}}{2} \,. \tag{6.28}$$

M is now the $z > 0$ part of $\mathbf{R}^{3,1}$, and ∂M denotes the surface $z = 0$, which is just $\mathbf{R}^{2,1}$. In (6.28), and in the rest of this section, we use the flat metric $\eta_{\mu\nu} = \operatorname{diag}\{-1, 1, 1, 1\}$ in all formulas: thus, for example, $\operatorname{tr} F_{\mu\nu}^2 = \eta^{\mu_1\mu_2}\eta^{\nu_1\nu_2} \operatorname{tr} F_{\mu_1\nu_1} F_{\mu_2\nu_2}$. Because there is now no distinction between "curved space" indices μ and tangent space indices $\underline{\mu}$, we simply use μ. Because the metric is flat, the spin connection vanishes. So

$$\begin{aligned} D_\mu \sigma &= (\partial_\mu - i g_{\text{YM}} A_\mu^a t^a) \sigma \\ D_\mu \psi &= \left(\partial_\mu - i g_{\text{YM}} A_\mu^a t^a \right) \psi \,. \end{aligned} \tag{6.29}$$

6.2.3 Scalar two-point functions

We define

$$G^R_\Sigma(x) = -i\theta(t)\langle[\mathcal{O}_\Sigma(t,\vec{x}), \mathcal{O}^\dagger_\Sigma(0,0)]\rangle = \int \frac{d^3k}{(2\pi)^3} e^{ik\cdot x} G^R_\Sigma(k)$$
$$G^F_\Sigma(x) = -i\langle T\mathcal{O}_\Sigma(t,\vec{x})\mathcal{O}^\dagger_\Sigma(0,0)\rangle = \int \frac{d^3k}{(2\pi)^3} e^{ik\cdot x} G^F_\Sigma(k)\,. \tag{6.30}$$

Here T denotes time-ordering, $x = (t, \vec{x})$, $k = (\omega, \vec{k})$, and $k \cdot x = -\omega t + \vec{k} \cdot \vec{x}$. We use $\langle A\rangle = \operatorname{tr} \rho A$ where ρ is the density matrix of the state under consideration. When the temperature and chemical potentials are zero this reduces to the vacuum expectation value $\langle 0|A|0\rangle$. The Green's functions (6.30) can be extracted from solutions to the wave equation for σ, as we now explain in some detail.

The scalar equation of motion is

$$D_\mu D^\mu \sigma = 0\,. \tag{6.31}$$

Because of the translation invariance in the $(t, \vec{x})$ directions, we can cast solutions in the form

$$\sigma(t, \vec{x}, z) = e^{ik\cdot x}\hat{\sigma}(z)\,. \tag{6.32}$$

A straightforward calculation shows that

$$D_\mu \sigma = e^{ik\cdot x}\hat{D}_\mu \hat{\sigma} \tag{6.33}$$

where

$$\hat{D}_m = iK_m \qquad \hat{D}_z = \partial_z \tag{6.34}$$

and

$$K_m = k_m - g_{\rm YM} A^a_m t^a\,. \tag{6.35}$$

(6.31) can be recast as

$$(\partial_z^2 - K_m K^m)\hat{\sigma} = 0\,, \tag{6.36}$$

so the solution is $\hat{\sigma} = e^{\pm Kz} v$, where $K = \sqrt{K^m K_m}$ and v is an arbitrary vector in $\mathbf{r}_\Sigma$. Recall that t^a is in the Cartan subalgebra $\mathbf{h}$ of $\mathbf{g}$ and we are working in a basis where all the t^a are diagonal. Thus, the K_m are diagonal, and one can define non-polynomial functions of the

K_m. Indeed, let v_λ be the weight space associated with weight vector λ^a, i.e., $t^a v_\lambda = \lambda^a v_\lambda$ for all $t^a \in \mathbf{h}$. Then $K_m v_\lambda = (k_m - k_{m,\lambda}) v_\lambda$ where

$$k_{m,\lambda} = g_{\rm YM} A^a_m \lambda^a \,. \tag{6.37}$$

When defining $K = \sqrt{K^m K_m}$ we need to specify which branch of the square root to pick. To start, let the spatial part $\vec{k}$ of k be large enough so that $k_m - k_{m,\lambda}$ is spacelike for all weights λ. Then the action of K on vectors in the λ eigenspace is simply $K v_\lambda = \sqrt{(k_m - k_{m,\lambda})(k^m - k^m_\lambda)} v_\lambda \equiv \sqrt{(k - k_\lambda)^2}\, v_\lambda$, where we pick the plus sign on the square root. Thus, in this purely spacelike case, where K^2 is a positive definite matrix acting on $\mathbf{r}_\Sigma$, we choose K also to be positive definite. Then the solutions to (6.36) which decay far from the boundary take the form

$$\hat{\sigma} = e^{-Kz} v \,. \tag{6.38}$$

Still assuming that K^2 is positive definite, one may extract the Green's function in the following manner. The on-shell action for the scalar is

$$S_{\rm on-shell} = -\int_M d^4x\, |D_\mu \sigma|^2 = -\int_M d^4x \left[\partial_\mu(\sigma^\dagger D^\mu \sigma) - \sigma^\dagger D_\mu D^\mu \sigma\right] = \int_{\partial M} d^3x\, \sigma^\dagger \partial_z \sigma \,, \tag{6.39}$$

where in the second step we used the equations of motion, and in the third step we used Stokes' Theorem and remembered that $D^z = \partial_z$. The basic premise of AdS/CFT is that the on-shell action is the generating functional for Green's functions of the boundary theory. In the current instance, this means that

$$S_{\rm on-shell} = W_2[\sigma_{\rm bdy}, \sigma^\dagger_{\rm bdy}] \equiv -\int_{\partial M} d^3x_1 d^3x_2\, \sigma^\dagger_{\rm bdy}(x_1) G_\Sigma(x_1 - x_2) \sigma_{\rm bdy}(x_2) \,, \tag{6.40}$$

where G_Σ is a two-point function of $\mathcal{O}_\Sigma$, and $\sigma_{\rm bdy}$ is simply σ evaluated at the boundary $z = 0$. The alert reader will note that we have not specified whether (6.44) is a retarded or time-ordered Green's function. At the moment we do not need to because the Hermitian parts of G^R_Σ and G^F_Σ coincide, and we are doing the computation for k_m such that K^2 is positive definite. To recover the full Green's function we will use an appropriate pole passing prescription to go to more general K^2.

Now consider the following linear combination of solutions to the equation of motion for σ:

$$\sigma = \xi_1 e^{ik\cdot x} e^{-Kz} v_1 + \xi_2 e^{iq\cdot x} e^{-Qz} v_2 \,, \tag{6.41}$$

where ξ_1 and ξ_2 are complex numbers, and Q is defined from the momentum q_m as K is from k_m. The on-shell action is now sesquilinear in ξ_1 and ξ_2. Plugging the boundary limit of the specific form (6.41) into the last expression in (6.40), one obtains immediately

$$\frac{\partial^2 W_2}{\partial \xi_1 \partial \xi_2^*} = -(2\pi)^3 \delta^3(q-k) v_2^\dagger G_\Sigma(k) v_1 \,. \tag{6.42}$$

On the other hand, plugging (6.41) into the last expression in (6.39) leads to

$$\frac{\partial^2 S_{\text{on-shell}}}{\partial \xi_1 \partial \xi_2^*} = \int_{\partial M} d^3x \, v_2^\dagger e^{-iq\cdot x} (-K) e^{ik\cdot x} v_1 \,. \tag{6.43}$$

Equating (6.42) and (6.43) leads to

$$G_\Sigma(k) = K \,. \tag{6.44}$$

This is almost our final result. The full retarded or Feynman Green's function can be obtained from (6.44) by an appropriate pole passing prescription:

$$\begin{aligned} &\omega \to \omega + i\epsilon &&\text{to obtain } G^R \\ &\omega \to \omega(1+i\epsilon) &&\text{to obtain } G^F . \end{aligned} \tag{6.45}$$

The subtleties of recovering the imaginary part of Green's functions from a supergravity action which is real have received significant attention [11, 12, 92, 57]. Here let us simply make the well-known observation that with the prescription (6.45) for retarded Green's functions, the scalar wave-functions are infalling: on eigenspaces where K_m acts as a timelike vector, K is a negative imaginary number, meaning that $e^{-Kz}v = e^{ipz}v$ with $p > 0$. In other words, the number flux of scalar quanta is away from the boundary, falling into the bulk.

Already from the simple expression (6.44) we can reach one of the main conclusions of this section: The spectral measure is supported in the timelike regions of light-cones in

k-space, one through $k_{m,\lambda}$ for each weight λ in the representation $\mathbf{r}_\Sigma$. To see this explicitly, we can simply note that $G_\Sigma(k)$ acts as

$$G_{\Sigma,\lambda}(k) = \sqrt{(k-k_\lambda)^2} \tag{6.46}$$

on the weight space associated with λ. This part of the Green's function has an imaginary part precisely when $k-k_\lambda$ is timelike, i.e. in the light-cone passing through k_λ. The spectral measure is essentially this imaginary part.

We have not concerned ourselves with the overall normalization of the action. If we had, we would have found an overall prefactor on G_Σ which scales as $N^{3/2}$ in constructions based on N coincident M2-branes.

Giving the scalar Σ an explicit mass term m, instead of the conformal coupling $-\frac{1}{6}|\Sigma|^2$ implies that the dual operator $\mathcal{O}_\Sigma$ has dimension Δ where $\Delta(\Delta-3) = m^2L^2$ and L is the radius of curvature of AdS$_4$. The calculation of the two-point functions proceeds almost identically to what we laid out above, except that it has to be done in AdS$_4$ rather than flat space, because the mass term is not conformally invariant. The radial parts of the wave-functions (without any conformal rescaling) come out proportional to $z^{3/2}\mathbf{K}_{\Delta-3/2}(Kz)$ instead of ze^{-Kz} as in (6.38). The pole passing prescription (6.45) will convert the modified Bessel function $\mathbf{K}_{\Delta-3/2}$ into an appropriate Hankel function when K_m acts as a timelike vector. When $\Delta \neq n + 3/2$ with n an integer, the result for the two-point function is $G_\Sigma(k) = c_\Delta K^{2\Delta-3}$, where c_Δ is a k-independent factor. Evidently, (6.44) corresponds to the case $\Delta = 2$. When $\Delta = n+3/2$ the Green's function takes the form $\tilde{c}_\Delta K^{2\Delta-3}\log K$. The limit $2\Delta - 3 \to n$ coincides with this form of the Green's function since c_Δ diverges in this limit.

6.2.4 Spinor and vector two-point functions

Our results for the scalar Green's functions G_Σ can be summarized in the following simple terms. With no gauge field present in the bulk, conformal invariance dictates $G_\Sigma(k) = c_\Delta k^{2\Delta-3}$. For $\Delta = 2$, the same expression can be deduced more generally for conformally flat backgrounds. The effects of the gauge field are simply to replace k with K, where $K_m = k_m - g_{\rm YM} A^a_m t^a$ as in (6.35).

In light of these results, it is reasonable to guess that Green's functions for spinor operators and conserved currents in the presence of a flat connection follow from similar replacements $k_m \to K_m$. More explicitly, the Green's functions we have in mind are defined as follows:

$$\begin{aligned} G^R_\Psi(x) &\equiv -i\theta(t)\langle\{\mathcal{O}_\Psi(t,\vec{x}), \mathcal{O}^\dagger_\Psi(0,0)\}\rangle = \int \frac{d^3k}{(2\pi)^3} e^{ik\cdot x} G^R_\Psi(k) \\ G^{R,ab}_{mn}(x) &\equiv -i\theta(t)\langle[J^a_m(t,\vec{x}), J^b_n(0,0)]\rangle = \int \frac{d^3k}{(2\pi)^3} e^{ik\cdot x} G^{R,ab}_{mn}(k)\,. \end{aligned} \tag{6.47}$$

Time-ordered Green's functions would be defined similarly. We usually omit the adjoint indices a, b. $\mathcal{O}_\Psi$ may have any dimension Δ, but because J^a_m is conserved, its dimension must be 2. Our expectation is that

$$G_\Psi(k) = -f_\Delta \frac{\gamma^m K_m}{K^{4-2\Delta}} \gamma^t \qquad\qquad G^{ab}_{mn}(k) = s_\infty \left(\frac{K^2\eta_{mn} - K_m K_n}{K}\right)^{ab}, \tag{6.48}$$

where f_Δ and s_∞ are constants that we do not propose to track at this stage, and the $i\epsilon$ prescription (6.45) is implied. Our notation, essentially following [57], is to represent the four-dimensional gamma matrices as

$$\Gamma^m = \begin{pmatrix} 0 & \gamma^m \\ \gamma^m & 0 \end{pmatrix} \qquad \Gamma^z = \begin{pmatrix} -1 & 0 \\ 0 & 1 \end{pmatrix}, \tag{6.49}$$

where

$$\gamma^t = i\sigma_2 \qquad \gamma^1 = \sigma_1 \qquad \gamma^2 = \sigma_3 \tag{6.50}$$

and σ_a denotes the Paul matrices. We decompose the Dirac spinor ψ as

$$\psi = \begin{pmatrix} \psi_+ \\ \psi_- \end{pmatrix}. \tag{6.51}$$

The operator $\mathcal{O}_\Psi$ transforms as a two-component spinor, like ψ_-. We sometimes consider the Dirac conjugate of a two component spinor: $\bar\psi_\pm \equiv \psi^\dagger_\pm \gamma^t$. The Green's function $G_\Psi(k)$ has the same spinor structure and group representation content as the bilinear $\psi_-\psi^\dagger_-$.

Just as in the case of scalar Green's functions, if u_- is a two-component spinor which belongs to a weight space of $\mathbf{r}_\Psi$ with weight vector λ then the action of G_Ψ on u_- is of the form $G_\Psi(k)u_- = G_{\Psi,\lambda}(k)u_-$, where

$$G_{\Psi,\lambda}(k) = -f_\Delta \frac{\gamma^m(k_m - k_{m,\lambda})}{(k-k_\lambda)^{4-2\Delta}}\gamma^t\,, \tag{6.52}$$

and k_λ is defined as in (6.37), only using weights of $\mathbf{r}_\Psi$ not $\mathbf{r}_\Sigma$. Likewise, if ϵ^n is a polarization vector which also belongs to a root space of $\mathbf{g}$ with root vector α, then $G_{mn}(k)\epsilon^n = G_{mn,\alpha}(k)\epsilon^n$ where

$$G_{mn,\alpha}(k) = s_\infty \frac{(k-k_\alpha)^2\eta_{mn} - (k_m - k_{m,\alpha})(k_n - k_{n,\alpha})}{\sqrt{(k-k_\alpha)^2}}\,, \tag{6.53}$$

and $k_{m,\alpha} = g_{\mathrm{YM}} A^a_m \alpha^a$. Evidently, the spectral measures of G_Ψ and G_{mn} are supported inside light cones, just as for G_Σ, but each light cone has its apex at the the momentum k_λ or k_α associated with a weight vector λ or a root vector α, as appropriate.

Let's sketch a derivation of the expression in (6.48) for G_Ψ in the case $\Delta = 3/2$, corresponding to a massless fermion, again focusing first on the situation where K^2 is positive definite. This is the case where we can do all the calculations in flat space, where the equation of motion is

$$\Gamma^\mu D_\mu \psi = 0\,. \tag{6.54}$$

This equation implies $D_\mu D^\mu \psi = 0$, which is identical to (6.31). So the allowed solutions are of the same form:

$$\psi = e^{ik\cdot x} e^{-Kz} u\,. \tag{6.55}$$

Here u is a four-component spinor transforming in the representation $\mathbf{r}_\Psi$. Plugging (6.55) into (6.54) provides a constraint on u:

$$(i\Gamma^m K_m - \Gamma^z K)\, u = 0\,. \tag{6.56}$$

Decomposing u as in (6.49), one can rewrite (6.56) as

$$u_- = i\frac{\gamma^m K_m}{K} u_+\,. \tag{6.57}$$

To compute the fermionic Green's function we plug a linear combination of solutions to the Dirac equation,

$$\psi = \xi_1 e^{ik\cdot x} e^{-Kz} u_1 + \xi_2 e^{iq\cdot x} e^{-Qz} u_2 \,, \tag{6.58}$$

into the on-shell action, which is simply the boundary term in (6.27):

$$S_{\text{on-shell}} = -\int_{\partial M} d^3x\, i\bar{\psi}\Gamma_- \psi = -i\xi_2^* \xi_1 (2\pi)^3 \delta^3(q-k)\bar{u}_{2+} u_{1-} + \dots \,. \tag{6.59}$$

In (6.59) we omitted terms involving different combinations of the ξ_i and their conjugates. Using (6.57) we find

$$\frac{\partial^2 S_{\text{on-shell}}}{\partial \xi_1 \partial \xi_2^*} = (2\pi)^3 \delta^3(q-k) \bar{u}_{2+} \frac{\gamma^m K_m}{K} u_{1+} \,. \tag{6.60}$$

On the other hand, essentially by definition,

$$\frac{\partial^2 W_2}{\partial \xi_1 \partial \xi_2^*} = -(2\pi)^3 \delta^3(q-k) \bar{u}_{2+} G_\Psi(k) \gamma^t u_{1+} \,. \tag{6.61}$$

Comparing (6.60) and (6.61) leads immediately to

$$G_\Psi(k) = -\frac{\gamma^m K_m}{K} \gamma^t \,. \tag{6.62}$$

Continuing to momenta where $K^2 < 0$ can be done using (6.45).

For the gauge field, the story is essentially the same. We start by perturbing the gauge field:

$$A = A_{\text{flat}} + a \,. \tag{6.63}$$

The field strength is $F = \frac{i}{g}(d - igA)^2 = f + O(a^2)$, where

$$f_{\mu\nu} = D_\mu a_\nu - D_\nu a_\mu \,, \tag{6.64}$$

where by convention $D = d - igA_{\text{flat}}$. The linearized equation of motion is

$$D^\mu f_{\mu\nu} = 0 \,. \tag{6.65}$$

It is most straightforward to proceed in a gauge where $a_z = 0$. Then one can show directly from (6.65), assuming as usual that K^2 is positive definite, that $a_m = e^{ik_m x^m} e^{-Kz} \epsilon_m$ if

$K^m \epsilon_m = 0$, and that $a_m = e^{ik_m x^m} \epsilon_m$ if $\frac{K_n K^m}{K^2} \epsilon_m = \epsilon_n$. Here ϵ_n is a constant polarization vector. The transverse modes, where $K^m \epsilon_m = 0$, are physical and the others are pure gauge. If we define

$$P_n{}^m = \delta_n{}^m - \frac{K_n K^m}{K^2}\,, \tag{6.66}$$

then we may compactly write the allowed solutions as

$$a = e^{ik\cdot x} e^{-KPz} \epsilon\,, \tag{6.67}$$

where Lorentz indices for the boundary directions are now implied. Plugging (6.67) into the quadratic on-shell action

$$S_{\text{on-shell}} = \int d^3x \; \operatorname{tr} a_m f^{zm}\,, \tag{6.68}$$

one finds more or less immediately that

$$G_{mn}(k) = K P_{mn}\,, \tag{6.69}$$

which indeed has the form indicated in (6.48).

We will not delve deeply into conductivity calculations in this paper, but it is worth noting that (6.69) contains a geometrical explanation of the hard-gap phenomenon remarked on in [85]. To understand this connection, first recall that the gauge potential in the infrared copy of AdS$_4$ is (in the notation of [85]) $A = B_0\, \tau^1\, dx$. So the Cartan subalgebra $\mathbf{h}$ is the one generated by τ^1. The conductivity studied in [85] is the one related to a perturbation $\delta A = e^{-i\omega t} a(z)\, \tau^3\, dy$. Now, $G^R_{mn}(k)$ acts in the adjoint representation, so it can be denoted $G^{R\,ab}_{mn}(k)$. The conductivity of interest is

$$\sigma_{yy,\tau^3}(\omega) = \frac{i}{\omega} v_a v_b G^{R\,ab}_{yy}(\omega, 0, 0)\,, \tag{6.70}$$

where v_a is the unit vector corresponding to the generator τ^3. Now we need to find a convenient basis in which to work out the right-hand-side of (6.70). The obvious basis for the adjoint representation, for our purposes, is the one in which τ^1 acts diagonally. The eigenvalues of its adjoint action are $\alpha = \pm 1$ and 0: these are the roots α of the adjoint representation of $SU(2)$, and they correspond to the c-number Green's functions $G^R_{mn,\alpha}$

defined in (6.53). In the basis for the adjoint representation where $(1,0,0)$ corresponds to $\alpha=1$, $(0,1,0)$ corresponds to $\alpha=-1$, and $(0,0,1)$ corresponds to $\alpha=0$, the unit vector corresponding to the generator τ^3 is $v=(1,1,0)/\sqrt{2}$. Plugging this expression for v into (6.70), we have

$$\sigma_{yy,\tau^3}(\omega)=\frac{i}{2\omega}\left[G^R_{yy,+}(\omega,0,0)+G^R_{yy,-}(\omega,0,0)\right]\,. \tag{6.71}$$

Now we can explain the geometric origin of the gap. From the explicit expression (6.53) we see that $G^R_{yy,+}$ is real except inside the light cone whose apex is at $k_{m,+}=g_{\rm YM}B_0\delta^x_m$. The distance along the ω axis one must go in order to cross into this light cone is $g_{\rm YM}B_0$. Likewise, $G^R_{yy,-}$ is real except inside a lightcone which one crosses into along the ω axis at the same value of ω. $G^R_{yy,0}$ has no gap, but it is not involved in $\sigma_{yy,\tau^3}(\omega)$. So the gap is $\Delta=g_{\rm YM}B_0$.

What we are neglecting is that there is asymmetric warping of time and space in the domain wall geometry of [85]. The t coordinate picks up a warp factor $e^{-\chi_0/2}$ in the infrared AdS$_4$ geometry relative to the ultraviolet, while the x coordinate picks up a factor c_0. Correspondingly, the wave-vector k_{m_+} at the apex of the light cone gets scaled by $1/c_0$ because it points in the x direction, and frequency gets scaled by $e^{\chi_0/2}$. Altogether, introducing these rescalings into the expression $\Delta=g_{\rm YM}B_0$ for the gap leads to

$$\tilde{\Delta}=\frac{e^{-\chi_0/2}g_{\rm YM}B_0}{c_0}\,. \tag{6.72}$$

$\tilde{\Delta}$ should match the gap found in [85], and it does. (Recall that their q is our $g_{\rm YM}$.) What we learn in addition is that if conductivity could be measured at finite wave-number, the gap would decrease as one goes toward the apex of one of the lightcones, and can be reduced to zero if the wave-number is chosen to lie at the apex. Similar analysis seems possible for σ_{xx,τ^3}, but we have not fully considered the consequences of mixing with the graviton and with timelike components of the gauge potential in this case.

It may seem striking that we are able to evaluate the gap by considering only the infrared limit of the geometry. This actually makes sense because there is a continuum contribution to the spectral measure of $G^{R\,ab}_{mn}$ only when the corresponding gauge-boson wave-function has some infalling component in the infrared geometry; otherwise the Green's function is purely real, with no dissipative part, except for δ-function localized contributions to the spectral measure like the one that signals infinite DC conductivity. The same reasoning, essentially, is behind the evaluation of the gap in [85]: the Schrodinger potential plateaus in the infrared at an energy that determines the gap.

6.2.5 Summary and an example

The upshot of the calculations in this section is that the Green's functions of operators dual to the conformally coupled scalar Σ, the massless Dirac fermion Ψ, and the non-abelian gauge fields A_μ in (6.19), are simple functions of modified momenta

$$K_m = k_m - g_{\rm YM} A^a_m t^a \,. \tag{6.73}$$

In particular, they all involve fractional powers of $K^2 = \eta^{mn} K_m K_n$. K^2 is always hermitian, but positive definite only for k outside all the shifted light-cones $(k_m - k_{m,\lambda})(k^m - k^m_\lambda) = 0$. As explained earlier, $k_{m,\lambda}$ is given by

$$k_{m,\lambda} = g_{\rm YM} A^a_m \lambda^a \,, \tag{6.74}$$

where λ is a weight vector for the representation in which the operator whose Green's function we are considering transforms. The spectral measure of these Green's functions comes entirely from the region where K^2 fails to be positive definite, i.e. the region where $k - k_\lambda$ is timelike for some weight λ.

It is interesting that the Green's functions have a pure power law form not only for an AdS_4 bulk, but for any conformally flat bulk geometry which is asymptotically AdS_4. This is a consequence of the invariance of the relevant part of the classical supergravity action under conformal transformations. Thus, power-law correlators, like those one sees in conformal theories, arise at leading order in a large N limit for special operators in backgrounds that are dual to non-conformal theories. At subleading orders in N, loop corrections in the bulk enter in, and one cannot expect the exact power-law behavior of the boundary theory correlators to persist unless there is conformal symmetry. All the backgrounds treatable by the methods of this section have exact boost invariance, $SO(2,1)$, as well as translational invariance. These symmetries would be preserved at all loop orders in the bulk, meaning all orders in N in the boundary theory.

As an example, consider $\mathbf{g} = so(4) = su(2)_A \oplus su(2)_B$, where the generators for the two $su(2)$ factors are labeled τ_A^a and τ_B^a. The standard Cartan subalgebra is generated by τ_A^3 and τ_B^3. Let the fermions Ψ transform in the $4 = 2_A \times 2_B$ of $so(4)$. Consider now the flat connection

$$A = W\,(dx\,\tau_A^1 + dy\,\tau_B^2)\,, \tag{6.75}$$

where W is a constant. Assuming that for $X = A, B$ the eigenvalues of each τ_X^a acting on the doublet of $su(2)_X$ are $\pm 1/2$, the images (6.74) of the weight vectors of the vector representation of $so(4)$ are

$$k_{s_1 s_2} = \frac{g_{\rm YM} W}{2}(s_1 \hat{k}_1 + s_2 \hat{k}_2) \tag{6.76}$$

where $s_i = \pm 1$ and $\hat{k}_i$ are unit vectors in momentum space. Thus the apexes of the Dirac cones pass through points at the corner of a square whose sides are aligned with the k_x and k_y axes.

The spectral measure of the retarded version of the Green's function (6.62) is

$$\rho(\omega, \vec{k}) \equiv -\operatorname{Im}\operatorname{tr} G_\Psi^R(k) = 2|\omega| \sum_{s_i = \pm 1} \frac{\theta(\omega^2 - |\vec{k} - \vec{k}_{s_1 s_2}|^2)}{\sqrt{\omega^2 - |\vec{k} - \vec{k}_{s_1 s_2}|^2}}\,, \tag{6.77}$$

where we have used (6.62) and (6.76). The most conspicuous feature of (6.77) is that $\rho(\omega, \vec{k})$ is supported in the union of four Dirac cones, whose apexes are the vectors $\vec{k}_{s_1 s_2}$. Plots of the Dirac cone and of $\rho(\omega, \vec{k})$ as a function of ω for fixed $\vec{k}$ are shown in figure 6.6. By adding a mass to the fermion, we can adjust the power in the denominator of (6.77) from a square root to $2 - \Delta$, where Δ is the dimension of the dual fermionic operator in the field theory: see (6.52).

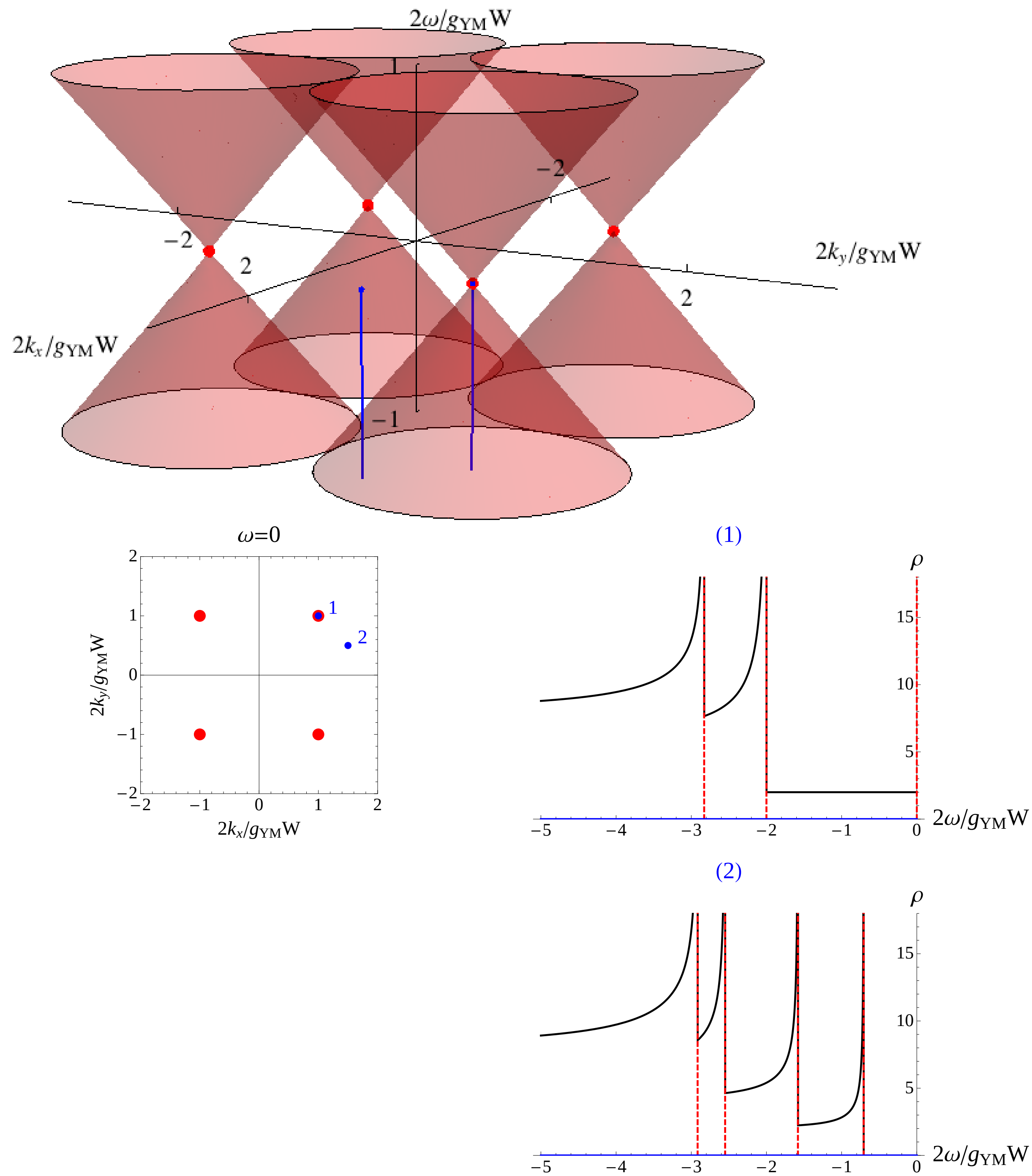

Figure 6.6: Features of the spectral function for the operator dual to a massless Dirac fermion in the **4** of $so(4)$, in a conformally flat background with the flat $so(4)$ connection (6.75). This is distinct from the spectral function in the p-wave superconductor to be discussed in the next section. Top: The Dirac cones inside which the spectral measure is supported. Bottom: Two representative plots of $\rho(\omega, \vec{k})$ as a function of ω for fixed values of $\vec{k}$.

6.3 Properties of the spectral function

We are interested in studying the Fourier space retarded Green's function $G^R(k^m)$ for fermions in the doublet of $SU(2)$ for the zero temperature p-wave superconductors discussed in section 6.1; Our conventions for G^R can be found in (6.47). Note that G^R has both spinor and gauge indices and a total of 16 *a priori* independent components. Here we will be interested in the spectral measure, ρ, defined by $\rho = -\operatorname{Im} \operatorname{tr} G^R$, where the trace is over both the gauge indices and the spinor indices. This quantity is gauge invariant, and it is interesting to consider because it gives a measure of the number of eigenstates of the theory that couple to the fermionic operator, with long lived excitations manifesting themselves as δ-functions peaks. In what follows we explain in some detail how to compute the spectral function (section 6.3.1), how it relates to normal modes of bulk fermions (section 6.3.2) and how positivity of ρ is guaranteed from a bulk point of view (section 6.3.3). The reader interested in the final numerical results for ρ may skip directly to section 6.4.

6.3.1 Green's functions from a gravity dual

In section 6.2 we computed the retarded Green's function for a configuration with a flat connection. In this section we consider the fermion Green's function for the zero temperature p-wave superconductor discussed in section 6.1 where the connection is flat only in the IR and UV. The action for the background is given by (6.1) and we use the notation in (6.4-6.5) to describe the metric and $SU(2)$ gauge fields. We introduce the spin-1/2 field Ψ which transforms in the doublet of $SU(2)$, whose action is given by

$$S_{\text{fermion}} = -i \int_M d^4x \sqrt{-g}\, \bar{\Psi} \Gamma^\mu D_\mu \Psi - i \int_{\partial M} d^3x \sqrt{-g g^{rr}}\, \bar{\Psi} \Gamma_- \Psi \ , \tag{6.78}$$

where D_μ is given in (6.21). Our conventions for the Γ matrices are largely as in section 6.2.4, but because we now work in curved spacetime, we must be careful to distinguish between curved and flat indices. Because the matrices γ^m are needed to describe the physics of the boundary theory, which is defined on a flat background, we persist in defining them as in

(6.50). In place of (6.49) we employ

$$\Gamma^{\underline{m}} = \begin{pmatrix} 0 & \gamma^m \\ \gamma^m & 0 \end{pmatrix} \qquad \Gamma^{\underline{r}} = -\Gamma^{\underline{z}} = \begin{pmatrix} 1 & 0 \\ 0 & -1 \end{pmatrix} . \tag{6.79}$$

The second term in (6.78) is a boundary term that does not affect the equations of motion but gives the only nonzero contribution to the on-shell action. We treat Ψ in the probe approximation and do not allow it to back-react on the geometry. The equation of motion for Ψ is $D_\mu \Psi = 0$. To write it explicitly, it is convenient to exploit translation invariance in the x^m directions and write Ψ in the form

$$\Psi(x^m, r) = (-g g^{rr})^{-\frac{1}{4}} e^{-i\omega t + i k_x x + i k_y y} \psi(r) . \tag{6.80}$$

Note that (6.80) reduces to (6.26) for a conformally flat metric. As in section 6.2, it is useful to split ψ into two chiral spinors

$$\psi = \begin{pmatrix} \psi_+ \\ \psi_- \end{pmatrix} . \tag{6.81}$$

The equations of motion for $\psi_\pm$ take the form:

$$\begin{aligned} \psi_+' + \frac{i}{\sqrt{\gamma} r^2} \left[\frac{e^{\frac{\chi}{2}}}{\sqrt{\gamma}} \left(-\omega - g_{\mathrm{YM}} \Phi\, \tau^3 \right) \gamma^t + \frac{1}{c} \left(k_x - g_{\mathrm{YM}} W\, \tau^1 \right) \gamma^x + k_y \gamma^y \right] \psi_- = 0 \\ -\psi_-' + \frac{i}{\sqrt{\gamma} r^2} \left[\frac{e^{\frac{\chi}{2}}}{\sqrt{\gamma}} \left(-\omega - g_{\mathrm{YM}} \Phi\, \tau^3 \right) \gamma^t + \frac{1}{c} \left(k_x - g_{\mathrm{YM}} W \tau^1 \right) \gamma^x + k_y \gamma^y \right] \psi_+ = 0 , \end{aligned} \tag{6.82}$$

where the prime denotes a derivative with respect to r and γ^μ are 2+1 dimensional boundary theory γ matrices related to the bulk Γ matrices through (6.49). Note that $\psi_\pm$ have both a boundary spinor index and an $SU(2)$ doublet index. We suppressed both types of indices in (6.82) but it should be clear how they are contracted. For instance $\left(\gamma^t \tau^1 \psi_+\right)^{(i)\,(b)} = \gamma^{t\,(ij)} \tau^{1\,(ab)} \psi^{(j)\,(b)}$, where $(i), (j), \ldots = 1, 2$ are spinor indices and $(a), (b), \ldots = 1, 2$ are $SU(2)$ doublet indices.

The asymptotic solution to (6.82) in the infrared is

$$\begin{aligned} \psi^{\mathrm{IR}} &= V_1 e^{-\kappa_+/r} + V_2 e^{-\kappa_-/r} + V_3 e^{\kappa_+/r} + V_4 e^{\kappa_-/r} \\ \kappa_\pm &\equiv \left(-e^{\chi_{\mathrm{IR}}} \omega^2 + \left(\frac{2k_x \pm g_{\mathrm{YM}} W_{\mathrm{IR}}}{2 c_{\mathrm{IR}}} \right)^2 + k_y^2 \right)^{\frac{1}{2}} , \end{aligned} \tag{6.83}$$

Here $c \underset{\text{IR}}{\longrightarrow} c_{\text{IR}}$ and similarly $W \underset{\text{IR}}{\longrightarrow} W_{\text{IR}}$ and $\chi \underset{\text{IR}}{\longrightarrow} \chi_{\text{IR}}$. The spinor integration constants V_1 and V_2 satisfy $\tau^1 V_i = \pm\frac{1}{2} V_i$ with the minus sign for $i = 1, 3$ and the plus sign for $i = 2, 4$. They must also satisfy a linear constraint that follows from (6.56). The equations $\kappa_\pm = 0$ define the two IR Dirac cones that we expect for $SU(2)$ doublet fermions. As discussed in section 6.2 if we are outside one of the Dirac cones, i.e, if for instance $\kappa_+^2 > 0$, then the corresponding term in (6.83) should be regular provided we pick the positive sign for the square root in the definition of κ_+. If we are inside one of the Dirac cones, the correct boundary conditions for computing the retarded Green's function are obtained by making the substitution $\omega \to \omega + i\epsilon$ and demanding regularity. In practice, this prescription amounts to keeping ω real and picking the sign of the square root such that the imaginary part has the same sign as ω. This is equivalent to requiring that the solutions are infalling in the IR. Thus, we set

$$V_3 = V_4 = 0\,. \tag{6.84}$$

The asymptotic behavior of the fermions in the UV takes the form

$$\begin{aligned} \psi^{\text{UV}} &= Q_1 e^{-\lambda_+/r} + Q_2 e^{\lambda_+/r} + Q_3 e^{-\lambda_-/r} + Q_4 e^{\lambda_-/r} \\ \lambda_\pm &\equiv \left(-e^{\chi_{\text{UV}}} \left(\omega \pm \frac{1}{2} g_{\text{YM}} \Phi_{\text{UV}} \right)^2 + \frac{k_x^2}{c_{\text{UV}}^2} + k_y^2 \right)^{\frac{1}{2}} , \end{aligned} \tag{6.85}$$

where $c \underset{\text{UV}}{\longrightarrow} c_{\text{UV}}$ and a similar definition for χ_{UV} and Φ_{UV}. The Q_i are constant spinors such that $\tau^3 Q_i = \pm\frac{1}{2} Q_i$ with the plus sign for $i = 3, 4$ and the minus for $i = 1, 2$. Like V_1 and V_2, each Q_i satisfies a linear constraint that follows from (6.56). As opposed to the IR asymptotics (6.83), in the UV there is no restriction on the choice of the sign of the square root in the definition of $\lambda_\pm$. The equations $\lambda_\pm = 0$ define two UV Dirac cones, different from the IR Dirac cones $\kappa_\pm = 0$. The IR Dirac cones are shifted in the k_x direction because in the IR only A_x is nonzero. The UV Dirac cones are shifted in the ω direction since in the UV only A_t is nonzero. Furthermore, since c and χ go to different constants in the UV and IR, the UV and IR Dirac cones are stretched by different factors in the ω and k_x directions: that is, they are characterized by different, anisotropic speeds of light.

The Green's function for the operator dual to Ψ can be found from the UV behavior of the fermions following the prescription given in [93, 94] and more recently in [57]. For the purpose of computing the Green's function we rewrite the UV asymptotics in the form

$$\begin{aligned}\psi_+^{\mathrm{UV}} &= A + B\frac{1}{r} + \mathcal{O}\left(\frac{1}{r^2}\right)\\ \psi_-^{\mathrm{UV}} &= D + C\frac{1}{r} + \mathcal{O}\left(\frac{1}{r^2}\right),\end{aligned} \tag{6.86}$$

where A, B, C and D are arbitrary chiral spinors with an $SU(2)$ doublet index which are linearly related to the Q_i. The linear constraints that follow from (6.56) can be used to solve for B and C in terms of D and A. Since the equations of motion are linear, requiring that the solutions are regular in the IR, (6.84), imposes a linear relation between A and D,

$$D^{(i)(a)} = \mathcal{M}^{(ij)(ab)} A^{(j)(b)}\,. \tag{6.87}$$

As explained in section 6.2, to obtain G^R we take the functional derivative of the on-shell action. The result is

$$G^R = -i\mathcal{M}\gamma^t\,, \tag{6.88}$$

where we suppressed the spinor and $SU(2)$ indices. The derivation is very similar to the one for uncharged fermions, and we refer the reader to [57] for details.

6.3.2 Normal modes

We are particularly interested in the regions in which $\rho \neq 0$. Consider the IR asymptotics for the fermions, (6.83). If $\kappa_+^2 > 0$ or $\kappa_-^2 > 0$ (i.e., we are inside the IR light-cone) then ψ_+ can be chosen to be everywhere real and consequently, $\rho = 0$ except perhaps for poles of $\mathrm{Re}\,\mathrm{tr}(\mathrm{G_R})$ which, together with the $i\epsilon$ prescription corresponds to ρ having δ-function support. In what follows, we argue that a divergence of G_{R} corresponds to a solution to (6.82) which is a normal mode.

We define a normal mode to be a solution of (6.82) which is regular in the IR and its near boundary expansion takes the form (6.86) with $A = 0$. This is a natural definition of a normal mode since A is the leading term in the UV asymptotic expansion of ψ. We can not require D to vanish as well since we are not free to choose D once we fix A. Normal modes will only occur for special values of k^m and V_i (i.e., the values of k^m for which there are normal modes will form a codimension one surface). The coefficients A and D in the UV expansion of ψ and V_1 and V_2 in the IR expansion of ψ are both integration constants of the same solution to a linear differential equation. Hence,

$$A = \mathcal{U}\, V \qquad D = \mathcal{V}\, V\,, \tag{6.89}$$

where V should be understood as a four component object that contains the four independent integration constants in the V_i. Using (6.87) the four by four matrices $\mathcal{U}$ and $\mathcal{V}$ are related to $\mathcal{M}$ through

$$\mathcal{M} = \mathcal{V}\mathcal{U}^{-1}\,, \tag{6.90}$$

where some care must be taken in interpreting the index structure. Since V, A and D are finite the entries of $\mathcal{U}$ and $\mathcal{V}$ can not diverge. From here it follows that if G^R has diverging entries then $\det \mathcal{U} = 0$; the only way that $\mathcal{M}$ (and hence G^R) can diverge is if $\mathcal{U}$ is not invertible, i.e., the solution is a normal mode.

By the same reasons as argued in Chapter 5, we expect normal modes only outside the IR Dirac cones. Let us briefly repeat this reasoning. If $\kappa_\pm^2 > 0$ then, as discussed earlier, ψ_+ can be chosen to be everywhere real and the condition $\det \mathcal{U} = 0$ is a real equation for which we can expect to find solutions for appropriate ω, k_x and k_y. On the other hand, if $\kappa_\pm^2 < 0$, ψ_+ cannot be chosen real and $\det \mathcal{U} = 0$ will be a complex equation whose solutions are expected to involve complex ω. Such a solution would correspond to a quasinormal mode rather than a normal mode.

There is also a somewhat weaker argument for expecting the normal modes to be inside at least one of the UV Dirac cones, ($\lambda_+^2 < 0$ or $\lambda_-^2 < 0$). According to (6.85), if $\lambda_+^2 > 0$ and $\lambda_-^2 > 0$ then the generic UV solution will grow exponentially and matching such a solution to the IR asymptotics seems improbable. If at least one of λ_+^2 and λ_-^2 is negative, then there is at least a two dimensional subspace of oscillatory solutions and there is no such obstruction. Our numerics indicate that the outermost UV light cone is indeed where the surface of normal modes ends. We conclude that the normal modes exist in a "preferred region"

$$\kappa_+^2 > 0 \text{ and } \kappa_-^2 > 0 \text{ and } \left(\lambda_+^2 < 0 \text{ or } \lambda_-^2 < 0\right). \tag{6.91}$$

This preferred region is bounded provided the UV Dirac cones have a narrower opening angle in both the k_x and k_y directions than the IR Dirac cones. This is certainly true of the $SU(2)$ backgrounds we have constructed. It may be possible to demonstrate in general that the region (6.91) is compact starting from an appropriate positive energy condition.

6.3.3 Positivity of the spectral measure

Unitarity requires that the spectral measure $\rho = -\operatorname{Im}\operatorname{tr} G_R$ is nonnegative for all real k^m in any field theory, as can be shown using a spectral decomposition. Instead of explaining the spectral decomposition argument (which is standard) we will show in this section how the positivity of the spectral measure follows from a computation in the gravity dual.

Consider the current

$$J^\mu \equiv -\bar{\Psi}\Gamma^\mu\Psi\,. \tag{6.92}$$

which is conserved in the sense that $\nabla_\mu J^\mu = 0$ provided the equations of motion that follow from (6.78) are obeyed. Not surprisingly, this conserved current is associated to the gauge invariance of the action (6.78). Here ∇ is a covariant derivative. From (6.80), we can write $\nabla_\mu J^\mu = 0$ as $Q'(r) = 0$, where

$$Q(r) \equiv \sqrt{-g}J^r = -\bar{\psi}\Gamma^{\underline{r}}\psi = -\bar{\psi}_+\psi_- + \bar{\psi}_-\psi_+ = -2\operatorname{Re}\left(\bar{\psi}_+\psi_-\right)\,. \tag{6.93}$$

where in the last line we used $\left(\bar{\psi}_-\psi_+\right)^\dagger = -\bar{\psi}_+\psi_-$. Using (6.86) we see that

$$Q = -2\operatorname{Re}\left(A^{a\dagger}\gamma^t D^a\right). \tag{6.94}$$

Combining (6.94) with (6.88), it follows that

$$Q = 2\operatorname{Im}\left(A^\dagger_{(b)}\gamma^t\, {G_R}^{(a)}{}_{(b)}\gamma^t A^{(b)}\right)\,. \tag{6.95}$$

Since, A is an arbitrary spinor and γ^t is invertible, $Q < 0$ implies that $\frac{1}{2i}\left(G - G^\dagger\right)$ is a nonpositive definite matrix and therefore, $\rho = -\operatorname{Im}\operatorname{tr} G$ is everywhere nonnegative.

It remains to show that with our IR asymptotics (6.83), $Q < 0$. To this end we work out the constraint on the V_i that follows from (6.57). If we split the V_i into chiral spinors, denoted by $V_i^{\pm}$, the constraint can be written as

$$V_1^- = i\frac{\alpha_+}{\kappa_+}V_1^+ \qquad V_2^- = i\frac{\alpha_-}{\kappa_-}V_2^+ \tag{6.96}$$

where

$$\alpha_\pm \equiv -e^{\frac{\chi_{\mathrm{IR}}}{2}}\omega\,\gamma^{\underline{t}} + \frac{2k_x \pm g_{\mathrm{YM}}W_{\mathrm{IR}}}{2c_{\mathrm{IR}}}\gamma^{\underline{x}} + k_y\gamma^{\underline{y}}. \tag{6.97}$$

There are now several different case we must consider. Suppose first that we are outside both IR Dirac cones. If we take the V_i^+ to be real and choose the Majorana basis for the γ matrices (making them real matrices) it follows from (6.96) that the V_i^- are pure imaginary. Therefore, $\bar{\psi}_+\psi_-$ is also pure imaginary and Q is identically zero leading us to conclude that $\rho = 0$ (up to, perhaps, a codimension one surface of normal modes.) Next, suppose that $\kappa_+^2 < 0$ and take $V_2 = 0$ for simplicity. If we choose V_1^+ real then V_1^- will also be real and Q is no longer zero. It is given by

$$Q = -\frac{2\,\mathrm{sgn}\,\omega}{|\kappa_+|}\,\mathrm{Re}\left(V_1^{+\dagger}\gamma^{\underline{t}}\alpha_+V_1^+\right). \tag{6.98}$$

It is now a simple exercise to compute the eigenvalues of the matrix $\gamma^{\underline{t}}\alpha_+$ and show that it is positive (negative) definite for $\omega > 0$ ($\omega < 0$). Therefore, Q is always negative for $\kappa_+^2 < 0$ and $V_2 = 0$. We can show in the same way that Q is negative for $\kappa_-^2 < 0$ and $V_1 = 0$. Since Q is given by a quadratic form, it follows that $Q \geq 0$.

6.4 Evaluating the spectral function

6.4.1 Numerical results

To obtain the spectral function $\rho = -\,\mathrm{Im}\,\mathrm{tr}\,G^R$ we solved (6.82) numerically with the initial conditions given in (6.83) for some small but nonzero r_i. We then extracted A and D from the behavior of the numerical solution at large r. This procedure was repeated for the four linearly independent choices of the V_i in (6.83). We then used (6.87) to obtain $\mathcal{M}$ and (6.88) to obtain G_{R}. To find the normal modes we looked for zeros of det $\mathcal{U}$.

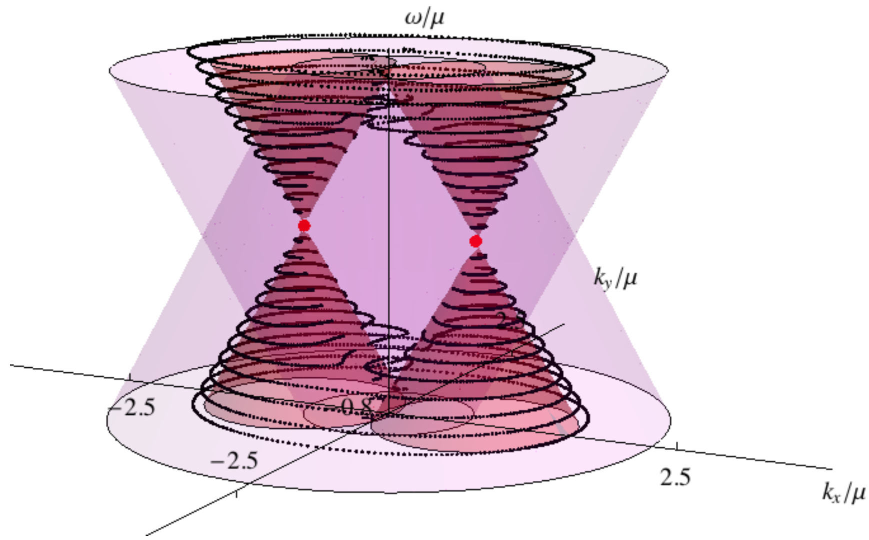

Figure 6.7: The normal mode surface for $g_{\mathrm{YM}} = 3$. The IR and UV Dirac cones are always drawn red and purple respectively. The normal mode surface is contained in the preferred region (6.91) and is shown as black dots.

Let us now discuss our numerical results. The spectral measure $\rho(k_m)$ is symmetric separately under the sign flips $\omega \to -\omega$, $k_x \to -k_x$, and $k_y \to -k_y$. Since we are restricting our attention to massless fermions the only free parameter is g_{YM}, the Yang-Mills coupling constant. Most of the features discussed in this section seem to be generic and independent of g_{YM}, with the obvious restriction that g_{YM} is at least large enough so that the $T = 0$ background we are considering exists. It seems possible that if we take g_{YM} large enough there could be several disconnected surfaces of normal mode, as we found in Chapter 5 for the s-wave background, but we were unable to check whether this happens as our numerics are not reliable for all of the "preferred region" for large g_{YM}. For g_{YM} as large as 10, there is only one distinct surface.

The surface of normal modes we obtained numerically can be roughly described as a truncated deformed version of the IR Dirac cones, as can be seen in Fig. 6.7. This surface does not extend indefinitely and is contained in the preferred region (6.91). It is perhaps more interesting to consider the shape of the normal mode surface near $\omega = 0$. The reason for this is that, in our conventions where $\Phi(0) = 0$, a fermion with $\omega = 0$ has energy equal to the chemical potential.[4] For the p-wave superconductor, Fig. 6.7 clearly shows as $\omega \to 0$ the surface of normal modes approaches the IR Dirac cones and that therefore the Fermi surface is given by two isolated points: the apexes of the IR Dirac cones.

To understand the behavior of ρ inside the IR Dirac cones it is useful to plot $\rho(k^m)$ as a function of ω for fixed k_x, k_y. Some of these plots are shown in Fig. 6.8. Outside the IR Dirac cones (the boundaries of which are shown as dashed red lines), ρ vanishes except for, perhaps, a δ-function peak that indicates the presence of a normal mode. Inside the IR Dirac cones, ρ is positive and smooth except for the intersection of two Dirac cones where there is a kink.

For k^m close to the apex of a Dirac cone, it is natural to expect that we will recover the behavior extracted from the infrared asymptotics. This behavior was discussion in section 6.2.5 for the $SO(4)$ case, and it is essentially the same in the $SU(2)$ case except in that there are only two Dirac cones rather than four. It is clear from plot (3) in Fig. 6.8 that ρ goes to a constant as $\omega \to 0$ when $\vec{k}$ is at the apex of the Dirac cone. Plot (1) in Fig. 6.8 reveals that there is almost a power-law singularity as soon as one crosses into the Dirac cone close to its apex. One does not see this dramatic near-singularity when crossing into a Dirac cone far from its apex.

To gain a better understanding of the spectral measure we provide some plots of constant ω slices in figure 6.9. At small ω we find that the normal modes surround each of the IR light cones. For the particular case of $g_{\text{YM}} = 3$ depicted in the top left corner of figure 6.9 the normal modes terminate on the light-cone leaving a "scar" in its interior. This is also seen more clearly in figure 6.10. This ridge inside the IR light-cone suggests that the normal mode has turned into a relatively long-lived quasinormal mode, or resonance.

Going back to figure 6.9, we observe that as ω is increased the shape of the surface of normal modes becomes more asymmetric until, eventually, the surface of normal modes

[4] If we wanted to treat Ψ beyond the probe approximation, the natural construction is to fill all the excitations with energy below the chemical potential, i.e, all the normal modes with $\omega < 0$. Once this is done, the Fermi surface will be given by the intersection of the normal mode surface with the $\omega = 0$ plane. But we don't understand how to systematically treat the back-reaction of the fermions on the geometry and the gauge field.

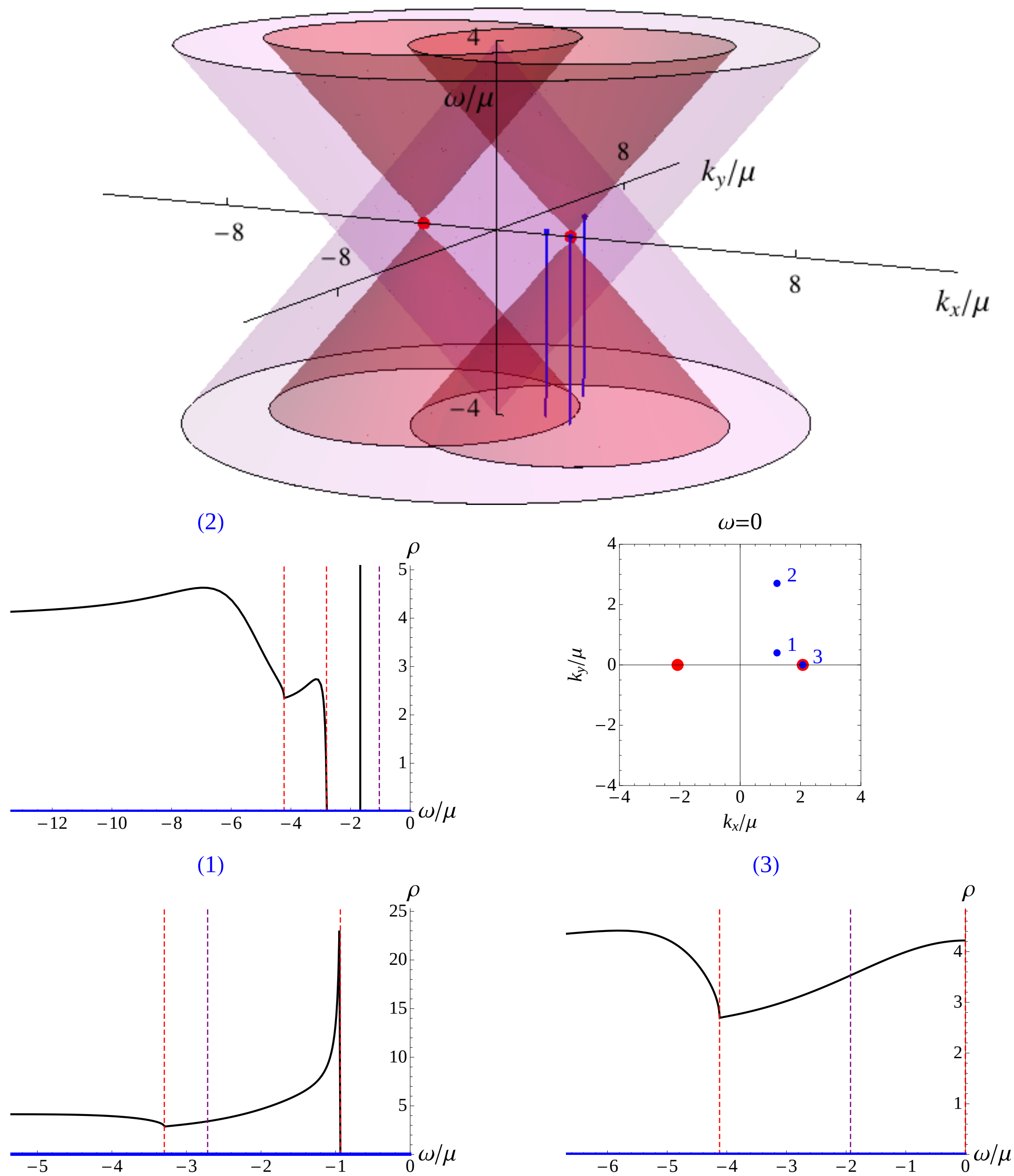

Figure 6.8: The preferred region and the spectral measure ρ as a function of ω for fixed k_x, k_y. The IR Dirac cones are shown in red, and UV Dirac cones in purple in the top figure. The blue lines are constant k_x and k_y lines and are the axes of the plots on the bottom. The limits of the IR and UV Dirac cones are marked in these plots as vertical dashed lines that are red and purple respectively. All the plots are for $g_{\rm YM} = 8$.

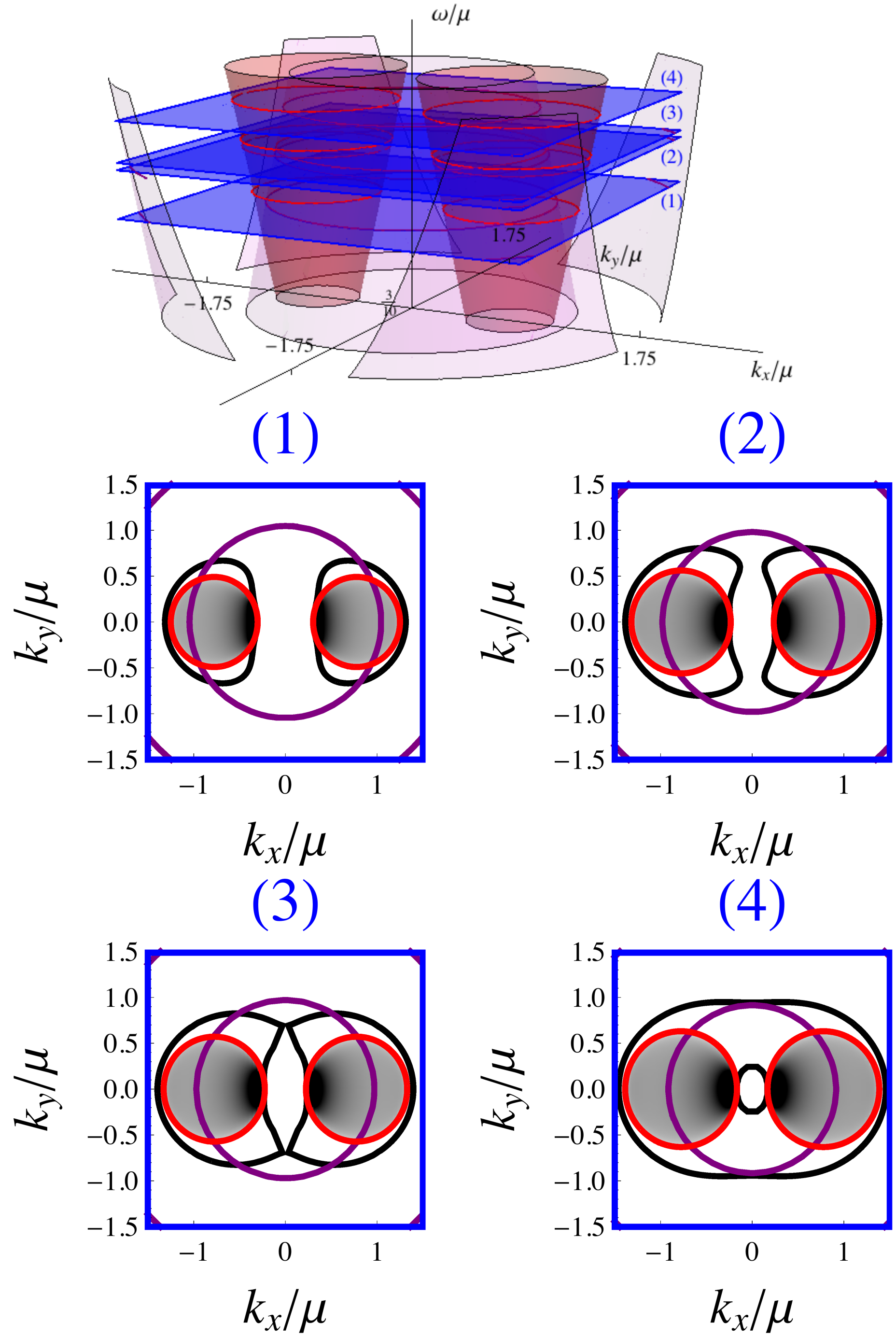

Figure 6.9: The spectral measure ρ for $\omega/\mu = 0.45$, 0.52, 0.53, 0.58 and $g_{\mathrm{YM}} = 3$. The UV and IR Dirac cones are shown in the top figure as red and purple surfaces respectively. The blue planes are the constant ω planes for which ρ is plotted in the bottom figure. In these plots, outside the the IR Dirac cones the surface of normal modes is shown as a black curve. This is overlaid with a density plot of the spectral measure ρ where black corresponds to large values of ρ.

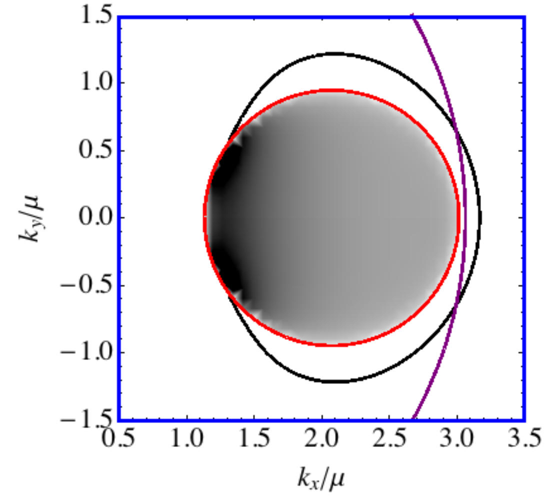

Figure 6.10: A contour plot of the spectral function ρ on a constant $\omega/\mu = 0.93$ slice for $g_{\rm YM} = 8$. The red and purple curves mark the location of the UV and IR cones respectively. The black line outside the IR light cone shows the location of the normal modes. The spectral function ρ develops a ridge between the points where the normal modes terminate on the light-cone.

around each of the light cones intersect (figure 6.9 (3)). At large ω the normal modes arrange themselves into an inner an outer closed surface. This inner surface disappears once the IR Dirac cones start overlapping. The outer surface will also disappear, eventually, and this happens as soon as the outermost UV Dirac cone is inside the IR Dirac cones.

6.4.2 Fermion correlators in the sudden approximation

The numerical work reported so far in this section turned up some interesting features in fermionic Green's functions: multiple thresholds associated with overlapping Dirac cones, normal modes in a preferred region, long-lived quasi-normal modes, and some signs of recovering the infrared approximations near the apex of a Dirac cone. We would like, if possible, some analytic approximation that exposes these features more clearly, so that we are not so dependent upon numerical integration of classical equations of motion. The obvious place to start is the probe approximation discussed in section 6.1.2. This approximation relies on having $g_{\rm YM}$ big so that the gauge field doesn't back-react appreciably on the AdS_4 geometry. Recall that in section 6.1.2 we rescaled fields as needed to eliminate explicit dependence of the equations of motion on $g_{\rm YM}$, and that at $T=0$ we were able to replace the AdS$_4$ geometry by the $z>0$ half of $\mathbf{R}^{3,1}$. For the sake of simplicity we will continue to restrict to a massless Dirac fermion, which (after a suitable rescaling) we denote ψ. It is dual to a spinorial operator $\mathcal{O}_\Psi$. We do *not* restrict ψ at this stage to be a doublet of $SU(2)$: it will become apparent that most of our discussion can be carried through straightforwardly for a domain wall configuration based on any semi-simple gauge group, with ψ transforming in any representation of it.

The two-point functions of $\mathcal{O}_\Psi$ are controlled by solutions to the linear equation of motion for ψ:

$$\Gamma^\mu(\partial_\mu - iA_\mu)\psi = 0\,. \tag{6.99}$$

Because we are working in the $z>0$ half of $\mathbf{R}^{3,1}$, we do not need to distinguish between Γ^μ and $\Gamma^{\underline{\mu}}$. A_μ is a domain wall solution to the flat-space Yang-Mills equations, so for the $SU(2)$ case it is takes the form

$$SU(2): \qquad A_m dx^m = \Phi(z)\, dt\, \tau^3 + W(z)\, dx^1\, \tau^1\,, \tag{6.100}$$

where Φ and W satisfy the equations (6.8). For $SO(4)$, an interesting solution generalizing (6.75) is

$$SO(4): \qquad A_m dx^m = \Phi(z)\, dt\, (\tau^3_A + \tau^3_B) + W(z)\, (dx^1\, \tau^1_A + dx^2\, \tau^2_B)\,, \tag{6.101}$$

with the same functions $\Phi(z)$ and $W(z)$ as in the $SO(4)$ case. Backgrounds based on more complicated gauge groups could also be constructed. All we require for the discussion of the next few paragraphs is that A_m depends only on z, and $A_z=0$ (a gauge choice).

Solutions to (6.99) can be cast in the form

$$\psi(x,z) = e^{ik\cdot x}\hat\psi(z)\,, \tag{6.102}$$

where, as usual, $k_m = (-\omega, \vec{k})$ and $x^m = (t, \vec{x})$. If we define

$$K_m(z) = k_m - A_m(z)\,, \tag{6.103}$$

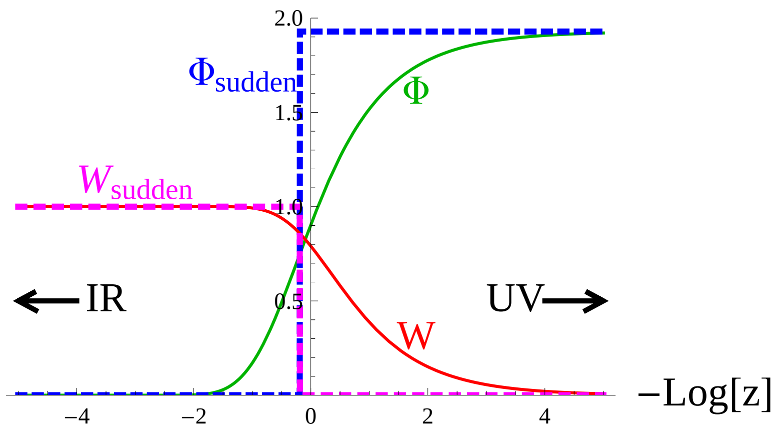

Figure 6.11: The functions Φ and W, with $W_{\rm IR} = 1$, together with the sudden approximations $\Phi_{\rm sudden}$ and $W_{\rm sudden}$ discussed in the main text.

then (6.99) becomes

$$(\partial_z + i\Gamma^z\Gamma^m K_m)\hat{\psi} = 0\,, \tag{6.104}$$

whose solutions can be formally expressed as

$$\hat{\psi}(z) = P\left\{\exp\left[-i\int_0^z dz'\,\Gamma^z\Gamma^m K_m(z')\right]\right\}\hat{\psi}(0)\,, \tag{6.105}$$

where P denotes ordering non-commuting matrices so that those coming from larger values of z go to the left. The allowed solutions satisfy boundary conditions in the infrared (large z) which can be compactly expressed as

$$\hat{\psi} \propto e^{-K_{\rm IR} z} u\,, \tag{6.106}$$

where restrictions on u come only from solving (6.104), and we define

$$\begin{aligned} K_m^{\rm IR} &= \lim_{z\to\infty} K_m(z) \qquad & K_{\rm IR} &= \sqrt{K_{\rm IR}^m K_m^{\rm IR}} \\ K_m^{\rm UV} &= \lim_{z\to\infty} K_m(z) \qquad & K_{\rm UV} &= \sqrt{K_{\rm UV}^m K_m^{\rm UV}}\,, \end{aligned} \tag{6.107}$$

and the $i\epsilon$ prescription (6.45) is implied.

It is hard to go further than (6.105) without some additional approximation because the path-ordered exponential is hard to compute. The domain wall structure suggests an obvious approximation, illustrated in figure 6.11: Let's replace $A_m \to A_m^{\rm sudden}$, where $A_m^{\rm sudden}$

is piecewise constant and piecewise flat, going straight from the UV flat connection to the IR flat connection at a special value z_* of z such that

$$\int_0^{z_*} dz\, A_t^{\rm sudden} = \int_0^{\infty} dz\, A_t\,. \tag{6.108}$$

A straightforward calculation based on the function $\tilde{\Phi}(\zeta)$ introduced in section 6.1.2 shows that in the $SU(2)$ and $SO(4)$ cases described by (6.100) and (6.101),

$$W_{\rm IR} z_* \approx 1.2058\,. \tag{6.109}$$

From now on we will set $W_{\rm IR} = 1$ for simplicity. It is easy to solve (6.99) with A_m replaced by $A_m^{\rm sudden}$: the solution is

$$\hat{\psi}_{\rm sudden}(z) = \begin{cases} e^{-iz\Gamma^z\Gamma^m K_m^{\rm UV}}\hat{\psi}_{\rm sudden}(0) & \text{for } 0<z<z_* \\ e^{-i(z-z_*)\Gamma^z\Gamma^m K_m^{\rm IR}} e^{-iz_*\Gamma^z\Gamma^m K_m^{\rm UV}}\hat{\psi}_{\rm sudden}(0) & \text{for } z_*<z\,. \end{cases} \tag{6.110}$$

Now let's see how to implement the boundary condition (6.106). Because $\hat{\psi}_{\rm sudden}$ satisfies the Dirac equation (with the replacement $A_m \to A_m^{\rm sudden}$), we have

$$\partial_z\hat{\psi}_{\rm sudden}(z) = -i\Gamma^z\Gamma^m K_m^{\rm IR}\hat{\psi}_{\rm sudden}(z) \qquad \text{for all } z>z_*. \tag{6.111}$$

On the other hand, $\partial_z\hat{\psi}_{\rm sudden}(z) = -K_{\rm IR}\hat{\psi}_{\rm sudden}(z)$ for large z because of (6.106). Since the $K_m^{\rm IR}$ commute with one another, it must be that

$$\partial_z\hat{\psi}_{\rm sudden}(z) = -K_{\rm IR}\hat{\psi}_{\rm sudden}(z) \qquad \text{for all } z>z_*\,. \tag{6.112}$$

Comparing (6.111) and (6.112), we arrive at

$$P\hat{\psi}_{\rm sudden}(0) = 0 \tag{6.113}$$

where

$$P \equiv (K_{\rm IR} - i\Gamma^z\Gamma^m K_m^{\rm IR})e^{-iz_*\Gamma^z\Gamma^n K_n^{\rm UV}}\,. \tag{6.114}$$

It will be useful to express

$$P = q + \Gamma^z\Gamma^m q_m + \Gamma^m\Gamma^n q_{mn} \tag{6.115}$$

where

$$\begin{aligned} q &= K_{\rm IR} \cosh(z_* K_{\rm UV}) \\ q_m &= -i \left[K_m^{\rm IR} \cosh(z_* K_{\rm UV}) + K_{\rm IR} K_m^{\rm UV} \frac{\sinh(z_* K_{\rm UV})}{K_{\rm UV}} \right] \\ q_{mn} &= K_m^{\rm IR} K_n^{\rm UV} \frac{\sinh(z_* K_{\rm UV})}{K_{\rm UV}} \,. \end{aligned} \tag{6.116}$$

Note that q, q_m, and q_{mn} have no spinor structure: they are purely gauge-theoretic quantities. In (6.115), the first term on the right hand side is implicitly multiplied by the unit matrix in spinor space.

The equation (6.113) determines the fermionic Green's function in the sudden approximation, as we now explain. If we use our usual basis for gamma matrices, (6.49), and express

$$\hat{\psi}_{\rm sudden}(0) = \begin{pmatrix} u_+ \\ u_- \end{pmatrix} , \tag{6.117}$$

then (6.113) can be recast as

$$\begin{pmatrix} P_{++} & P_{+-} \\ P_{-+} & P_{--} \end{pmatrix} \begin{pmatrix} u_+ \\ u_- \end{pmatrix} = 0 \,, \tag{6.118}$$

where

$$\begin{pmatrix} P_{++} & P_{+-} \\ P_{-+} & P_{--} \end{pmatrix} = \begin{pmatrix} q + \gamma^m \gamma^n q_{mn} & -\gamma^m q_m \\ \gamma^m q_m & q + \gamma^m \gamma^n q_{mn} \end{pmatrix} . \tag{6.119}$$

Comparing to (6.86) and using (6.87), we arrive at

$$G_{\rm sudden}(k) = i P_{+-}^{-1} P_{++} \gamma^t = i P_{--}^{-1} P_{-+} \gamma^t \,. \tag{6.120}$$

A more explicit form, based on the middle expression in (6.120), is

$$G_{\rm sudden}(k) = -i(\gamma^m q_m)^{-1} (q + \gamma^m \gamma^n q_{mn}) \gamma^t \,. \tag{6.121}$$

We further define $\rho_{\rm sudden}(k) \equiv -\operatorname{Im} \operatorname{tr} G^R_{\rm sudden}(k)$. We note that $\operatorname{tr} G^R_{\rm sudden}(k)$ and hence $\rho_{\rm sudden}(k)$ can in principle be found in closed form as functions of k_m, μ, $W_{\rm IR}$, and z_*. In practice, the closed-form expressions for q, q_m, and q_{mn} in terms of k_m, μ, $W_{\rm IR}$, and z_* are already quite complicated, and we were unable to find a closed-form expression for the inverse matrix $(\gamma^m q_m)^{-1}$ that was sufficiently compact to be useful.

Although we did not succeed in finding a simple enough closed form expression for the spectral measure to record here, the expression (6.121) is simple enough to expose most of the qualitative features of the analytic structure of $G_{\text{sudden}}(k)$. First we claim that branch cuts in q and q_m, as functions of k_m, arise only when K_{IR} has a branch cut, while q_{mn} has no branch cuts at all. To demonstrate this claim, we observe that $\cosh(z_* K_{\text{UV}})$ and $\frac{\sinh(z_* K_{\text{UV}})}{K_{\text{UV}}}$ are analytic functions of K_{UV}^2, which in turn is a quadratic expression in the momenta k_m; so $\cosh(z_* K_{\text{UV}})$ and $\frac{\sinh(z_* K_{\text{UV}})}{K_{\text{UV}}}$ have no branch cuts at all as functions of the k_m. More trivially, K_m^{IR} and K_m^{UV} also have no branch cuts. Our first claim now follows by inspection of the formulas (6.116) for q, q_m, and q_{mn}.

It follows from our first claim that the continuum part of $\rho_{\text{sudden}}(k)$ is supported precisely where K_{IR} has a branch cut, which is to say inside the Dirac cones. This feature of the spectral function has been discussed extensively in section 6.3 and is essentially as expected on intuitive grounds: The retarded Green's function can have a dissipative part iff some component of the fermion wave-function is infalling in the infrared, rather than exponentially decaying there.

Our second claim is that, at least for ψ in a real representations of $\mathbf{g}$ and for generic values of $\vec{k} = (k_x, k_y)$, δ-function singularities in $\rho_{\text{sudden}}(\omega, k_x, k_y)$ as a function of ω can only occur outside the IR Dirac cones. Recall that a δ-function in $\rho_{\text{sudden}}(\omega, k_x, k_y)$ is associated with a pole in $\operatorname{Re}\operatorname{tr} G^R_{\text{sudden}}(\omega, k_x, k_y)$ for real ω. Thus our claim is that any such pole must arise outside the Dirac cones. To demonstrate the claim, first note that q, q_m, and q_{mn} never diverge. So the only way to get a pole is if $\gamma^m q_m$ is non-invertible, which is to say $\det i\gamma^m q_m$ vanishes. The γ^m may be chosen in a Majorana basis, where all entries are real: indeed, (6.50) is such a basis. In a real representation of the gauge group, all the K_m^{IR} and K_m^{UV} are real symmetric matrices, as are $\cosh(z_* K_{\text{UV}})$ and $\frac{\sinh(z_* K_{\text{UV}})}{K_{\text{UV}}}$. K_{IR} is also real and symmetric provided we are outside the Dirac cones. Thus the iq_m are real matrices, and we see that $\det i\gamma^m q_m$ must indeed be real. More precisely, for real k_x and k_y, $\det i\gamma^m q_m$ is a real function of the variable ω outside the Dirac cones. Inside the Dirac cones, K_{IR} has an imaginary part, and $\det i\gamma^m q_m$ is *not* a real function of ω. All that we need to note now in order to complete our argument is that real analytic functions of a single variable generically can have zeros on the real axis, but general complex analytic functions do not. It is tempting to speculate that this argument could be extended to fermions in complex representations. Certainly there is intuitive reason to think that when a delta-function contribution to the spectral measure crosses into a continuum, it will spread out into a finite-width resonance—as we saw numerically in Fig. 6.10.

We caution the reader that the sudden approximation is *not* controlled in the sense of becoming good when some parameter is taken large or small. Usually, sudden approximations are justified when wave-functions are slowly varying as compared to the features of the underlying background that one is approximating. Optimistically, one might expect our sudden approximation to be good near the infrared light-cone, because then the fermion wave-functions are slowly varying in the region $z > z_*$. But these wave-functions are not necessarily slowly varying for $z < z_*$. Thus we regard (6.121) as useful in the sense of providing an in-principle closed-form expression that captures some of the relevant physics: namely a continuous part of the spectral measure inside the Dirac cones, with the possibility (at least on genericity grounds) of normal modes only outside the cones.

6.5 Discussion

The starting point of our analysis is the classical action

$$S = \int_M d^4x \sqrt{-g} \left(R + \frac{6}{L^2} - \frac{1}{2} \operatorname{tr} F_{\mu\nu}^2 - i\bar{\Psi}\Gamma^\mu D_\mu \Psi \right) + \text{boundary terms}\,, \tag{6.122}$$

which is essentially the lagrangian of QCD coupled to gravity with a negative cosmological constant, except that we choose the gauge group to be $SU(2)$ or $SO(4)$, while the fermion transforms either as the doublet of $SU(2)$ or the fundamental $\mathbf{4}$ of $SO(4)$. The lagrangian (6.122) describes the bulk dynamics dual to a field theory in $2+1$ dimensions whose continuous symmetries form the same group as the gauge group in (6.122). We treat the dynamics of (6.122) classically, which is understood to be dual to a large N approximation in the field theory.

One output of our analysis is the phase diagram of superconducting black holes based on the $SU(2)$ gauge group. This phase diagram is shown in Fig. 6.2. We demonstrated, largely through a numerical study, that black holes charged under the τ^3 generator of $SU(2)$ spontaneously break that symmetry through a p-wave condensate similar to the one originally studied in [76]. A conspicuous feature of the phase diagram is a tricritical point separating second order and first order behavior at the symmetry breaking phase transition. We also showed that at low temperatures, the symmetry-breaking solutions approach the AdS_4-to-AdS_4 domain wall geometries of [85], similar to domain walls found in the Abelian Higgs model in Chapter 2 except for anisotropic alteration of the coordinate speed of light in the infrared. Our analysis is not complete in that we did not systematically study the stability of the symmetry-breaking solutions, and it is possible that there are other symmetry-breaking configurations that we missed. Thus we cannot rule out the existence of a more complicated phase diagram than we plotted in Fig. 6.2, with (for example) symmetry-breaking phases present below $g_{\mathrm{YM}} = 0.710$.

A second output of our analysis is two-point functions of the fermionic operators dual to Ψ. These two-point functions show some intriguing parallels with ARPES data on high-temperature superconductors. Relationships between holographic fermionic correlators and ARPES data were emphasized early in [41] in the context of the non-superconducting phase, following earlier work [84, 57, 40]. Studies in the superconducting phase include [83, 82] and our work in Chapter 5. These works all focused on rotationally symmetric backgrounds. By contrast, our Fermi surface at $T = 0$ consists of isolated points: two in the $SU(2)$ example, and four in the $SO(4)$ example. Above each isolated point, a Dirac cone rises, as can be seen in Fig. 6.8 for the $SU(2)$ case and in Fig. 6.6 for the $SO(4)$ case. In the $SO(4)$ case, the nodes are positioned at $45°$ degrees relative to the axes along which the gauge potentials are aligned, reminding us of the positioning of nodes in the gap in $d_{x^2-y^2}$ superconductors.

The structure of normal modes is also favorable to the comparison with ARPES data. As shown in Fig. 6.7, there is a normal mode slightly outside each Dirac cone. And as shown in Fig. 6.8 (plot (2) especially), the spectral measure significantly away from the tip of the

Dirac cone exhibits a peak-dip-hump structure. The peak comes from the normal mode, which shows up in the spectral measure at $T = 0$ as a δ-function, like an infinitely sharp quasi-particle. The hump comes from the continuum part of the spectral measure, which is entirely inside the Dirac lightcone. At the tip of the light cone (plot (2) of Fig. 6.8) or just slightly away from it (plot (1)), there is less structure: the peak goes away or merges into the hump. Again we see a point of comparison with ARPES: the classic peak-dip-hump structure arises away from the node in the gap.

There is a twist in our discussion of Dirac cones, normal modes, and continuum structures relative to the usual story based on quasi-particles, where continuum structures arise because of two- or three-particle states, where each particle by itself is on-shell when its momentum lies on the Dirac cone. In our case, the Dirac cone characterizes the edge of the continuum rather than the dispersion relation for the quasi-particle. We see already from formulas like (6.62) that if only the infrared dynamics are accounted for, a continuum supported inside each Dirac cone is the *only* feature of the spectral measure. There are no quasi-particles in sight in this infrared limit. The quasi-particles (or, at least, the normal modes of the bulk fermions) come from the more intricate domain wall structure of the full bulk geometry, as discussed in section 6.3.2. The dispersion relation of these quasi-particles is not perfectly linear. This is striking because, even in the full domain wall geometry, the continuum part of the spectral measure is supported in Dirac cones which are perfectly linear. In fact, close inspection of Fig. 6.7 shows that the normal modes cross into the Dirac cones in certain regions. This behavior is brought out better in Figs. 6.9 and 6.10. Moreover, the normal modes disappear altogether once one passes outside the preferred region described in (6.91). So for large enough ω and $\vec{k}$ there are no normal modes, and therefore no well-defined quasi-particle δ-functions in the spectral measure. But one still finds that the edge of the continuous part of the spectral measure defines a perfect Dirac cone. In short, the continuum part of the spectral measure is the fundamental feature, while the quasi-particle δ-function appears only under the right circumstances.

We were able to produce an explicit formula (6.121) which captures the main features of the fermionic Green's function, including the perfect Dirac cones enclosing the continuous part of the spectral measure and the normal mode outside the Dirac cones. Previous works, notably [42], have provided analytic approximations to interesting fermionic correlators; moreover, the ones in [42] are based on a controlled approximation, whereas ours is not. The analytic forms found in [42] for the non-superconducting state rely upon the existence of an AdS_2 near-horizon region. This feature of the geometry is double-edged: While it does provide tractable asymptotics, it also forces the existence of non-zero entropy density at zero temperature, which remains unexplained and seems to us peculiar in a theory whose underlying formulation is a continuum field theory rather than a lattice. Limited analytic information about fermionic two-point functions is available in the backgrounds studied in Chapter 4, where also entropy vanishes linearly with temperature. A more powerful understanding might be forthcoming if one better exploited the AdS_3 near-horizon region of the ten-dimensional embedding of these backgrounds.

There are some good reasons to be suspicious of the relevance of our setup to real high-T_c materials with a d-wave gap:

- As already remarked in the introduction, the field theory dual to the AdS_4 bulk is a large N field theory formulated in the continuum rather than on the lattice.

- The condensate in the $SO(4)$ case is not described in terms of a spin-2 bulk field, as one might expect, but rather in terms of gauge potentials involving off-diagonal generators of $SO(4)$. It's not at all clear that the classic phase-sensitive features of the d-wave gap would show up in our system.

- Off-diagonal gauge potentials are dual to persistent currents of global symmetries in the boundary theory. This seems rather different from the usual language for discussing d-wave superconductivity. It would be interesting to see if the notion of persistent currents as an order parameter might be translated into lattice language, and how it might interact with constraints such as those discussed in [95].

- In addition to the $SO(4)$ gauge symmetry, the field theory dual to (6.122) has $SO(2,1)$

Lorentz symmetry and also relativistic conformal invariance. These symmetries are largely broken by the condensates, but the fermion operator $\mathcal{O}_\Psi$ transforms as a doublet under $SO(2,1)$. This has no immediate analog in spin systems relevant to high-T_c materials, where the spins are doublets under the $SU(2)_{\rm spin}$ and have no further structure under the Lorentz group in $2+1$ dimensions.

- The $SO(4)$ symmetry of the Hubbard model is composed of $SU(2)_{\rm spin}$ and $SU(2)_{\rm pseudospin}$. The definition of the latter seems to require the lattice. Doping amounts to adding a chemical potential for the τ^3 component of pseudospin, whereas in (6.101) we added equal chemical potentials for the τ^3 components of both $SU(2)$'s in $SO(4)$.

Nevertheless, the resemblance of our results for the spectral measure of fermionic Green's functions to the spectral properties revealed in real materials by ARPES are striking enough that we should inquire what underlying physics is driving it. At one level there is no puzzle: as soon as we note that the infrared Green's functions depend on Lorentz-invariant combinations of $K_m = k_m - g_{\rm YM} A_m$, where $k_m = (-\omega, \vec{k})$ and A_m is a flat connection in the gauge group of (6.122), we see that the displaced Dirac cones are just a consequence of the Lorentz invariance plus the eigenvalues of the non-zero components of A_m. At another level, it may seem strangely suggestive that $SO(4)$ is the symmetry group of the Hubbard model on a bipartite lattice, and the fermion creation and annihilation operators transform as the **4** of $SO(4)$.[5] Precisely this choice of gauge group and fermion representation gave us the Dirac cone structure reminiscent of $d_{x^2-y^2}$ pairing. Did we get approximately right answers for ARPES-like spectra because we have captured some correct features of the Hubbard model? A positive answer to this question would be fairly exciting.

[5] A theory of phase competition between anti-ferromagnetic order and superconductivity has been advanced based on an approximate $SO(5)$ symmetry [96]; for a review see [97].

Chapter 7

Conclusions

The gauge-gravity dualities provide a new paradigm to understand strongly coupled quantum field theories. Through the dualities, these strongly interacting systems are mapped to classical gravitational problems for which both the general conceptual framework and computational methods are significantly more developed. In light of this, significant interest has attached to the idea of bringing this new paradigm to bear on problems from other areas of physics in which strong interactions play a role. In this dissertation, we have pursued this idea in the direction of applications to condensed matter physics. The interest of applying methods based on the dualities to condensed matter topics stems from the fact that more traditional approaches based on a weakly-coupled quasi-particle paradigm have met with difficulties when applied to some heavily studied materials such as non-conventional superconductors. Of course, some caution is necessary since the quantum field theories with well understood gravity duals are large-N_c supersymmetric gauge theories, which do not seem likely to have direct connections to the underlying physics of materials of current interest in condensed matter research. However, by studying gravitational duals that capture phenomena such as superconductivity in a strongly coupled setting, it seems eminently reasonable to expect to gain insights and abstract principles that will be useful in more general settings than the specific gravitational duals being considered.

In this spirit, in this dissertation we have considered gravitational duals that exhibit features such as superconductivity, quantum criticality and Fermi surfaces. We began by introducing a class of zero temperature geometries that arise has extrema of the holographic Abelian Higgs model for some scalar potentials. These geometries have a domain wall structure with two asymptotic Anti de Sitter regions. Their dual field theory interpretation is as zero temperature but finite density states. Even though this density breaks scale and Lorentz invariance, these states have an emergent conformal symmetry at low energies. Another important feature is the global symmetry associated to the current with a nonzero density is spontaneously broken. We identified these geometries, that can arise as zero temperature limits of holographic superconductors, as gravitational duals of quantum critical points in light of this emergent symmetry and also of the low-frequency power-law behavior of the conductivity they exhibit. The relationship between these domain wall geometries and the better known holographic renormalization group flow geometries led us to formulate the Criticality Pairing Conjecture, relating symmetry breaking renormalization group flows to finite-density states with quantum critical behavior. An interesting direction for future research would be to test this conjecture in more general situations, including both more intricate gravitational duals and in frameworks that do not rely on the AdS/CFT correspondence.

A topic that has been the subject of a lot of attention recently is the study of the properties of spin-$\frac{1}{2}$ fields in gravity duals. One of the most interesting findings [41, 40] was that extremal RNAdS blackholes admit stable fermionic excitations with finite momentum and zero frequency. This has been interpreted as signaling a presence of a Fermi surface in the dual field theory. Furthermore, the features of the correlators of these fermionic fields deviate from those in Landau Fermi liquid theory in interesting ways. In this dissertation, we considered spin-$\frac{1}{2}$ fields in different gravitational backgrounds and studied their properties. One of the puzzling features of extremal RNAdS is that it possesses finite entropy density even at zero temperature. We considered analytic dilatonic blackhole backgrounds whose entropy density goes to zero in the zero temperature limit and in fact have T-linear specific heat at low temperatures, much like Fermi liquids. Moreover, they can (like extremal

RNAdS) exhibit isolated stable fermionic excitations at finite momentum and therefore are interesting candidates for gravitational duals of Fermi liquids. These backgrounds can be embedded in larger string theory constructions, although in this setting they display thermodynamical instabilities. The fermionic sector we studied was, however, an *ad hoc* addition and it would be interesting to repeat this study with a fermionic sector that can also be embedded in string theory.

We also introduced spin-$\frac{1}{2}$ fields into holographic superconductor backgrounds. We first considered s-wave holographic superconductors, more specifically in the zero temperature domain wall geometry from Chapter 3. We found that the Dirac cones associated to the infrared and ultraviolet conformal symmetries were key in determining the properties of fermionic correlators and normal modes. More specifically, the stable fermionic excitations were constrained to lie in a region in Fourier space, the "preferred wedge", with boundaries given by these Dirac cones (in [83], similar results were found for zero temperature geometries with emergent Poincaré symmetry). According to the choice of parameters these bands can be either partially filled (and therefore exhibit a Fermi surface) or totally empty and gapped. In future research, it would interesting to generalize these studies to finite temperature.

The other gravitational backgrounds for which we studied fermionic fields were p-wave holographic superconductors or, more specifically, their zero temperature limit, which has somewhat similar structure to the domain wall geometries of Chapters 2 and 3 as first found in [85]. These geometries are extrema of gravitational Lagrangians containing a non-Abelian gauge field and we were led to consider bulk fermions with non-Abelian charge. As happened for the s-wave holographic superconductors, we found continuous surfaces of normal modes constrained to lie in regions delimited by Dirac cones. Due to the non-Abelian nature of the fermions, the structure of light cones was more complex and we found that surface of normal modes was consistent with a Fermi surface for the dual field theory that consisted of isolated points. This lead us to speculate on possible connections with results from angle resolved photoemission spectroscopy experiments for the cuprate high-T_c superconductors. We did detailed numerical studies for $SU(2)$ non-Abelian gauge field and fermions in its doublet representation and argued how our results should generalize for arbitrary gauge group and fermion representation. Of particular phenomenological interest is the $SO(4)$ case with the fermions in the **4** representation, since this would seem to be the closest approach to the d-wave symmetry of the cuprates. Repeating our numerical analysis for this case is an appealing future avenue of research, as would be generalizing it to finite temperature.

The study of gravitational duals with fermionic sectors has far from been exhausted. We have already outlined some possible future direction connected to the research in this dissertation. A further promising direction is developing methods to treat the fermions beyond the probe approximation and allow them to back-react on the geometry. This necessarily involves going beyond the strictly classical approximation and has already been found to lead to some interesting effects such as de Haas-van Alphen oscillations [45], emergent Lifshitz symmetries [98], T-linear contributions to the resistivity [99] and Cooper pairing on the gravity side [100]. In different direction, much could be learned from considering gravitational actions with fermionic sectors that can be embedded in string theory or M-theory as a more complete picture of the dual field theory would result. In [101], an example of such a construction was already given and it would be interesting to find more general examples.

In conclusion, the program of applying the gauge-gravity duality to condensed matter topics is still at its beginning. Although the prospect of finding an exact gravity dual to a real world condensed matter system seems unlikely at the present time, what the gauge-gravity duality does is provide a new framework to conceptualize systems at strong coupling. Continued study of holographic realizations of features such as Fermi surfaces and superconductivity will lead to a more general understanding of these phenomena that does not rely on a quasi-particle description. Expecting these developments to shed light on condensed matter topics does not seem far-fetched.

References

[1] Juan M. Maldacena. The large n limit of superconformal field theories and supergravity. *Adv. Theor. Math. Phys.*, 2:231–252, 1998.

[2] S. S. Gubser, Igor R. Klebanov, and Alexander M. Polyakov. Gauge theory correlators from non-critical string theory. *Phys. Lett.*, B428:105–114, 1998.

[3] Edward Witten. Anti-de sitter space and holography. *Adv. Theor. Math. Phys.*, 2:253–291, 1998.

[4] Christopher P. Herzog. Lectures on Holographic Superfluidity and Superconductivity. *J. Phys.*, A42:343001, 2009.

[5] Sean A. Hartnoll. Lectures on holographic methods for condensed matter physics. *Class. Quant. Grav.*, 26:224002, 2009.

[6] John McGreevy. Holographic duality with a view toward many-body physics. 2009.

[7] Gary T. Horowitz. Introduction to Holographic Superconductors. 2010.

[8] Ofer Aharony, Oren Bergman, Daniel Louis Jafferis, and Juan Maldacena. N=6 superconformal Chern-Simons-matter theories, M2-branes and their gravity duals. *JHEP*, 10:091, 2008.

[9] Peter Breitenlohner and Daniel Z. Freedman. Stability in gauged extended supergravity. *Ann. Phys.*, 144:249, 1982.

[10] Peter Breitenlohner and Daniel Z. Freedman. Positive energy in anti-de sitter backgrounds and gauged extended supergravity. *Phys. Lett.*, B115:197, 1982.

[11] Dam T. Son and Andrei O. Starinets. Minkowski-space correlators in AdS/CFT correspondence: Recipe and applications. *JHEP*, 09:042, 2002.

[12] C. P. Herzog and D. T. Son. Schwinger-Keldysh propagators from AdS/CFT correspondence. *JHEP*, 03:046, 2003.

[13] Steven Weinberg. Superconductivity for particular theorists. *Prog. Theor. Phys. Suppl.*, 86:43, 1986.

[14] Steven S. Gubser. Breaking an Abelian gauge symmetry near a black hole horizon. *Phys. Rev.*, D78:065034, 2008.

[15] Sean A. Hartnoll, Christopher P. Herzog, and Gary T. Horowitz. Holographic Superconductors. 2008.

[16] Steven S. Gubser and Fabio D. Rocha. The gravity dual to a quantum critical point with spontaneous symmetry breaking. *Phys. Rev. Lett.*, 102:061601, 2009.

[17] Steven S. Gubser, Silviu S. Pufu, and Fabio D. Rocha. Quantum critical superconductors in string theory and M- theory. *Phys. Lett.*, B683:201–204, 2010.

[18] Steven S. Gubser, Fabio D. Rocha, and Pedro Talavera. Normalizable fermion modes in a holographic superconductor. 2009.

[19] Steven S. Gubser and Fabio D. Rocha. Peculiar properties of a charged dilatonic black hole in AdS_5. *Phys. Rev.*, D81:046001, 2010.

[20] Steven S. Gubser, Fabio D. Rocha, and Amos Yarom. Fermion correlators in non-abelian holographic superconductors. 2010.

[21] Christopher P. Herzog, Pavel Kovtun, Subir Sachdev, and Dam Thanh Son. Quantum critical transport, duality, and M-theory. *Phys. Rev.*, D75:085020, 2007.

[22] Sean A. Hartnoll, Pavel K. Kovtun, Markus Muller, and Subir Sachdev. Theory of the nernst effect near quantum phase transitions in condensed matter, and in dyonic black holes. *Phys. Rev.*, B76:144502, 2007.

[23] Sean A. Hartnoll and Christopher P. Herzog. Ohm's law at strong coupling: S duality and the cyclotron resonance. *Phys. Rev.*, D76:106012, 2007.

[24] Matthew P. A. Fisher, Peter B. Weichman, G. Grinstein, and Daniel S. Fisher. Boson localization and the superfluid-insulator transition. *Phys. Rev.*, B40:546–570, 1989.

[25] D. Z. Freedman, S. S. Gubser, K. Pilch, and N. P. Warner. Renormalization group flows from holography: supersymmetry and a c-theorem. *Adv. Theor. Math. Phys.*, 3:363–417, 1999.

[26] Sean A. Hartnoll, Christopher P. Herzog, and Gary T. Horowitz. Building a Holographic Superconductor. *Phys. Rev. Lett.*, 101:031601, 2008.

[27] Steven S. Gubser and Abhinav Nellore. Low-temperature behavior of the Abelian Higgs model in anti-de Sitter space. *JHEP*, 04:008, 2009.

[28] Steven S. Gubser, Christopher P. Herzog, Silviu S. Pufu, and Tiberiu Tesileanu. Superconductors from Superstrings. *Phys. Rev. Lett.*, 103:141601, 2009.

[29] Jerome P. Gauntlett, Julian Sonner, and Toby Wiseman. Holographic superconductivity in M-Theory. *Phys. Rev. Lett.*, 103:151601, 2009.

[30] Richard Corrado, Krzysztof Pilch, and Nicholas P. Warner. An N = 2 supersymmetric membrane flow. *Nucl. Phys.*, B629:74–96, 2002.

[31] Dario Martelli and James Sparks. Toric geometry, Sasaki-Einstein manifolds and a new infinite class of AdS/CFT duals. *Commun. Math. Phys.*, 262:51–89, 2006.

[32] Jerome P. Gauntlett, Seok Kim, Oscar Varela, and Daniel Waldram. Consistent supersymmetric Kaluza–Klein truncations with massive modes. *JHEP*, 04:102, 2009.

[33] Frederik Denef and Sean A. Hartnoll. Landscape of superconducting membranes. *Phys. Rev.*, D79:126008, 2009.

[34] L. Girardello, M. Petrini, M. Porrati, and A. Zaffaroni. Novel local CFT and exact results on perturbations of N = 4 super Yang-Mills from AdS dynamics. *JHEP*, 12:022, 1998.

[35] L. J. Romans. New compactifications of chiral $N = 2$ $d = 10$ supergravity. *Phys. Lett.*, B153:392, 1985.

[36] Gary T. Horowitz and Matthew M. Roberts. Holographic Superconductors with Various Condensates. *Phys. Rev.*, D78:126008, 2008.

[37] C. N. Pope and N. P. Warner. An SU(4) invariant compactification of $d = 11$ supergravity on a stretched seven sphere. *Phys. Lett.*, B150:352, 1985.

[38] C. N. Pope and N. P. Warner. Two new classes of compactifications of d = 11 supergravity. *Class. Quant. Grav.*, 2:L1, 1985.

[39] Sean A. Hartnoll and Pavel Kovtun. Hall conductivity from dyonic black holes. *Phys. Rev.*, D76:066001, 2007.

[40] Hong Liu, John McGreevy, and David Vegh. Non-Fermi liquids from holography. 2009.

[41] Mihailo Cubrovic, Jan Zaanen, and Koenraad Schalm. String Theory, Quantum Phase Transitions and the Emergent Fermi-Liquid. *Science*, 325:439–444, 2009.

[42] Thomas Faulkner, Hong Liu, John McGreevy, and David Vegh. Emergent quantum criticality, Fermi surfaces, and AdS2. 2009.

[43] Soo-Jong Rey. String Theory on Thin Semiconductors: Holographic Realization of Fermi Points and Surfaces. *Progr. Theor. Phys. Suppl.*, 177:128–142, 2009.

[44] Sang-Jin Sin and Ismail Zahed. Holographic dual of Cold Trapped Fermions. *JHEP*, 12:015, 2009.

[45] Frederik Denef, Sean A. Hartnoll, and Subir Sachdev. Quantum oscillations and black hole ringing. *Phys. Rev.*, D80:126016, 2009.

[46] Igor R. Klebanov. World-volume approach to absorption by non-dilatonic branes. *Nucl. Phys.*, B496:231–242, 1997.

[47] Steven S. Gubser, Igor R. Klebanov, and Arkady A. Tseytlin. String theory and classical absorption by three-branes. *Nucl. Phys.*, B499:217–240, 1997.

[48] Steven S. Gubser and Igor R. Klebanov. Absorption by branes and Schwinger terms in the world volume theory. *Phys. Lett.*, B413:41–48, 1997.

[49] M. Gunaydin, L. J. Romans, and N. P. Warner. Compact and Noncompact Gauged Supergravity Theories in Five-Dimensions. *Nucl. Phys.*, B272:598, 1986.

[50] M. Cvetic et al. Embedding AdS black holes in ten and eleven dimensions. *Nucl. Phys.*, B558:96–126, 1999.

[51] S. S. Gubser, C. P. Herzog, F. D. Rocha, and S. Pufu, unpublished.

[52] Steven S. Gubser. Thermodynamics of spinning D3-branes. *Nucl. Phys.*, B551:667–684, 1999.

[53] Mirjam Cvetic and Steven S. Gubser. Thermodynamic Stability and Phases of General Spinning Branes. *JHEP*, 07:010, 1999.

[54] R. Gregory and R. Laflamme. Black strings and p-branes are unstable. *Phys. Rev. Lett.*, 70:2837–2840, 1993.

[55] Ruth Gregory and Raymond Laflamme. The Instability of charged black strings and p-branes. *Nucl. Phys.*, B428:399–434, 1994.

[56] Steven S. Gubser and Jonathan J. Heckman. Thermodynamics of R-charged black holes in AdS(5) from effective strings. *JHEP*, 11:052, 2004.

[57] Nabil Iqbal and Hong Liu. Real-time response in AdS/CFT with application to spinors. *Fortsch. Phys.*, 57:367–384, 2009.

[58] K. Behrndt, Mirjam Cvetic, and W. A. Sabra. Non-extreme black holes of five dimensional N = 2 AdS supergravity. *Nucl. Phys.*, B553:317–332, 1999.

[59] Andrew Chamblin, Roberto Emparan, Clifford V. Johnson, and Robert C. Myers. Charged AdS black holes and catastrophic holography. *Phys. Rev.*, D60:064018, 1999.

[60] Steven S. Gubser and Indrajit Mitra. Instability of charged black holes in anti-de Sitter space. 2000.

[61] Steven S. Gubser and Indrajit Mitra. The evolution of unstable black holes in anti-de Sitter space. *JHEP*, 08:018, 2001.

[62] John McGreevy, Leonard Susskind, and Nicolaos Toumbas. Invasion of the giant gravitons from anti-de Sitter space. *JHEP*, 06:008, 2000.

[63] Vijay Balasubramanian, Micha Berkooz, Asad Naqvi, and Matthew J. Strassler. Giant gravitons in conformal field theory. *JHEP*, 04:034, 2002.

[64] Vijay Balasubramanian and Asad Naqvi. Giant gravitons and a correspondence principle. *Phys. Lett.*, B528:111–120, 2002.

[65] Andrew Strominger and Cumrun Vafa. Microscopic Origin of the Bekenstein-Hawking Entropy. *Phys. Lett.*, B379:99–104, 1996.

[66] Curtis G. Callan and Juan Martin Maldacena. D-brane Approach to Black Hole Quantum Mechanics. *Nucl. Phys.*, B472:591–610, 1996.

[67] Robert C. Myers and Oyvind Tafjord. Superstars and giant gravitons. *JHEP*, 11:009, 2001.

[68] Hai Lin, Oleg Lunin, and Juan Martin Maldacena. Bubbling AdS space and 1/2 BPS geometries. *JHEP*, 10:025, 2004.

[69] Juan Martin Maldacena, Andrew Strominger, and Edward Witten. Black hole entropy in M-theory. *JHEP*, 12:002, 1997.

[70] Steven S. Gubser. Curvature singularities: The good, the bad, and the naked. *Adv. Theor. Math. Phys.*, 4:679–745, 2000.

[71] Steven S. Gubser and Abhinav Nellore. Ground states of holographic superconductors. *Phys. Rev.*, D80:105007, 2009.

[72] Debaprasad Maity, Swarnendu Sarkar, Nilanjan Sircar, B. Sathiapalan, and R. Shankar. Properties of CFTs dual to Charged BTZ black-hole. 2009.

[73] Gary T. Horowitz and Matthew M. Roberts. Zero Temperature Limit of Holographic Superconductors. 2009.

[74] Jan de Boer, Kyriakos Papadodimas, and Erik Verlinde. Holographic Neutron Stars. 2009.

[75] Steven S. Gubser. Colorful horizons with charge in anti-de Sitter space. 2008.

[76] Steven S. Gubser and Silviu S. Pufu. The gravity dual of a p-wave superconductor. *JHEP*, 11:033, 2008.

[77] Matthew M. Roberts and Sean A. Hartnoll. Pseudogap and time reversal breaking in a holographic superconductor. *JHEP*, 08:035, 2008.

[78] Sebastian Franco, Antonio Garcia-Garcia, and Diego Rodriguez-Gomez. A general class of holographic superconductors. 2009.

[79] Francesco Aprile and Jorge G. Russo. Models of Holographic superconductivity. 2009.

[80] Sebastian Franco, Antonio M. Garcia-Garcia, and Diego Rodriguez-Gomez. A holographic approach to phase transitions. *Phys. Rev.*, D81:041901, 2010.

[81] Andrea Damascelli, Zahid Hussain, and Zhi-Xun Shen. Angle-resolved photoemission studies of the cuprate superconductors. *Rev. Mod. Phys.*, 75(2):473–541, Apr 2003.

[82] Jiunn-Wei Chen, Ying-Jer Kao, and Wen-Yu Wen. Peak-Dip-Hump from Holographic Superconductivity. 2009.

[83] Thomas Faulkner, Gary T. Horowitz, John McGreevy, Matthew M. Roberts, and David Vegh. Photoemission 'experiments' on holographic superconductors. 2009.

[84] Sung-Sik Lee. A Non-Fermi Liquid from a Charged Black Hole: A Critical Fermi Ball. *Phys. Rev.*, D79:086006, 2009.

[85] Pallab Basu, Jianyang He, Anindya Mukherjee, and Hsien-Hang Shieh. Hard-gapped Holographic Superconductors. 2009.

[86] Pallab Basu, Jianyang He, Anindya Mukherjee, and Hsien-Hang Shieh. Superconductivity from D3/D7: Holographic Pion Superfluid. 2008.

[87] Christopher P. Herzog and Silviu S. Pufu. The Second Sound of SU(2). *JHEP*, 04:126, 2009.

[88] Martin Ammon, Johanna Erdmenger, Viviane Grass, Patrick Kerner, and Andy O'Bannon. On Holographic p-wave Superfluids with Back-reaction. 2009.

[89] Hua-Bi Zeng, Zhe-Yong Fan, and Hong-Shi Zong. Superconducting Coherence Length and Magnetic Penetration Depth of a p-wave Holographic Superconductor. 2009.

[90] Amos Yarom. Fourth sound of holographic superfluids. 2009.

[91] G. K. Savvidy. Yang-mills classical mechanics as a kolmogorov k-system. *Phys. Lett.*, B130:303, 1983.

[92] Steven S. Gubser, Silviu S. Pufu, and Fabio D. Rocha. Bulk viscosity of strongly coupled plasmas with holographic duals. *JHEP*, 08:085, 2008.

[93] Mans Henningson and Konstadinos Sfetsos. Spinors and the AdS/CFT correspondence. *Phys. Lett.*, B431:63–68, 1998.

[94] Wolfgang Mueck and K. S. Viswanathan. Conformal field theory correlators from classical field theory on anti-de Sitter space. II: Vector and spinor fields. *Phys. Rev.*, D58:106006, 1998.

[95] Felix Bloch. Flux quantization and dimensionality. *Physical Review*, 166(2):415–423, 1968.

[96] Shou-Cheng Zhang. A unified theory based on $so(5)$ symmetry of superconductivity and antiferromagnetism. *Science*, 275(5303):1089–1096, 1997.

[97] Eugene Demler, Werner Hanke, and Shou-Cheng Zhang. $so(5)$ theory of antiferromagnetism and superconductivity. *Rev. Mod. Phys.*, 76(3):909–974, Nov 2004.

[98] Sean A. Hartnoll, Joseph Polchinski, Eva Silverstein, and David Tong. Towards strange metallic holography. *JHEP*, 04:120, 2010.

[99] Thomas Faulkner, Nabil Iqbal, Hong Liu, John McGreevy, and David Vegh. From black holes to strange metals. 2010.

[100] Thomas Hartman and Sean A. Hartnoll. Cooper pairing near charged black holes. 2010.

[101] Martin Ammon, Johanna Erdmenger, Matthias Kaminski, and Andy O'Bannon. Fermionic Operator Mixing in Holographic p-wave Superfluids. *JHEP*, 05:053, 2010.